AD-A103 083 UNITED TECHNOLOGIES RESEARCH CENTER EAST HARTFORD CT F/G 20/4
TWO-PHASE NOZZLE THEORY AND PARAMETRIC ANALYSIS, PHASE II, PARA--ETC(U)
JUL 81 S C KUO, C W DEANE N00014-79-C-0344
UNCLASSIFIED UTRC/R81-955229-4 NL

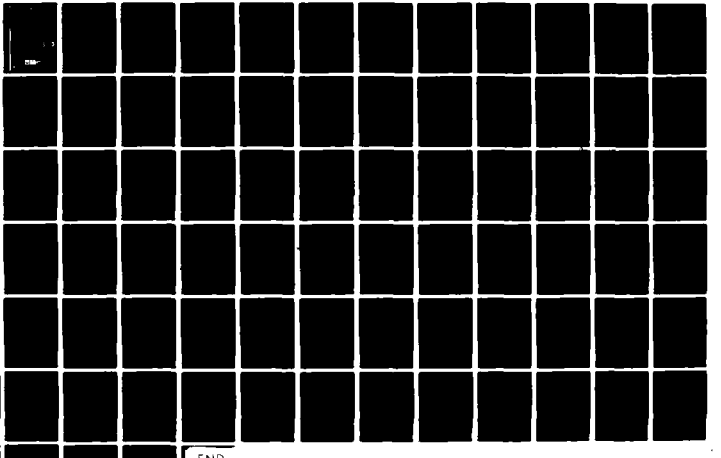

END
DATE FILMED
9-81
DTIC

(12) LEVEL III

UTRC Report R81-955229-4

AD A103083

Two-Phase Nozzle Theory and Parametric Analysis

Phase II — Parametric Analysis and Optimization

Annual Technical Report
July 1981

C.W. Deane

S.C. Kuo, Principal Investigator

Prepared for

The Office of Naval Research, Arlington, Virginia
Under Contract No. N00014-79-C-0344, Modification P00002

UNITED TECHNOLOGIES RESEARCH CENTER
East Hartford, Connecticut 06108

UNCLASSIFIED

SECURITY CLASSIFICATION OF THIS PAGE (When Data Entered)

REPORT DOCUMENTATION PAGE	READ INSTRUCTIONS BEFORE COMPLETING FORM
1. REPORT NUMBER: UTRC R81-955229-4	2. GOVT ACCESSION NO.: AD-A103083
3. RECIPIENT'S CATALOG NUMBER:	
4. TITLE (and Subtitle): Two-Phase Nozzle Theory and Parametric Analysis. (Phase II - Parametric Analysis and Optimization)	5. TYPE OF REPORT & PERIOD COVERED: Annual Technical Report. July 15, 1980 to July 14, 1981
	6. PERFORMING ORG. REPORT NUMBER: UTRC/R81-955229-4
7. AUTHOR(s): Simion C. Kuo; Charles W. Deane	8. CONTRACT OR GRANT NUMBER(s): N00014-79-C-0344; Modification P00002
9. PERFORMING ORGANIZATION NAME AND ADDRESS: United Technologies Research Center, Silver Lane, East Hartford, CT 06108	10. PROGRAM ELEMENT, PROJECT, TASK AREA & WORK UNIT NUMBERS: Program Element: 61153N; Project: RRO 24-03; Task Area: RRO 24-03-02; Work Unit: NR 097-411
11. CONTROLLING OFFICE NAME AND ADDRESS: Office of Naval Research, 800 North Quincy Street, Arlington, VA 22217	12. REPORT DATE: July 1981
	13. NUMBER OF PAGES:
14. MONITORING AGENCY NAME & ADDRESS (if different from Controlling Office)	15. SECURITY CLASS. (of this report): Unclassified
	15a. DECLASSIFICATION/DOWNGRADING SCHEDULE

16. DISTRIBUTION STATEMENT (of this Report)

Approved for public release; Distribution unlimited

17. DISTRIBUTION STATEMENT (of the abstract entered in Block 20, if different from Report)

Same as block 16

18. SUPPLEMENTARY NOTES

19. KEY WORDS (Continue on reverse side if necessary and identify by block number)

Two-Phase Gas-Liquid Flow
Two-Phase Nozzle
Two-Phase Engine
Droplet Breakup
Droplet Heat Transfer

20. ABSTRACT (Continue on reverse side if necessary and identify by block number)

A working theory of two-component two-phase (gas-liquid) nozzles developed earlier (as part of the Phase I work on this program) was used to conduct parametric performance analyses over a wide range of flow conditions and for varied fluid properties. Droplet breakup and the interface transport of momentum and thermal energy were considered in the analyses, but mass transfer and wall friction losses were excluded. Results from the

DD FORM 1 JAN 73 1473 EDITION OF 1 NOV 65 IS OBSOLETE S/N 0102-014-6601

UNCLASSIFIED

SECURITY CLASSIFICATION OF THIS PAGE (When Data Entered)

parametric analyses compare favorably with experimental data and other theoretical analyses available in the literature. The sensitivity of the predicted nozzle performance to the assumptions concerning the droplet characteristics was examined, and criteria were developed for optimum nozzle designs based on the parametric analyses. A simplified procedure was developed for the quick estimation of the major dimensions for two-phase nozzles. Finally, the work extraction potential of two-phase nozzles was examined in terms of their performance criteria and system integration characteristics.

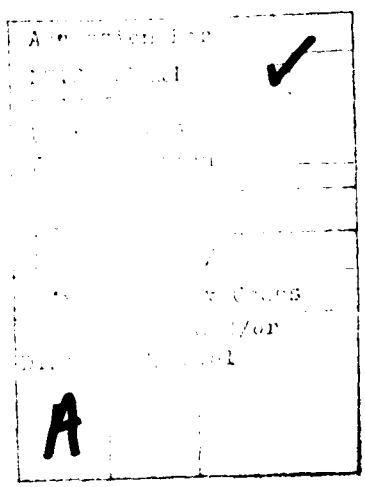

R81-955229-4

Two-Phase Nozzle Theory and Parametric Analysis Phase II-Parametric Analysis and Optimization

Annual Technical Report

Dr. Simion C. Kuo
Principal Investigator
(203) 727-7258

Prepared for:
The Office of Naval Research, Arlington, Virginia
Under Contract No. N00014-79-C-0344, Modification P00002
Mr. M. Keith Ellingsworth, Program Monitor

July 1981

FOREWORD

The work described in this Annual Technical Report was performed at the United Technologies Research Center (UTRC) under Contract N00014-79-C-0344, Modification P00002, entitled "Parametric Analysis and Optimization of Two-Phase Nozzles", for the Office of Naval Research (ONR). This report summarizes results obtained for the Phase II - (second year) study indicated above which is an integral part of a three-year study program on Two-Phase Gas-Liquid Nozzle Flow Theory. Dr. Simion C. Kuo is the Principal Investigator for this contract, and Dr. C. W. Deane is the major contributor for this phase of the study.

The contract program was initiated with ONR on May 15, 1980, and the ONR Program Manager is Mr. M. Keith Ellingsworth, Power Program, ONR, Arlington, Virginia. Valuable guidance and comments received from Mr. Ellingsworth are gratefully acknowledged.

Two-Phase Nozzle Theory and Parametric Analysis
Phase II - Parametric Analysis and Optimization

SUMMARY

The objectives of the work presented in this report were to analyze the parametric performance and to identify the optimum design criteria for two-phase nozzles. A working theory of two-component two-phase (gas-liquid) nozzles developed earlier (as part of the Phase I work on this program) was used to conduct these parametric analyses over a wide range of flow conditions and fluid properties; this working theory includes droplet breakup and the interphase transport of momentum and thermal energy but excludes mass transfer and frictional losses. The sensitivity of the predicted nozzle performance to the assumptions concerning the droplet characteristics was examined, and criteria were developed for optimum nozzle designs based on the parametric analyses. A simplified procedure was developed for the purpose of estimating the approximate dimensions of two-phase nozzles. The performance criteria of two-phase nozzles were then assessed for the nozzle as an integral part of an energy conversion system.

The sensitivity of the predicted nozzle performance to the droplet characteristics was examined by varying the correlations assumed in the formulation of the working theory and then estimating the resulting changes in nozzle performance. Then, using the Model with Droplet Heat Transfer, parametric performance analyses of two-phase nozzles were conducted as a function of the governing flow parameters, including loading ratio, inlet and exit pressures, inlet temperatures of the gas and of the liquid, thermophysical properties of the liquid and of the gas, inlet velocities, droplet size, and nozzle length. Efficiency maps of a two-phase nozzle were then constructed based on the results of these analyses, and the power split between the liquid and the gas streams was estimated under different operating conditions.

Based on the parametric analyses, criteria for optimum nozzle designs were developed, and desirable liquid/gas combinations were investigated in terms of three criteria: maximum operating temperatures of the liquid, degradation characteristics of the liquid, and desirable thermophysical properties. A simplified nozzle sizing procedure, based on isothermal theory, was devised for the quick calculation of the approximate dimensions of the nozzle. Finally, the work extraction potential of two-phase nozzles was examined by identifying nozzle performance criteria and by assessing the attributes of a nozzle suitable for incorporation in an energy conversion system in terms of the off-design performance characteristics of the nozzle.

This study program was conducted by the Energy Conversion Systems Analysis Group at UTRC under Contract N00014-79-C-0344, Modification P00002, from the Office of Naval Research, Power Program, Arlington, Virginia.

INTRODUCTION

Power conversion systems involving two-phase working fluids are of potential interest in a number of applications because of several inherent advantages. For example, two-phase work extraction can be directly applied to harness geothermal energy, where the working fluid is initially available as a two-phase mixture of steam and brine. Another potentially attractive application is in the marine propulsion field where the low exit velocities of a high-density two-phase mixture from a two-phase nozzle (coupled with a two-phase turbine and other components to form a work extraction system) can advantageously drive the propulsion turbines with shaft speeds significantly lower than those in more conventional turbomachinery (steam or gas turbine) power systems. Lower shaft speeds, in turn, would allow the typically massive gearbox (that couples the turbine shaft to the thrustor shaft) to be much smaller and lighter (because less speed reduction would be required), thereby allowing increased payload or range. Another potential advantage in marine propulsion applications is the possible elimination of the boiler. This might be possible if the liquid phase (for example, a heat transfer oil with low vapor pressure) were heated, under pressure without boiling, and then used to flash the condensate of the second component (for example, water) into the gas phase (steam in this example).

In general, a two-phase (gas-liquid) mixture can contain the same amount of enthalpy at a much lower stagnation temperature than a single-phase gas such as steam. Because of the relatively high density of the liquid, the two-phase mixture can also carry the same amount of kinetic energy in the nozzle exit stream at a much lower velocity than the single-phase gas. For example, the differences in velocity and temperature levels between the single-phase ($1-\phi$) and the two-phase ($2-\phi$) streams are indicated in Fig. II.1 where both streams have the same gas mass flow rate (of steam), but the two-phase stream contains liquid. For equal amounts of exit kinetic energy and at loading rates greater than ten, the exit velocities of the two-phase mixture are generally less than one-third of the exit velocities of the single-phase system. These lower nozzle exit velocities then allow lower turbine shaft speeds. Further, to achieve the same exit gas temperature, the nozzle inlet temperatures of the single-phase system with steam are generally a minimum of 350 R higher than the inlet temperatures of a two-phase system with steam and Dowtherm A (DTA), for example. Hence the two-phase system also has the potential to operate with lower heat source temperatures.

In addition to the two applications cited above for two-phase work extraction systems, many other applications involve flows of a substance that is a suspension of liquid droplets in a gas. The particular area of interest in this investigation is a two-phase nozzle where a gas and a liquid at conditions of high pressure and low velocity are mixed at the nozzle inlet and then expanded through the nozzle to conditions of low pressure and high velocity. Previous investigators have proposed physical models for two-phase flows in nozzles, but these models generally display one

of two drawbacks in terms of conducting parametric analyses. Either: only some of the significant effects of momentum and heat transfer were considered (e.g., Refs. 1 to 7); or these effects were considered but the model (e.g., Refs. 8 and 9) was formulated essentially for the purpose of detailed theoretical computation and not for the purpose of conducting parametric analyses and optimization where many cases must be examined quickly yet with reasonable accuracy. Hence, to avoid these drawbacks, a more practical working theory was formulated during Phase I of this study program (Ref. 10). This working theory, developed and computerized as a Model with Droplet Heat Transfer, is suitable for parametric analyses and optimization and is formulated for a wide range of operating conditions because it includes the significant effects of velocity slip, droplet breakup, and droplet heat transfer.

The Model with Droplet Heat Transfer assumes a two-component, two-phase mixture, where the liquid phase is in the form of droplets. One-dimensional flow, with variables changing only in the axial flow direction of the nozzle, was selected for study so that both the model and the results will be tractable. Numerical marching-type solutions with the nozzle divided into numerous small axial segments of equal length were chosen because closed-form analytical solutions are possible only for certain simplified situations. The variations of the thermophysical properties of the gas and the liquid with temperature and/or pressure along the nozzle are included in the marching-type solution by recalculating the value of the property for the local temperature or pressure at each segment.

The Model with Droplet Heat Transfer uses the following six basic equations to describe the adiabatic one-dimensional two-phase nozzle flow:

Continuity
Momentum
Droplet Drag
Droplet Breakup
Energy
Heat Transfer

These equations describe the flow conditions in and across each segment of finite length, and each equation has been transformed into a form suitable for computerized numerical solutions, as described in detail in Ref. 10.

The objectives of the Phase II - Two-Phase Nozzle study program were to conduct parametric analyses using the Model with Droplet Heat Transfer that was developed during Phase I, and to identify optimum design criteria for two-phase nozzles. The results of this Phase II study program are presented in this report.The sensitivity of the two-phase nozzle performance (Model with Droplet Heat Transfer) to the assumptions concerning the droplet characteristics was analyzed in Task II.1 by varying the correlations assumed in the formulation of the theory. Then this theory was

used to conduct parametric performance analyses in Task II.2 by examining the effect of the governing flow parameters on nozzle performance predictions and efficiency, including the effects of loading ratio, nozzle pressure ratio, nozzle length, liquid surface tension and the related droplet size, as well as the effects of other flow parameters. Based on these parametric analyses, criteria were developed in Task II.3 for optimum nozzle designs; desirable liquid/gas combinations were investigated, and a simplified procedure for two-phase nozzle sizing was developed. Finally, two-phase nozzle performance criteria applicable to work extraction were identified in Task II.4, and a simplified procedure was developed for the calculation of off-design nozzle performance characteristics.

INTRODUCTION REFERENCES

1. Tangren, R. F., C. H. Dodge and H. S. Siefert: Compressibility Effects in Two-Phase Flow. J. Appl. Phys., Vol. 20, No. 7, pp. 637-645, 1949.

2. Kliegel, J. R.: One Dimensional Flow of a Gas-Particle System. Report No. TR-59-0000-00746, Space Technology Laboratories, Los Angeles, 1959.

3. Rudinger, G.: "Relaxation in Gas-Particle Flow," Chapter in Nonequilibrium Flows -- Part I, P. P. Wegener, ed., pp. 119-161. Marcel Dekker, Inc., 1969.

4. Netzer, D. W.: Calculations of Flow Characteristics for Two-Phase Flow in Annular Converging-Diverging Nozzles. Report No. TM-62-3, Jet Propulsion Center, School of Mechanical Engineering, Purdue University, 1962.

5. Hultberg, J. A. and S. L. Soo: Two-Phase Flow Through a Nozzle. Astronautica Acta, Vol. 11, No. 3, pp. 207-216, 1965.

6. Crowe, C. T., M. P. Sharma and D. E. Stock: The Particle-Source-In Cell (PSI-Cell) Model for Gas Droplet Flows. ASME J. of Fluids Eng'g., pp. 325-332, 1977.

7. Comfort, W. J., T. W. Alger, W. H. Giedt and C. T. Crowe: Calculation of Two-Phase Dispersed Droplet-in-Vapor Flows Including Normal Shock Waves. ASME J. of Fluids Eng'g., pp. 355-362, 1978.

8. Elliott, D. G.: "Theoretical and Experimental Investigation of a Gas-Driven Jet Pump for Rocket Engines", in Liquid Rockets and Propellants, Progress in Astronautics and Rocketry - Vol. 2, pp. 497-541. Academic Press, 1960.

9. Elliott, D. G. and E. Weinberg: Acceleration of Liquids in Two-Phase Nozzles. JPL Report 32-987, 1968.

10. Deane, C. W. and S. C. Kuo: Two-Phase Nozzle Theory and Parametric Analysis, UTRC Report R80-954624-2, 1980.

CONCLUSIONS

1. The expected efficiency (in percent) of a two-phase two-component nozzle would range between the mid 60's and the high 80's depending on the loading ratio (the ratio of the liquid-to-gas mass flowrates), the nozzle pressure ratio, the nozzle length, and to a lesser degree the inlet conditions and properties of the two fluids. In contrast, a properly designed single-phase (gas) nozzle with a straight axis can achieve efficiencies ranging between 94 and 99 percent.

2. Generally speaking, the higher end of the efficiency range indicated above can be achieved in a long nozzle (say greater than 10 inches) operating at a relatively low pressure ratio (say under 50) while the lower efficiency range is for shorter nozzles particularly with a very high pressure ratio (up to several hundreds). Using a mixture of steam and Dowtherm A(DTA), a six inch nozzle operating at a loading ratio of 40 and a pressure ratio of 40 would have an efficiency between 70 and 75 percent.

3. At a given pressure ratio, the nozzle efficiency goes through a minimum as the loading ratio is increased -- at first decreasing because of the presence of more liquid, reaching a minimum value (at a loading ratio in the vicinity of 10), before increasing gradually because the slip velocity between the two phases is decreasing as the loading ratio is increased to approximately 60. At higher loading ratios, the flow regime may no longer be droplet flow, as assumed in the working theory.

4. The exit specific power (flux of kinetic energy at the nozzle exit) decreases when either the loading ratio or the pressure ratio or both is increased. As the loading ratio is increased (more liquid), the required nozzle exit area also increases because the gas exit velocity is decreasing and more flow area is needed to pass the lower-velocity mixture.

5. For a mixture of steam and Dowtherm A(DTA) flowing at a loading ratio of 40, the power split (between the liquid-phase kinetic energy and the gas-phase kinetic energy at the nozzle exit) is 24 for a nozzle operating at an inlet pressure of 1000 psia and a pressure ratio of 10. With the pressure ratio increased to 40 for these inlet conditions, the power split is 20. Further, for loading ratios greater than five for steam/DTA mixtures at those operating conditions, over 75 percent of the mixture kinetic energy is carried by the liquid phase.

6. The sensitivity of the predicted nozzle performance to assumptions of droplet breakup was found to be significant (as much as four percentage points in nozzle efficiency over the expected range of maximum Weber number). In contrast, the droplet drag coefficient and the droplet heat transfer coefficient were found to have a lesser influence on the nozzle performance.

7. Performance criteria of two-phase nozzles applicable to work extraction systems were identified to be nozzle efficiency and mixture velocity at the nozzle exit. But the performance and design of the selected nozzle must be carefully integrated with the overall work extraction system to yield the optimum overall system.

8. Using a simplified sizing procedure based on isothermal theory, estimates of off-design gas and liquid flow rates indicate that the kinetic energy profiles at off-design can be made relatively flat by tailoring the flow rates.

Two-Phase Nozzle Theory and Parametric Analysis
Phase II - Parametric Analysis and Optimization

The overall objective of this analytical study program is to advance the basic understanding of two-phase nozzles, particularly from the energy conversion point of view. To meet this overall objective, the specific objectives of the Phase II work described herein are to conduct parametric analyses in terms of the effect of the governing parameters on two-phase nozzle performance characteristics and to identify optimum design criteria for two-phase nozzles. As part of the earlier Phase I work (which is described in detail in Ref. 1), a working theory of two-component two-phase (gas-liquid) nozzles, identified as the Model with Droplet Heat Transfer, was developed which includes droplet breakup and the interphase transport of momentum and thermal energy but excludes mass transfer and frictional losses. This working theory was computerized in a form suitable for parameteric and optimization analyses of these two-phase nozzles. The Phase II work described herein consists of results obtained from four study tasks: II.1) Sensitivity Analysis of Droplet Characteristics; II.2) Parametric Performance Analysis; II.3) Optimum Nozzle Designs; and II.4) Assessment of Work Extraction Potential. The results obtained in each of these four tasks are presented in the following sections.

II.1 Sensitivity Analysis of Droplet Characteristics

The sensitivity of the two-phase nozzle performance predictions (obtained from the working theory that was developed during Phase I of this program and is presented in Ref. 1) to assumptions and simplifying correlations concerning droplet characteristics was examined by varying the correlations and then comparing the change in the predicted performance. To make numerical estimates of nozzle performance characteristics, correlations of experimental data are required in three areas: droplet breakup, the droplet drag coefficient, and the droplet heat transfer coefficient. Estimates of the sensitivities of the nozzle performance predictions to these three droplet characteristics were made in this portion of the study.

The sensitivity of the predicted nozzle efficiency to the assumptions made for droplet breakup was found to be significant. In contrast, the sensitivities of the predicted nozzle efficiency to the assumptions for the droplet drag coefficient and the droplet heat transfer coefficient were found to be low, in part because of the relatively high heat transfer coefficient (from the liquid droplet to the gas) inherent with the very small droplets.

II.1.1 Droplet Breakup

As discussed in Ref. 1 and elsewhere, droplet breakup in a two-phase mixture is governed primarily by the ratio of two forces: the aerodynamic pressure forces, and the surface tension forces. The ratio of these two forces is known as the Weber Number, which is defined as:

$$We \equiv \frac{\rho_g V_{slip}^2 D}{2\sigma} \qquad (II.1)$$

where ρ_g is the gas density, V_{slip} is the slip velocity ($V_{slip} \equiv V_\ell - V_g$), D is the droplet diameter, and σ is the surface tension of the liquid. The subscript "ℓ" refers to the liquid phase, and the subscript "g" refers to the gas phase.

In the computerized model, the critical value of the Weber Number, $We)_{crit}$, would limit the maximum droplet size, D_{MAX}, that can exist at the local flow conditions in a two-phase flow:

$$D_{MAX} = \frac{2\sigma\ We)_{Crit}}{\rho_g V_{slip}^2} \qquad (II.1a)$$

The generally accepted value of $We)_{crit}$ is 6.0 (Ref. 2), within a factor of about 2 (for example, see Ref. 3). However, recent experiments by Alger (Ref. 4) with steam-water nozzles suggest that the appropriate value of $We)_{crit}$ should be approximately 1.0. Areas of high acceleration in the nozzle could produce greater droplet deformation as compared to nearly spherical droplets in less accelerated regions.

The sensitivity of the nozzle performance predictions to droplet breakup in terms of the exit velocities and temperatures and the nozzle efficiency is shown in Table II.1 for three values of the critical Weber Number. These values generally cover the range found experimentally by previous investigators and represent the range over which the sensitivity of nozzle performance predictions is of interest. In Table II.1, V is velocity, r is the loading ratio ($r \equiv \dot{m}_\ell/\dot{m}_g$) where $\dot{m}$ is mass flow rate, T is temperature, and η is the nozzle efficiency (which is defined later in Eq. II.9). Droplet breakup is seen to have a significant effect on the predicted efficiency because the smaller droplets have a lower slip velocity ($V_g - V_\ell$) and a higher rate of heat transfer to the gas because of the increased total surface area of the droplets. At the selected operating conditions (given in

Table II.1) of a nozzle with a two-phase mixture of steam and Dowtherm A (DTA), decreasing the value of the critical Weber Number by a factor of six results in an increase in the predicted nozzle efficiency of 2.7 percentage points at a loading ratio of one, while at a loading ratio of 40, the increase in predicted nozzle efficiency is 4.3 percentage points.

II.1.2 Droplet Drag

As discussed in Ref. 1, the empirical data base for the drag coefficient (C_D) was developed from previous investigations published in the literature, and the comprehensive expression that was selected for use in the computerized model is:

$$\ell n\ C_D = 3.271 - 0.8893\ L_{Re} + 0.03417\ L_{Re}^2 + 0.001443\ L_{Re}^3 \qquad \text{(II.2)}$$

where $L_{Re} \equiv \ell n\ (Re_{Rel})$. Re_{Rel} is the relative Reynolds number ($Re_{Rel} \equiv \rho_g\ V_{slip}\ D/\mu_g$), and μ_g is the gas viscosity. Stonecypher (as cited in Ref. 5) developed this expression by making a least-squares fit of the drag data for spherical particles that was tabulated by Perry, et al. (Ref. 6).

Using the computerized model, the sensitivity of the nozzle performance predictions to the droplet drag coefficient was calculated and is shown in Table II.2 for three values of the coefficient: 1) 80 percent of the value predicted by the drag coefficient correlation of Eq. II.2 at the local relative Reynolds number for each of the axial nozzle segments, 2) 100 percent of this value, and 3) 120 percent of this value. This range of values (plus and minus 20 percent of the nominal value) brackets a reasonable range of scatter that might exist in the original experimental drag data. The sensitivity of the calculated exit velocities and temperatures was found to be small at a loading ratio of 40, with only a 0.7 percentage point increase in the calculated efficiency as the drag coefficient is increased over the range. Conversely, at a loading ratio of one, the sensitivity of the calculated nozzle efficiency was found to be extremely low because the relative impact of the liquid is less, and the sensitivities of the exit velocities and temperatures are greater than at higher values of the loading ratio but are still relatively low.

II.1.3 Droplet Heat Transfer

The heat transfer coefficient (h) between the liquid droplets and the gas is numerically evaluated in the computerized model, as discussed in Ref. 1, with a dimensionless correlation recommended by McAdams (Ref. 7) for relative Reynolds numbers in the range of 25 to 10,000:

$$\frac{hD}{k_g} = 0.37\ Re_{Rel}^{0.6} \qquad (II.3)$$

where k_g is the thermal conductivity of the gas. For relative Reynolds numbers in the range of 1.0 to 25, the expression recommended by Kreith (Ref. 8) is used to calculate the heat transfer coefficient:

$$\frac{hD}{k_g} = \frac{\mu_g C_{pg}}{k_g} \left[2.2 + 0.48\ Re_{Rel}^{0.5}\right] \qquad (II.4)$$

where C_{pg} is the specific heat (at constant pressure) of the gas.

Using the computerized model, the sensitivity of the nozzle performance predictions to the heat transfer coefficient was calculated and is shown in Table II.3 for three values of the coefficient: 1) 80 percent of the value predicted by the heat transfer coefficient correlations of Eqs. II.3 and II.4 at the local relative Reynolds number for each of the axial nozzle segments, 2) 100 percent of this value, and 3) 120 percent of this value. This range of values brackets the ± 20-percent scatter that is typical of heat transfer data. The sensitivity of the calculated efficiency and the exit velocities and temperatures to heat transfer was found to be low over the loading ratio range of 1.0 to 40., and decreases as the loading ratio is increased. The low sensitivity is attributable, in part, to the fact that the heat transfer coefficient is already very high because the liquid droplets are very small in diameter at the operating conditions of Table II.3.

II.2 Parametric Performance Analysis

Using the working theory (identified as the Model with Droplet Heat Transfer) that was previously developed on Phase I of this program (Ref. 1), parametric performance analyses were made for selected two-phase nozzles in terms of the operating conditions. The effects of all the governing parameters on nozzle performance were investigated, and efficiency maps of a two-phase nozzle were constructed based on these analyses. The power split between the liquid and the gas streams was estimated under different operating conditions. Table II.4 summarizes the relative effect, qualitatively rated, of the governing flow parameters on nozzle performance predictions in terms of the exit temperatures and velocities of each phase and of the nozzle efficiency. The parameters that have the most significant effect on nozzle efficiency are: loading ratio, nozzle pressure ratio (or exit pressure), gas density, liquid surface tension and the related droplet size, and nozzle length. The results of the parametric analyses which form the base for the ratings of the relative effects shown in Table II.4 are presented and discussed in this section. Generally, the value of the Weber Number was set at 6.0, the value of the inlet gas velocity was set at 100 ft/sec, the value of the inlet liquid velocity was set at 70 ft/sec, and a nozzle length of six inches was selected for the parametric analyses, unless otherwise stated.

II.2.1 Effect of Liquid/Gas Ratio

The effect of the liquid/gas ratio was investigated in terms of the ratios of mass, volume, and thermal capacity of the two streams. The mass ratio of the two streams is generally known as the loading ratio ($r \equiv \dot{m}_\ell/\dot{m}_g$), while the ratios of volume and thermal capacity are directly related to this loading ratio. For two-component two-phase nozzle flow without mass transfer between the two phases (which is the situation for the working theory developed during Phase I of this program), the loading ratio is constant throughout the nozzle, but the ratios of volume and thermal capacity will vary as the two-phase mixture flows through the nozzle, depending on the effect of local temperature and pressure on the density and specific heat of the gas and the liquid. The volume ratio is defined as the ratio of the volumetric flows of the two streams:

$$r_v \equiv \frac{\dot{m}_\ell/\rho_\ell}{\dot{m}_g/\rho_g} = r\,\frac{\rho_g}{\rho_\ell} \qquad \text{(II.5)}$$

where ρ_ℓ is the density of the liquid. The thermal capacity ratio is correspondingly defined as the ratio of the thermal capacities (per unit temperature rise) of the two streams:

$$r_t \equiv \frac{C\,\dot{m}_\ell}{C_{pg}\,\dot{m}_g} = r\,\frac{C}{C_{pg}} \qquad \text{(II.6)}$$

where C is the specific heat of the liquid. This definition is analogous to the definition of capacity ratio in heat exchanger design theory (Ref. 9).

Figure II.2 shows the effect of the (mass) loading ratio on performance predictions of nozzle throat and exit conditions. P is the local pressure, and the subscript "in" refers to the nozzle inlet while the subscript "exit" refers to the nozzle exit. As the loading ratio is reduced, both throat and exit velocities of both phases increase, and both throat and exit temperatures of both phases decrease. These situations are explained by reasoning that the effect of the liquid phase decreases as the loading ratio is decreased, and hence the gas phase tends to behave increasingly as a pure gas. The slip velocity increases as the loading ratio is reduced and the droplet size decreases as a result, because the higher slip velocity means higher aerodynamic forces which tend to break up the droplets. The nozzle efficiency goes through a minimum, at first decreasing because of the higher slip when the loading ratio is reduced, but then increasing because the presence of the liquid phase has a lesser effect when the loading ratio is reduced further.

As indicated above, both the volume ratio and the thermal capacity ratio are proportional to the mass loading ratio. Hence, the effects of the volume and thermal capacity ratios, evaluated at the nozzle inlet conditions (of temperature and pressure) are the same as the effect of the mass loading ratio, and are shown in Fig. II.2.

The exit specific power is shown in Fig. II.3 as a function of (mass) loading ratio and pressure ratio ($PR = P_{in}/P_{exit}$). The exit specific power is the time rate of flow of kinetic energy of the two-phase mixture at the nozzle exit, divided by the exit flow area (A_{exit}):

$$\text{Specific Power})_{exit} \equiv \frac{\frac{1}{2}\,\dot{m}\,\bar{V}^2_{exit}}{A_{exit}} \qquad \text{(II.7)}$$

where $\dot{m}$ is the total mass flow rate ($\dot{m} = \dot{m}_\ell / + \dot{m}_g$) and $\bar{V}_{exit}$ is the mass-weighted exit velocity. The mass-weighted velocity is defined as: $\bar{V} = (V_g + r\,V_\ell)/(1 + r)$. As seen in Fig. II.3, the specific power increases when either the loading ratio or the pressure ratio is decreased. As the loading ratio is decreased, the required exit area decreases because the gas exit velocity is increasing (as seen in Fig. II.2), and less flow area is needed to pass the higher-velocity mixture; with less liquid relative to the gas mass, the gas exit velocity is higher at the lower loading ratio. As the pressure ratio decreases (and hence the exit pressure increases, for fixed inlet pressure), the exit gas is denser and less exit area is needed to pass the same mass flow at a given loading ratio. With less nozzle exit flow area, then, the specific power increases.

II.2.2 Pressure and Temperature Effects

Pressure and temperature effects on nozzle performance predictions were investigated parametrically in terms of inlet pressure, exit pressure, pressure ratio (P_{in}/P_{exit}), inlet temperature, and inlet temperature difference between the gas and the liquid.

Pressure Effects

With the exit pressure held constant, Fig. II.4 shows the effect of inlet pressure on nozzle performance predictions for a two-phase mixture of steam and DTA, for two values of loading ratio which span the range of interest for propulsion applications. The effect on nozzle efficiency is small, with the nozzle efficiency increasing slightly as the inlet pressure is increased. The exit velocities increase and the exit temperatures decrease as the inlet pressure is increased, because the gas phase (steam) is being expanded through a larger pressure ratio.

Figure II.5 shows the parametric effect of nozzle exit pressure, with a fixed inlet pressure of 1000 psia. As the exit pressure is decreased, the gas phase is expanded more, and the gas exit velocity increases substantially while the liquid exit velocity increases by a lesser amount. Hence, the slip velocity ($V_g - V_\ell$) between the two phases increases, and the nozzle efficiency decreases as a result. In addition, with the greater expansion of the gas phase when the exit pressure is decreased, the gas exit temperature also decreases substantially. Here, the liquid phase acts as a heat source to the gas phase, and heat transfer from the hotter liquid retards this gas temperature decrease, but the short residence time of the two-phase mixture in the nozzle does limit the amount of heat that can be transferred from the liquid to the gas. At the lower loading ratio ($r = 10$), the liquid exit temperature is lower and the effect of the lower exit pressure is larger, in both instances because the liquid heat source is relatively smaller than at a loading ratio of 40.

Shown in Fig. II.6 is the effect of pressure ratio (P_{in}/P_{exit}), over an extremely wide range, at a fixed inlet pressure. As the pressure ratio is increased, both the efficiency and the exit gas temperature decrease, the exit gas velocity rises sharply, while the exit liquid temperature falls and the exit liquid velocity rises only for pressure ratios less than about 50 and are otherwise little affected by the pressure ratio. For the results of Fig. II.6, the pressure ratio is increased by decreasing the exit pressure to lower values. For example, at a pressure ratio of 400 and an inlet pressure of 600 psia, the exit pressure is 1.5 psia. Figure II.7 shows a nozzle design at this low exit pressure. In the last 0.2 ft of the nozzle, the gas temperature drops rapidly while the liquid temperature drops only moderately, and the gas velocity rises sharply while the liquid velocity

rises only moderately. In general, at low exit pressures, for a pressure profile linear with nozzle length, the local expansion ratio near the exit is large relative to design conditions that have higher exit pressures. This large local expansion ratio then results in large increases in gas velocity and large decreases in gas temperature as the gas expands. The residence time is too short at the high velocities (both for momentum transfer from the gas to the liquid and for heat transfer from the liquid to the gas), to narrow the velocity and temperature differences between the gas and the liquid, respectively. The effect of exit pressure on nozzle shape is shown in Fig. II.8, in terms of the relative nozzle diameter at the throat and at the exit, for a six-inch-long nozzle with the pressure profile linear with length. Exit pressure has no effect on throat diameter, but the exit diameter must be increased to accommodate the lower-density exit gas at the lower exit pressure, even though the exit gas velocity increases as the exit pressure is reduced; this trend of gas velocity was seen in Fig. II.6. In general, the nozzle exit area (which is proportional to d^2_{exit}) in Fig. II.8 is increasing faster than the inverse of the exit gas density (this inverse is proportional to $1/P_{exit}$) because the exit gas velocity is not increasing as fast as the exit gas density is decreasing.

Temperature Effects

Table II.5 shows the effect of inlet temperature on nozzle performance predictions, at two values of the loading ratio. At a given loading ratio, the effect of inlet temperature on the liquid temperature drop through the nozzle $[T_\ell)_{in} - T_\ell)_{exit}]$ is small, as is the effect on the temperature differential between the liquid and the gas at the nozzle exit. As the inlet temperature is reduced from 1160 R to 960 R, the liquid and gas velocities and the nozzle efficiency decrease, while the slip velocity increases because the liquid droplets are larger at the lower temperature where the liquid surface tension is larger. With the higher slip velocity, the nozzle efficiency is expected to be lower.

The effect of the inlet temperature difference on nozzle performance predictions is shown in Fig. II.9. The only major effect of this temperature difference is seen in the exit temperatures of the gas and the liquid, where the exit temperatures fall when the gas temperature is reduced to provide the temperature difference. This trend is expected from enthalpy considerations. The nozzle efficiency also decreases slightly as the inlet temperature is increased, because the colder two-phase mixture means that the liquid surface tension is higher and hence the liquid droplets are larger according to the Weber Number breakup criterion (Eq. II.1a). This data on the effect of inlet temperature difference is replotted in Fig. II.10 as a function of loading ratio. The effect is relatively larger at the lower values of the loading ratio, where the gas phase is a larger fraction of the two-phase mixture.

II.2.3 Effects of Thermophysical Properties

The effects of thermophysical properties of the gas and of the liquid on nozzle performance characteristics were investigated by judiciously varying these properties.

Effects of Gas Thermophysical Properties

Table II.6 shows the effect of the gas specific heat, at three values relative to the specific heat of steam: twice the specific heat of steam, equal to that, and half of that value. As expected, the effect on exit velocities, which are primarily governed by momentum transfer, is negligible. The effect on nozzle efficiency is small and decreasing as the loading ratio is increased, and the effect on exit temperatures is also small, in part because the gas phase is only one-eleventh of the total mass at a loading ratio of ten, for example.

The effect of gas-phase density on nozzle performance predictions is shown in Fig. II.11. The calculations were made by varying the molecular weight of the gas (hence the gas density which is calculated with the perfect gas law), while the relationships for the other thermophysical properties (viscosity, thermal conductivity, and specific heat) of the gas were not changed and were those of steam. As the gas density increases, the nozzle efficiency increases, and the exit velocities and the slip velocity ($V_g - V_\ell$) both decrease. The lower velocities mean both a longer residence time in the nozzle for increased heat transfer from the liquid to the gas, and higher exit temperatures for both phases because a lower fraction of the constant total energy is in the form of kinetic energy. If the other thermophysical properties of the gas remain unchanged, a heavier gas, therefore, results in higher nozzle efficiencies.

Effects of Liquid Thermophysical Properties

The effects of the thermophysical properties of the liquid were also investigated, and Fig. II.12 shows the relative effect of liquid specific heat on nozzle performance characteristics (all other liquid properties being those of Dowtherm A). Three values of liquid specific heat were investigated: the specific heat of Dowtherm A, and half and twice that value. At a loading ratio of ten, halving the liquid specific heat results in only a 0.15 percentage increase in the predicted nozzle efficiency, and the effect is smaller at larger values of the loading ratio. Of course, the effect on the calculated exit temperatures of the liquid and of the gas are much larger: the liquid with the lower specific heat

has a lower exit temperature and the accompanying gas exit temperature is also lower, because the liquid is a relatively smaller heat source at the same loading ratio than is a liquid with a higher specific heat. Overall, the effect of liquid specific heat on the nozzle efficiency, hence its performance, is small.

Figure II.13 shows the effect of liquid surface tension on nozzle performance predictions. As discussed previously in connection with the Weber Number breakup criterion (Eq. II.1a), liquid surface tension is a primary factor in the determination of the droplet size. And, as the surface tension is decreased, the liquid droplets will break up into smaller sizes. With smaller droplets, at a given loading ratio, the velocity slip (V_g-V_ℓ) between the two phases is lower, the heat transfer between the liquid and the gas is higher because there is more droplet surface area, and the nozzle efficiency is higher as a result. These are the trends displayed as a function of loading ratio, in Fig. II.13, which shows results for three values of the liquid surface tension: the real value of DTA, half of that value, and twice that value. Except for the surface tension, the thermophysical properties of the liquid phase are those of DTA, and the thermophysical properties of the gas phase are those of steam. If the other thermophysical properties of the liquid remain unchanged, lower liquid surface tension, therefore, results in higher nozzle efficiency.

The effect of liquid density is shown in Fig. II.14 in terms of three values of density: the density of DTA, and both 20 percent above and 20 percent below the value for the DTA density. All other liquid properties are those of DTA. The effect of liquid density on the gas and liquid exit temperatures is negligible and is not shown. At a given value of the loading ratio, the lower liquid density leads to higher velocities, lower slip velocity (V_g-V_ℓ), and higher nozzle efficiency. With a given amount of momentum transfer from the gas to the liquid, the lower liquid density means that the liquid velocity will be higher. For a 20 percent decrease in liquid density, the nozzle efficiency increases by 1.6 percentage points at a loading ratio of 40, and by 1.1 percentage points at a loading ratio of 10.

II.2.4 Effects of Inlet Velocity, Droplet Size, and Nozzle Length

The effect of inlet velocity on nozzle performance predictions is summarized in Table II.7 and is seen to be small. Part a) of this table presents nozzle exit results at three levels of inlet gas velocity, with the velocity ratio (V_ℓ/V_g) held constant at 0.7, for three values of the loading ratio. Part b) shows results for a loading ratio of 20, but at three values of the inlet velocity ratio, 0.7, 0.8, and 0.9, at two levels of inlet gas velocity. In all cases, the effect on exit temperatures is negligible. As the inlet velocity is increased, the nozzle

efficiency increases slightly, as do the exit velocities, but by much smaller amounts than the increase in inlet velocity. At a given inlet gas velocity, the effect of velocity ratio is negligible. Hence, in general, the effect of inlet velocity on nozzle performance predictions is minor.

The effect of droplet size is shown in Fig. II.15. As expected from discussions above, the effect of droplet size on nozzle efficiency is significant because of its impact on the transfer of momentum and heat. The results in Fig. II.15 are presented in terms of the maximum Weber Number, $We)_{max}$, because this is the factor which is postulated to control droplet size in the Model with Droplet Heat Transfer. The droplets break up until their diameter results in a droplet Weber Number equal to the maximum. A smaller value of the maximum Weber Number results in smaller droplet sizes, as indicated by the results in Fig. II.15 for droplet diameter (D), but the droplet diameter does not vary proportionately with the maximum Weber Number because the slip velocity also changes when the droplet size changes. The droplet drag force, which is influenced by the droplet size, couples the gas to the liquid and is indirectly related, through the force balance on the droplet, to the velocity difference between the two phases. As seen in Fig. II.15, the major effect of the droplet size is to increase the nozzle efficiency by about two percentage points when the critical Weber Number (for droplet breakup) is cut by a factor of two, and the corresponding droplet size is then about 25 percent smaller. The smaller droplets result in a higher velocity ratio (V_g/V_ℓ), which means lower slip velocity and higher nozzle efficiency.

Figure II.16 shows the effect of nozzle length on performance predictions. The main effect is on nozzle efficiency which increases as nozzle length increases because the residence time of the two-phase mixture is longer. And the longer residence time means more transfer of momentum and heat between the two phases. Hence, as the nozzle length is increased, the velocity slip ($V_g - V_\ell$) is reduced, as is the temperature difference between the hot liquid and the cold gas. As mentioned previously, the Model with Droplet Heat Transfer neglects friction, and this is a reasonable assumption for shorter nozzles to be used in propulsion applications where space is likely to be limited.

II.2.5 Power Split of Two-Phase Nozzles

The power split of the nozzle is defined as the ratio of the kinetic energy of the liquid fraction at the nozzle exit to the kinetic energy of the gas fraction at the nozzle exit:

$$\left(\frac{KE_{liq}}{KE_{gas}}\right)_{exit} = \left(\frac{\frac{1}{2}\dot{m}_\ell V_\ell^2}{\frac{1}{2}\dot{m}_g V_g^2}\right)_{exit} = r K_{exit}^2 \qquad \text{(II.8)}$$

where K_{exit} is the exit value of the velocity ratio ($K \equiv V_\ell/V_g$). Because of the assumption that no mass transfer occurs between the gas and the liquid phases, the mass loading ratio does not change from the inlet value. Therefore, to estimate the power split, the inlet loading ratio and the velocity ratio at the nozzle exit must be obtained. The drag force on the liquid droplets accelerate the droplets, but the droplet velocity lags the gas velocity throughout the nozzle. The velocity ratio at the nozzle exit is calculated as one of the results from the computerized Model with Droplet Heat Transfer and was shown earlier in the parametric results (as in Fig. II.2). Generally, the range of values of K_{exit} is limited to about 0.5 to 0.9, but the value of the loading ratio is much higher, ranging from zero (all-gas flow) to 50 and higher, depending on the design conditions. Hence, the loading ratio which is one part of the specified inlet operating conditions is the more important factor in the estimation of the power split. At a loading ratio of 40 for the steam/DTA mixture and the nozzle inlet conditions specified in Fig. II.2, the value of the exit velocity ratio is $K_{exit} = 0.78$ and the power split is then 24.4, as estimated with Eq. II.8. As expected, the bulk of the kinetic energy is carried at this loading ratio by the liquid phase despite the higher exit velocity of the gas phase. If the pressure ratio is increased to 40 with the loading ratio still at 40, then the exit velocity is about 0.72 and the power split is 20.7. Figure II.17 shows the power split as a function of the loading ratio. Also shown in Fig. II.17 is the same information replotted as the liquid energy fraction, which is the fraction of the total kinetic energy of the mixture that is carried by the liquid phase.

II.2.6 Efficiency Maps of Two-Phase Nozzles

Based on the parametric performance analyses discussed above, efficiency maps for a nozzle with a two-phase mixture of steam and Dowtherm A (DTA) were constructed. As noted previously (Ref. 1), the isentropic efficiency is a measure of nozzle efficiency and is defined as:

$$\eta \equiv \frac{\frac{1}{2}\,\dot{m}\,(\bar{V}^2_{exit} - \bar{V}^2_{inlet})}{\dot{m}\,\Delta h)_{max}} = \frac{\bar{V}^2_{exit} - \bar{V}^2_{inlet}}{2\,\Delta h)_{max}} \qquad \text{(II.9)}$$

This efficiency is the ratio of the change in kinetic energy per unit mass of the mixture to the ideal change of enthalpy (into kinetic energy) for the isentropic expansion of a homogeneous two-phase mixture. (For operating conditions where the nozzle inlet velocity ($\bar{V}_{inlet}$) is very low when compared to the exit velocity ($\bar{V}_{exit}$), then $\bar{V}^2_{exit} >> \bar{V}^2_{inlet}$ and the inlet velocity term can be neglected.)

The maximum enthalpy change through the nozzle, $\Delta h)_{max}$, is given by the expression:

$$\Delta h)_{max} = \left\{\left(\frac{1}{1+r}\right) C_{pg}\left[T_g)_{inlet} - T_{exit}\right]\right\} + \left\{\left(\frac{r}{1+r}\right)\left(C\left[T_\ell)_{inlet} - T_{exit}\right] + \frac{\Delta P}{\rho_\ell}\right)\right\} \qquad \text{(II.10)}$$

where ΔP is the pressure drop through the nozzle. Efficiency maps are shown in Figs. II.18, II.19, and II.20 in terms of pressure effects, temperature effects, and inlet temperature difference effects, respectively.

Effect of Pressure Ratio

The effect of pressure ratio ($PR = P_{in}/P_{exit}$) on nozzle efficiency at two levels of inlet pressure is seen in Fig. II.18 over a range of loading ratio. At a given inlet pressure, as the exit pressure is reduced (and hence PR increased), the nozzle efficiency decreases. At the lower exit pressure, the gas expands to a higher exit velocity, but the liquid velocity does not increase by a proportionate amount because momentum transfer from the gas to the liquid is a rate process which therefore requires time to reach equilibrium. Hence, at the lower exit pressure, because the residence time of the mixture in the nozzle is shorter, less momentum is transferred from the gas to the liquid and the nozzle efficiency is lower. At a given pressure ratio but at a lower inlet pressure, the exit pressure is lower, and the same rationale of less momentum transfer also explains the trend to lower efficiency.

Effect of Inlet Temperature

In Fig. II.19, the increase in efficiency as the inlet temperature is increased can be explained by the smaller droplet sizes at the higher temperature. The liquid surface tension (which in part determines the maximum droplet size through the critical Weber Number for droplet breakup, Eq. II.1a) decreases as the temperature increases. Hence, the droplets are smaller, momentum transfer between the smaller droplets and the gas is better, the exit liquid velocity is therefore higher, and the nozzle efficiency is higher as a result.

Effect of Inlet Temperature Difference

Figure II.20 shows that for a constant liquid inlet temperature, the effect of inlet temperature difference on nozzle efficiency is small for values of the loading ratio greater than about five, above which point the liquid phase dominates the exit temperature of the two-phase mixture. Near the nozzle inlet, the inlet temperature difference will have a greater effect, however, on local conditions, as seen earlier in the Phase I work (Fig. I.26 of Ref. 1). Thus, the inlet temperature itself has a much larger effect on nozzle efficiency than the inlet temperature difference.

II.2.7 Comparisons with Experimental Results

As discussed in Ref. 1, experimental data have been taken for a number of two-phase nozzles, but only some of this data was taken with a two-component mixture - the type of mixture to which the Model with Droplet Heat Transfer

applies. Figures II.21, II.22 and II.23 compare calculated results from the Model with Droplet Heat Transfer to experimental measurements made by Elliott and Weinberg (Ref. 5) at three levels of inlet pressure with a water-nitrogen mixture flowing through a 50-inch-long nozzle. The Model with Droplet Heat Transfer is a design model, and as such is normally used to plan families of nozzles for one set of operating conditions. Hence, the results from the Model with Droplet Heat Transfer in these three figures are actually a series of nozzle designs, over a range of loading ratios; the profile of pressure drop was selected to be linear with axial distance through the nozzle. Also shown in these three figures are performance lines predicted by Elliott and Weinberg with their models (Ref. 5) for the actual nozzle contour. The Elliott and Weinberg prediction labeled "Real" is based on a model that includes velocity slip, droplet breakup, and heat transfer but no friction; while their prediction labeled "Friction" includes friction in terms of wall boundary layer losses.

The design-point performances shown in Figs. II.21, II.22 and II.23 as calculated for a series of nozzles by the Model with Droplet Heat Transfer compare well with the experimental data of Elliott and Weinberg and show the same trend as the off-design performance of one nozzle.

As seen by the definition of Eq. II.9, the nozzle efficiency is essentially a function of the mass-weighted velocity at the nozzle exit. Hence, the comparisons of the measured exit velocities with the predictions from the Model with Droplet Heat Transfer in Figs. II.21, II.22, and II.23 are essentially a comparison of the measured and predicted efficiencies as well.

II.3 Optimum Nozzle Designs

Based on the parametric analyses presented in Section II.2, criteria were developed for optimum nozzle designs. Desirable liquid/gas combinations were investigated in terms of three criteria: maximum allowable operating temperatures of the liquid, degradation characteristics of the liquid, and desirable thermophysical properties. Maximum efficiencies for two-phase nozzles were estimated based on the parametric analyses of Section II.2. Finally, a simplified design procedure was developed for the quick, first-cut sizing by hand calculation of two-phase nozzle geometry.

II.3.1 Criteria for Optimum Nozzle Designs

The parametric analyses presented in Section II.2 are the bases for developing the criteria for optimum nozzle designs. First, considering the selection of nozzle geometry, nozzle efficiency increases as nozzle length is increased, as seen from Fig. II.16. The increased length provides more residence time for the exchange of momentum and heat between the two phases, and the nozzle efficiency is therefore higher. Hence, within the geometric constraints of the given application, longer nozzles result in higher nozzle efficiency.

Second, the other governing flow parameters of the nozzle design are generally set by overall system considerations. The effect of these parameters on nozzle performance can be studied for parametric trends that can be used to influence the selection of the overall system operating conditions at the design point. For example, the effect of increasing the nozzle pressure ratio, seen in Fig. II.6 (obtained by reducing the exit pressure), is to reduce the design point nozzle efficiency. The effect of nozzle inlet pressure (for a given exit pressure) was seen in Fig. II.4, wherein lower nozzle inlet pressure was seen to reduce the nozzle efficiency and can be significant in the selection of overall system operating conditions. In general, higher pressure ratio can be obtained by: increasing the nozzle inlet pressure (this increase has side effects on the sizing of the pump); and/or by decreasing the exit pressure (this decrease has side effects both on the sizing of the turbine with the concomitant lower turbine inlet pressure and on the design of the condenser where the steam is condensed before being repressurized as a liquid).

The effect of inlet temperature on nozzle performance predictions was seen in Table II.5, wherein reducing the inlet temperature was seen to reduce the nozzle efficiency (because the droplets are larger). The effect of loading ratio was seen in Fig. II.2, wherein the shape of the curve results in a shallow minimum (instead of a maximum of any kind). Hence, loading ratio would probably be a secondary factor from the viewpoint of nozzle efficiency when selecting overall

system design conditions, unless a loading ratio lower than about five was being contemplated (which is the approximate value where the efficiency begins to change quickly). Thus, the nozzle performance trends that are caused by the effects of pressure, temperature, and loading ratio can be inspected and used to assist in the selection of the value of these parameters for the overall system conditions. The nozzle performance, however, is only one factor in the overall design-point selection, because all the components in the system must be considered collectively to select the overall system performance.

II.3.2 Liquid/Gas Combinations

Suitable liquid/gas combinations were examined in terms of three criteria: maximum allowable operating temperatures of the liquid, degradation characteristics of the liquid, and desirable thermophysical properties. The first two of these three criteria themselves rule out many possible combinations, but other important criteria could include cost, availability, and toxicity, depending upon the application. High-temperature organic heat transfer fluids with a low vapor pressure were surveyed as candidate liquids by examining reports in the literature and manufacturers' data brochures (which sometimes compare their own fluids with those of their competitors). One problem with some of the fluids is that the thermophysical properties have been measured only at temperatures near room temperature.

The maximum allowable operating temperature is an important consideration and may represent a limitation on the selection of design conditions. Table II.8 summarizes this maximum temperature for a number of organic heat transfer fluids of possible interest. The degradation data in this table were assembled from research published by Dow Chemical (Refs. 10 and 11) and show their Dowtherm A (DTA) to have relatively low degradation characteristics at 1060 R; for DTA, their extrapolated measurements indicate a degradation rate of 0.0035 weight percent per week at 1060 R, or approximately 0.2 weight percent of the DTA will degrade in one year. This degradation is essentially a thermally-induced breakdown, in a clean closed system, of the petroleum oils into primarily volatile materials. Furthermore, these degradation tests were conducted in a clean system, with no oxygen or water present. In a telephone conversation with Monsanto (Ref. 12), their representative indicated that Therminol 66 becomes highly oxidized in the presence of air or water at temperatures higher than about 610 R, and they would not recommend the use of Therminol 66 in a two-phase system with steam as the gas phase. This breakdown problem exacerbated by the presence of water could conceivably exist for the other heat transfer oils, because "contamination" by impurities is known to promote degradation.

Nevertheless, based on the information in Table II.8, DTA has a high maximum operating temperature and relatively favorable degradation characteristics, pending experimental evidence for mixtures of DTA and steam at temperatures of interest.

Sufficiently complete sets of thermophysical data were available only for DTA and Dowtherm G (DTG), as surface tension data (needed for estimation of droplet size) is frequently unavailable, except sometimes for a value at room temperature. And the use of Therminol 66 was definitely ruled out on the basis of discussion with the manufacturer's representative.

Figure II.24 compares the nozzle performance characteristics for DTA and DTG. Basically, the main differences in the thermophysical properties at 1060 R are that, for DTG, the density is about ten percent higher, the specific heat is about seven percent lower, and the extrapolated surface tension is about 42 percent higher than the corresponding properties of DTA. For loading ratios in the range of 5 to 40, the use of DTG instead of DTA would lead to a one percentage point drop in nozzle efficiency. The exit temperatures are slightly lower because of the lower liquid specific heat, while the exit liquid velocities are about one percent lower and the exit gas velocities are about one percent higher primarily because of the higher surface tension of DTG. From the viewpoint of nozzle efficiency, DTA is therefore better than DTG as the liquid-phase fluid.

In the absence of actual thermophysical data for other liquids, the parametric effects of the thermophysical properties on nozzle performance can be examined for clues to be used in searching for liquid/gas combinations with favorable property characteristics. Of course, the effects of these properties on nozzle performance may be quite different from their effects on overall system performance, and the selected liquid/gas combination must obviously have favorable overall system performance characteristics rather than just favorable nozzle performance characteristics. As seen earlier, Fig. II.13 shows the effect of liquid surface tension on nozzle performance predictions. With the other liquid properties being those of DTA, a reduction in surface tension results in an increase in nozzle efficiency. Similarly, a decrease in liquid density as seen earlier in Fig. II.14, or a decrease in liquid specific heat as seen earlier in Fig. II.12, will tend to increase the nozzle efficiency. As for the effect of the gas-phase properties, an increase in gas density as seen earlier in Fig. II.11 will also tend to increase the nozzle efficiency, but an increase in gas specific heat as seen in Table II.6 will result in only a slight increase in nozzle efficiency. Thus, the trends in nozzle efficiency caused by the thermophysical properties of the liquid and of the gas can be used as preliminary guidance in examining candidate liquids and gases.

II.3.3 Maximum Nozzle Efficiencies

The effects of all the governing flow parameters on nozzle efficiency have been investigated and the results presented above in Section II.2. Figure II.6 is a particularly relevant figure to examine for the level of maximum nozzle efficiencies that can be expected, because those operating conditions are possibly typical of those expected for a two-phase propulsion system with a two-phase turbine. In this figure, the nozzle inlet temperatures are 960 R, and the inlet pressure is

600 psia. A loading ratio in the range of 20 to 40 is quite reasonable. Then, for a nozzle exit pressure of 15 psia, the pressure ratio is 40, and the efficiency of a six-inch-long nozzle with a steam/DTA mixture at a loading ratio of 40 is therefore 74 percent. For a steam/DTG mixture with these operating conditions, the design efficiency would be about one percentage point lower, based on the relative results of Fig. II.24; a nozzle efficiency of 73 percent is therefore predicted with DTG as the liquid phase.

II.3.4 Simplified Procedure for Nozzle Sizing

Although the computerized model developed during Phase I (Ref. 1) is relatively straightforward to use because it is oriented toward engineering results, the code still requires a computer to obtain the results. As such, the process to obtain results is still more complicated than a procedure for the quick estimation, by hand, of first-cut sizing numbers for the nozzle, such as the diameters at the inlet, throat, and exit. Hence, a simplified sizing procedure was developed to obtain quickly the approximate values of these diameters. This procedure is based on the isothermal theory developed by Rudinger (Ref. 13) because this is the most complex theory that can still be solved with just a few hand calculations.

Estimation of Nozzle Geometry

Five geometric parameters can be used to approximate the nozzle shape. These parameters are: nozzle length and throat location, and the nozzle diameters (or flow areas if the nozzle is not axisymmetric) at the inlet, throat, and exit locations. Based on the parametric analysis of Section II.2, in order to maximize nozzle efficiency, the nozzle length should be as long as possible within the geometric constraints of the proposed application. Then the nozzle throat is placed at the half-way point of the nozzle length, with the throat pressure assigned a value half-way between the inlet and exit pressures. The selection of the throat location is also based on the parametric analysis of Section II.2, where the flow area in the vicinity of the throat was seen to have a shallow shape as a function of nozzle length and where the location of the throat generally occurred near the mid-point of the nozzle. Hence, for the purpose of the first-cut sizing calculations, these assumptions pin down two of the geometric parameters of the nozzle design: the nozzle throat location and the nozzle length.

Estimation of Inlet Diameter

The inlet diameter (or flow area) is estimated using the continuity equation and assuming that the total flow area is the sum of the flow areas required for each of the two phases:

$$A_{in} = \left(A_g + A_\ell\right)_{in} = \left(\frac{\dot{m}_g}{\rho_g V_g} + \frac{\dot{m}_\ell}{\rho_\ell V_\ell}\right)_{in} = \left(\frac{\dot{m}_g}{\rho_g V_g}\left[1 + \frac{\dot{m}_\ell}{\dot{m}_g}\frac{\rho_g}{\rho_\ell}\frac{V_g}{V_\ell}\right]\right)_{in} \quad \text{(II.11)}$$

The quantities needed to estimate the nozzle inlet flow area are all known from the assumed inlet conditions, and the perfect gas law is used to calculate the gas density. For the propulsion application, the velocity ratio (V_ℓ/V_g) is generally in the range of 0.6 to 0.8, so a value of 0.7 is generally a good choice to be used for the first-cut sizing calculations. Hence, the nozzle inlet diameter (d_{in}) can be estimated from the inlet flow area:

$$d_{in} = \sqrt{4\ A_{in}/\pi} \tag{II.12}$$

Estimation of Throat Diameter

The nozzle throat diameter is estimated by using the continuity equation in conjunction with the velocity equation which results from the momentum balance in the isothermal theory developed by Rudinger (Ref. 13). The gas velocity at the nozzle throat is estimated with the expression:

$$V_{g,thr} = \sqrt{V_{g,in}^2 + \frac{2R\ T_{g,in}}{1 + rK}\left[\ell n\left(\frac{P_{in}}{P_{thr}}\right) + \left(\frac{\epsilon_{in}}{1-\epsilon_{in}}\right)\left(1 - \frac{P_{thr}}{P_{in}}\right)\right]} \tag{II.13}$$

where r is the loading ratio, K is the velocity ratio (V_ℓ/V_g), P_{thr} is the pressure at the throat and is assumed to be half way between the inlet and exit pressures, R is the gas constant, and ϵ_{in} is the inlet value of the liquid volume fraction:

$$\epsilon_{in} = \frac{1}{1 + \frac{K\rho_\ell}{r\ \rho_{g,in}}} \tag{II.14}$$

The velocity ratio is assumed constant at the inlet value, because this assumption was made by Rudinger in order to obtain a closed-form analytical solution. The throat liquid velocity is calculated from the velocity ratio: $V_{\ell,thr} = K\ V_{g,thr}$. Then by continuity, the throat diameter (d_{thr}) is estimated with the expression:

$$d_{thr} = d_{in}\sqrt{\frac{V_{g,in}}{V_{g,thr}}\ \frac{P_{in}}{P_{thr}}\left(\frac{1-\epsilon_{in}}{1-\epsilon_{thr}}\right)} \tag{II.15}$$

where the liquid volume fraction at the throat is estimated with:

$$\varepsilon_{thr} = \frac{1}{1 + \frac{K\rho_\ell}{r\rho_{g,thr}}} \qquad \text{(II.16)}$$

The gas density at the throat, $\rho_{g,thr}$ is calculated from the perfect gas law with the assumed throat pressure and from the inlet value of the gas temperature because the flow is assumed to be isothermal.

Estimation of Exit Diameter

A similar approach is used to estimate the nozzle exit diameter. The gas velocity at the nozzle exit is estimated with the momentum-derived expression:

$$V_{g,exit} = \sqrt{V_{g,in}^2 + \frac{2RT_{g,in}}{1 + rK}\left[\ell n \frac{P_{in}}{P_{exit}} + \left(\frac{\varepsilon_{in}}{1-\varepsilon_{in}}\right)\left(1 - \frac{P_{exit}}{P_{in}}\right)\right]} \qquad \text{(II.17)}$$

Then the nozzle exit diameter is estimated with the continuity expression:

$$d_{exit} = d_{in}\sqrt{\frac{V_{g,in}}{V_{g,exit}}\frac{P_{in}}{P_{exit}}\left(\frac{1-\varepsilon_{in}}{1-\varepsilon_{exit}}\right)} \qquad \text{(II.18)}$$

where the liquid volume fraction is estimated with:

$$\varepsilon_{exit} = \frac{1}{1 + \frac{K\rho_\ell}{r\rho_{g,exit}}} \qquad \text{(II.19)}$$

The gas temperature and both the loading ratio and the velocity ratio are constant throughout the nozzle, as per the original assumptions for the Isothermal Theory. Thus, the nozzle diameters at the three locations of especial interest (inlet, throat, and exit) can be estimated with Eqs. II.12, II.15, and II.18, respectively. Table II.9 summarizes the equations for the Simplified Nozzle Sizing Procedure.

Comparison of Calculations

Calculations were made to obtain an indication of the differences that might be expected between the diameters from the Simplified Nozzle Sizing Procedure and the diameters obtained from the computerized Model with Droplet Heat Transfer. Figure II.25 compares the results for nozzle geometry from the two models. At these operating conditions, the results for nozzle diameter from the simplified sizing procedure at a velocity ratio of either 0.7 or 0.8 are within eight percent of the more exact results from the computerized model. The results for nozzle efficiency, obtained by inserting the velocity results into the definition of nozzle efficiency (Eq. II.9), also show reasonable agreement, except at the lower end of the loading ratio where the assumption of isothermal conditions throughout the nozzle is least defendable. The drop in gas temperature increases as the loading ratio is reduced (as seen earlier in Fig. II.2) in the actual situation, whereas increased amounts of heat addition would be required if the isothermal assumption were to be maintained in the Isothermal Model. Furthermore, as seen in Fig. II.26, the exit velocities of the liquid that are calculated with the Simplified Sizing Procedure are lower than those calculated with the computerized Model with Droplet Heat Transfer, and the liquid phase carries the bulk of the kinetic energy for loading ratios greater than about three (as seen earlier in Fig. II.17). Thus, a lower calculated liquid exit velocity explains the lower calculated values of nozzle efficiency from the Simplified Nozzle Sizing Procedure. Further, because the exit value of the velocity ratio is actually closer to 0.8 for the operating conditions of Fig. II.26, the nozzle efficiencies in Fig. II.25 that were calculated from the Simplified Sizing Procedure at a velocity ratio of 0.8 are much closer to the more exact results for nozzle efficiencies from the Model with Droplet Heat Transfer.

Figure II.27 compares the results for nozzle efficiency and diameters from the two models at a different set of operating conditions. Here, at a velocity ratio of 0.7, the results from the Simplified Sizing Procedure for the throat diameter are about four percent lower than the results from the Droplet Heat Transfer Model, and the nozzle efficiency results agree within two percent except for loading ratios lower than about five, while the results for the exit diameter are about 18 percent higher than those from the Droplet Heat Transfer Model. Thus, the comparison of results in Figs. II.25 and II.27 are an indication of the differences that can be expected between the quick first-cut calculations of the Simplified Nozzle Sizing Procedure and the more exact results of the Model with Droplet Heat Transfer.

II.4 Assessment of Work Extraction Potential

In this section, performance criteria of two-phase nozzles applicable to work extraction systems are identified, and the attributes of a nozzle suitable for inclusion in a system that converts kinetic energy into work are assessed in terms of the off-design performance characteristics of a two-phase nozzle. These off-design characteristics are also of interest because in real applications, the nozzle will most certainly operate at conditions other than the design-point conditions for which it was designed.

II.4.1 Performance Criteria for Work Extraction

One of the two-phase nozzle performance criteria applicable to work extraction systems is the nozzle efficiency, which is defined as the increase in kinetic energy of the two-phase mixture relative to the ideal change in enthalpy if the two-phase mixture were to be expanded isentropically as a homogeneous mixture to the same exit pressure. The kinetic energy of the two-phase mixture at the nozzle exit is in turn converted into work, as seen in the schematic flow diagram of Fig. II.28. Thus, the maximum nozzle efficiency corresponds to the maximum level of conversion to kinetic energy that is possible by the nozzle at the assumed operating conditions. At the nozzle inlet, the heated liquid (DTA, for example) is mixed with the condensate stream (water, for example) to produce the gas phase by flashing the condensate stream if the enthalpy of the heated liquid is sufficiently high. Then the mixture is expanded and the enthalpy of the mixture is converted into kinetic energy for subsequent conversion to shaft power in the two-phase turbine. As seen in Fig. II.17, most of the kinetic energy is carried by the liquid stream over the range of loading ratios which are of interest for propulsion applications. Hence in order to extract most of the mixture's energy, the liquid-phase kinetic energy must obviously be extracted.

A second nozzle performance criterion applicable to work extraction systems is the mixture velocity at the nozzle exit. For the shaft speed of the two-phase turbine to be advantageously lower than that of an all-gas turbine, the nozzle exit velocity must be reasonably low. Otherwise, the low-speed advantage of a two-phase turbine will not be gained, and a large gearbox would still be required to reduce the turbine shaft speed down to the thrustor shaft speed. As presented in Section II.2, high nozzle exit velocities occur when the loading ratio or the nozzle exit pressure is very low. Hence, very low levels of loading ratio or nozzle exit pressure should be avoided if the advantage of low turbine shaft speed is to be realized in the work extraction system.

The most significant factors for the work extraction system are the overall system efficiency and design, not just the nozzle efficiency which itself might be favorably enhanced by factor(s) that could ultimately result in a lower system efficiency, or a less attractive system design. As discussed above, the two-phase nozzle is only one of several components in a work extraction system. For example, a lower nozzle pressure ratio (obtained by increasing the nozzle exit pressure) would result in a higher nozzle efficiency, but the effect of this lower nozzle pressure ratio on the overall system efficiency must also be examined. Generally, as the nozzle exit pressure increases, the mixture velocity at the nozzle exit will decrease, the turbine speed will be lower and lower cycle efficiency may result (Ref. 14). Hence, the favorable reduction in gearbox size that is derived from the lower nozzle exit velocity must be balanced against any potential reduction in cycle efficiency of the work extraction system, and this trade-off optimization may depend in part on the particular application.

II.4.2 Nozzle Attributes for Energy Conversion Systems

In order to assess the attributes of a nozzle suitable for inclusion in a work extraction system, a simplified calculation procedure was developed to estimate the off-design performance characteristics of two-phase nozzles. The off-design performance characteristics are important in assessing the attractiveness of the two-phase nozzle over the entire range of expected operating conditions because the overall system will undoubtedly have to operate at conditions quite different from the design-point conditions. As in the development of the Simplified Nozzle Design Procedure, the isothermal theory of Rudinger (Ref. 13) was again adapted for the off-design calculations because this is the most complex theory that is still tractable in terms of doing calculations reasonably quickly by hand.

Continuity equations and the momentum equation are used to estimate the off-design nozzle performance.

Continuity Requirements

At a given set of operating conditions, the continuity equation for the gas flow can be written for flow conditions anywhere in the nozzle:

$$\dot{m}_g = \left(1-\varepsilon_{in}\right) \rho_{g,in} V_{g,in} A_{in} = \left(1-\varepsilon\right) \rho_g V_g A \qquad \text{(II.20)}$$

where ε is the local liquid volume fraction and is calculated with the expression:

$$\varepsilon = \frac{1}{1 + \frac{K\rho_g}{r\rho_\ell}} \qquad \text{(II.21)}$$

Again K is the velocity ratio (V_ℓ/V_g) and is assumed to be constant throughout the nozzle at a given set of operating conditions (as per the original assumption that Rudinger made in order to obtain the version of the momentum equation that will be used later). Hence from Eq. II.20, the gas velocity at any location in the nozzle, relative to the inlet gas velocity, is then known as:

$$\frac{V_g}{V_{g,in}} = \frac{\rho_{g,in}}{\rho_g}\,\frac{A_{in}}{A}\left(\frac{1-\varepsilon_{in}}{1-\varepsilon}\right) = \frac{P_{in}}{P}\,\frac{A_{in}}{A}\left(\frac{1-\varepsilon_{in}}{1-\varepsilon}\right) \qquad \text{(II.22)}$$

where the perfect gas law is used to convert density into pressure, for the assumption of isothermal conditions in the nozzle at one set of operating conditions.

A second group of continuity equations is used to describe the gas flow rates at different possible operating conditions at the nozzle inlet, where the superscript (*) denotes the design-point (or reference) operating conditions:

$$\dot{m}_g = \left(1-\varepsilon_{in}\right)\rho_{g,in}\,V_{g,in}\,A_{in} \qquad \text{(II.23)}$$

$$\dot{m}^*_g = \left(1-\varepsilon^*_{in}\right)\rho^*_{g,in}\,V^*_{g,in}\,A_{in} \qquad \text{(II.24)}$$

These equations can be combined to obtain the inlet gas velocity at any operating conditions, relative to the inlet gas velocity at the design-point conditions:

$$V_{g,in} = V^*_{g,in}\,\frac{\dot{m}_g}{\dot{m}^*_g}\,\frac{\rho^*_{g,in}}{\rho_{g,in}}\left(\frac{1-\varepsilon^*_{in}}{1-\varepsilon_{in}}\right) \qquad \text{(II.25)}$$

If the assumption is made that the inlet conditions of temperature and pressure are the same at both design and off-design, then $\rho_{g,in} = \rho^*_{g,in}$, and Eq. II.25 simplifies to:

$$V_{g,in} = V^*_{g,in}\,\frac{\dot{m}_g}{\dot{m}^*_g}\left(\frac{1-\varepsilon^*_{in}}{1-\varepsilon_{in}}\right) \qquad \text{(II.25a)}$$

Further, if the special operating conditions of the same gas flow also obtain at both design and off-design conditions, then Eq. II.25a further reduces to:

$$V_{g,in} = V^*_{g,in} \left(\frac{1-\varepsilon^*_{in}}{1-\varepsilon_{in}} \right) \qquad \text{(II.25b)}$$

Equations II.25a and II.25b obviously represent special circumstances.

Now, to calculate the gas velocity throughout the nozzle at off-design, Eq. II.25 is combined with Eq. II.22 to obtain:

$$\frac{V_g}{V^*_{g,in}} = \frac{\rho^*_{g,in}}{\rho_g} \frac{A_{in}}{A} \frac{\dot{m}_g}{\dot{m}^*_g} \left(\frac{1-\varepsilon^*_{in}}{1-\varepsilon} \right) \qquad \text{(II.26)}$$

which is valid for all combinations of inlet conditions and for all variations in gas flow rates. However, if the assumption is made that the inlet conditions of temperature and pressure are the same for all operating conditions, then $\rho^*_{g,in} = \rho_{g,in}$. And by the perfect gas law, $\rho_{g,in}/\rho_g = P_{in}/P = PR$, where PR is the nozzle pressure ratio at that location in the nozzle where the flow area is A. Then, using Eq. II.21 for the definition of ε, Eq. II.26 can be rewritten as:

$$\frac{V_g}{V^*_{g,in}} = PR \frac{A_{in}}{A} \frac{\dot{m}_g}{\dot{m}^*_g} \left\{ \frac{1 + \dfrac{r\rho^*_{g,in}}{(PR)K\rho_\ell}}{1 + \dfrac{r^*\rho^*_{g,in}}{K^*\rho_\ell}} \right\} \qquad \text{(II.26a)}$$

which is valid for off-design operation at unchanged values of the inlet temperature and pressure, but at various gas flow rates and loading ratios. Equation II.26a expresses the off-design gas velocity (V_g), at the location where the nozzle flow area is A, in terms of the gas velocity ($V^*_{g,in}$) at the nozzle inlet at the design-point conditions. If the nozzle flow area (A) is selected to be the exit flow area, then the gas velocity (V_g) is the nozzle-exit gas velocity.

But still another expression is required in order to obtain the nozzle exit pressure. After all, when the nozzle was designed, the inlet conditions and the pressure ratio were selected. Now, at off-design, the inlet conditions are again selected, but the exit area is fixed, and the exit pressure (hence the pressure ratio) must then be calculated to be consistent with the requirements of the continuity and momentum equations. The continuity requirements have been developed above, and now the equation to satisfy the momentum requirements will be developed.

Momentum Requirements

The expression for gas velocity at the location in the nozzle where the pressure is P was obtained for the isothermal theory by Rudinger (Ref. 13), from momentum considerations. This expression is:

$$V_g^2 = V_{g,in}^2 + \frac{RT_{g,in}}{1+rK}\left[\ell n\left(\frac{P_{in}}{P}\right) + \left(\frac{\epsilon_{in}}{1-\epsilon_{in}}\right)\left(1 - \frac{P}{P_{in}}\right)\right] \qquad \text{(II.27)}$$

where R is the perfect gas constant. In addition to the isothermal assumption discussed above, the assumption of constant velocity ratio (K) throughout the nozzle at a given set of operating conditions was made by Rudinger to obtain Eq. II.27.

From the continuity relationship of Eq. II.22, for a given set of operating conditions, the gas velocity at any location is related to the inlet gas velocity, and Eq. II.22 can then be substituted into Eq. II.27 to obtain the result:

$$V_{g,in}^2 = \frac{\frac{2RT_{g,in}}{1+rK}\left[\ell n\left(\frac{P_{in}}{P}\right) + \left(\frac{\epsilon_{in}}{1-\epsilon_{in}}\right)\left(1 - \frac{P}{P_{in}}\right)\right]}{\left(\frac{P_{in}}{P}\frac{A_{in}}{A}\frac{1-\epsilon_{in}}{1-\epsilon}\right)^2 - 1} \qquad \text{(II.28)}$$

Calculation Procedure

Now that the continuity and momentum relations in their adapted form are available for the simplified off-design performance predictions, the calculation procedure can be discussed.

The off-design gas inlet velocity is calculated from Eq. II.25, which is an expression based solely on continuity. Here, the off-design conditions (of inlet gas velocity, inlet liquid volume fraction, velocity ratio, loading ratio, gas mass flow rate, etc.) relative to the design-point values are used. The off-design velocity ratio must be assumed, and one possible estimation method (that was used here) is to use the values from the design-point calculations with the Model with Droplet Heat Transfer at other values of the loading ratio (for example, the series of design-point values of V_ℓ/V_g in Fig. II.2 at the inlet conditions of temperature and pressure of interest).

Then, because Eq. II.28 cannot be solved explicitly for the exit pressure ratio (P_{in}/P), a trial-and-error solution is required to obtain the value of P_{in}/P that yields the value of $V_{g,in}$ that agrees with the value from Eq. II.25. (The pressure term (P) occurs in four places, including the ϵ term, in the right-hand side of Eq. II.28, and an explicit solution for P does not seem possible.) Then, knowing the values of the pressure ratio (P_{in}/P) and the inlet gas velocity ($V_{g,in}$) that satisfy Eqs. II.25 and II.28 at the off-design conditions, the exit gas velocity can be calculated with Eq. II.27.

With the off-design velocities at the nozzle inlet and exit now known, the conversion of enthalpy into kinetic energy by the nozzle can then be estimated. The change in kinetic energy of the two-phase mixture as it passes through the nozzle is given by the expression:

$$\Delta KE = \frac{1}{2}\dot{m}\left(\overline{V}^2 - \overline{V}_{in}^2\right) = \frac{1}{2}\left(\dot{m}_\ell+\dot{m}_g\right)\left[\left(\frac{V_g + rV_\ell}{1+r}\right)^2 - \left(\frac{V_{g,in} + rV_{\ell,in}}{1+r}\right)^2\right] \quad (II.29)$$

where $\dot{m}$ is the total mass flow rate ($\dot{m} = \dot{m}_\ell + \dot{m}_g$) and $\overline{V}$ is the mass-weighted velocity: $\overline{V} = (V_g + r\,V_\ell)/(1 + r)$. Recalling that the velocity ratio in the isothermal theory is assumed to be constant throughout the nozzle at a given operating point, then Eq. II.29 can be rewritten as:

$$\Delta KE = \frac{1}{2}\dot{m}_g\,\frac{(1+rK)^2}{1+r}\left(V_g^2 - V_{g,in}^2\right) \quad (II.29a)$$

Then the kinetic energy conversion at off-design relative to the design-point conversion is:

$$\frac{\Delta KE}{\Delta KE^*} = \frac{\dot{m}_g}{\dot{m}_g^*}\left(\frac{1+rK}{1+r^*K^*}\right)^2\left(\frac{1+r^*}{1+r}\right)\left(\frac{V_g^2 - V_{g,in}^2}{V_g^{*2} - V_{g,in}^{*2}}\right) \quad (II.30)$$

And if the gas flow rate is the same at both design and off-design, then the flow rate factor in Eq. II.30 is unity.

Calculated Results

Results calculated from the simplified procedure developed above were used to investigate the effect of off-design operation on the nozzle performance characteristics. For the purpose of examining off-design trends, the inlet conditions of temperature and pressure were kept constant at their design-point values. In actual operation, the nozzle inlet temperature and pressure could vary dramatically at the off-design operating conditions, depending on the operation of the other components in the work extraction system (Fig. II.28) at off-design, but these off-design inlet conditions were arbitrarily chosen because no actual schedule was available. Figure II.29 shows results for the off-design performance of the two-phase nozzle, assuming that the gas flow rate is kept constant at the design-point value while the liquid flow rate (and hence the loading ratio) is varied. Other schedules of gas flow rate could easily be chosen, but this schedule was chosen for this set of calculations. The velocity ratio selected was based on the design-point values over the range of loading ratio calculated previously with the Model with Droplet Heat Transfer. As the loading ratio is reduced in Fig. II.29, the inlet gas velocity is seen to decrease, as required by continuity considerations for the same inlet conditions (this is due to the

fact that less mass is going through the nozzle inlet), while the exit gas velocity increases and the nozzle pressure ratio increases (actually the exit pressure decreases, because the nozzle inlet pressure is held constant in these calculations). With a reduced loading ratio but at a fixed gas flow rate, the gas will expand more because less liquid mass is present to retard the gas expansion. Generally, as seen earlier in the design-point calculations (for example, Fig. II.2), as the loading ratio is reduced, the gas velocity increases because the gas expands more in the presence of less liquid. Further, to allow the increased gas expansion, the nozzle exit pressure will be lower (hence, the gas density will be lower, to satisfy continuity for the isothermal expansion). The relative kinetic energy conversion, calculated with Eq. II.30, shows an increase of less than five percent above the design-point value. Similar results are shown in Fig. II.30 for different inlet conditions, and with the same assumption of the same gas flow rate at design as at off-design conditions. Here, the expected range of the velocity ratio as a function of loading ratio was assumed to be wider (based on previous design point calculations from the Model with Droplet Heat Transfer, at the lower values of inlet temperature and pressure). This larger range may explain why the effect of loading ratio on the relative kinetic energy conversion is slightly larger while overall it is still a small effect in that it varied by less than eight percent over a range of loading ratio from double to half the design-point value.

Another possible mode of off-design operation is for the loading ratio to be kept constant over the entire range of operating conditions. In this mode, both the liquid flow rate and the gas flow rate are varied in tandem to maintain a constant value of the loading ratio. Figure II.31 shows the results calculated for such a mode, wherein the inlet conditions of temperature and pressure were again held constant at the design-point values, throughout the off-design operation. As the gas flow rate decreases (while still at constant loading ratio), the inlet gas velocity decreases because less total mass is flowing through the nozzle, while the exit gas velocity is increasing. The inlet gas velocity is lower because of continuity (Eq. II.25); while to satisfy the momentum equation in the form of Eq. II.28, the pressure ratio must be increased (by reducing the exit pressure in this instance because the inlet pressure is held constant) and an increased pressure ratio means a higher exit gas velocity, Eq. II.27. Simplified, in terms of the isothermal theory, a lower total mass flow through a nozzle that is designed for a higher mass flow, will be expanded further than the higher mass flow, for these levels of the loading ratio.

The relative kinetic energy conversion for the operating mode of constant loading ratio is also shown in Fig. II.31 and is seen to decrease as the loading ratio is decreased, because the lower mass flow rate more than makes up for the higher exit gas velocity. Actually the increase in gas exit velocity

is relatively small as compared to the increase seen in Fig. II.30 for the mode of operation where the loading ratio varies. This mode (with the constant gas flow rate over the off-design conditions) has a much flatter profile of kinetic energy conversion at off-design than for the mode where the gas flow rate is varied (and the loading ratio is held constant). This difference could possibly be useful when the off-design conditions for the work extraction system are defined because the liquid flow rates and the gas flow rates could conceivably be scheduled independently to obtain the flatter profile.

Thus, using the simplified calculation procedure described here, and within the limitations and assumptions of this procedure, the off-design performance of two-phase nozzles can be estimated. Consequently, the off-design flow rates might be tailored to vary the shape of the off-design profile of kinetic energy conversion by the nozzle, for appropriate integration of the nozzle into an energy conversion system. A valuable design-procedure outgrowth of these studies is that, because the exit gas velocity for the two-phase nozzle does decrease as the mass flow is increased, consideration should be given to selecting the design-point condition for the nozzle as a condition where the mass flow is relatively low in comparison to the overall schedule of mass flows, so that the nozzle exit velocity will be lower at the other expected (off-design) operating points where the mass flow rates would be higher. This selection would then tend to retain the advantage of low nozzle exit velocities throughout the entire expected range of nozzle operation.

REFERENCES

1. Deane, C. W. and S. C Kuo: Two-Phase Nozzle Theory and Parametric Analysis: Phase I - Two-Phase Nozzle Theory. UTRC Report R80-954624-2, 1980.

2. Wallis, G. B.: One-Dimensional Two-Phase Flow. McGraw-Hill, 1969.

3. Hanson, A. R., E. G. Domich, H. S. Adams: Shock Tube Investigation of the Breakup of Drops by Air Blasts. Physics of Fluids, Vol. 6, No. 8, pp. 1070-1080, 1963.

4. Alger, T. W.: Droplet Phase Characteristics in Liquid-Dominated Steam-Water Nozzle Flow. Report UCRL-52534, Lawrence Livermore Laboratory, 1978.

5. Elliott, D. G. and E. Weinberg: Acceleration of Liquids in Two-Phase Nozzles. JPL Report 32-987, 1968.

6. Perry, R. H., C. H. Chilton, and S. D. Kirkpatrick: Chemical Engineers' Handbook. Fourth Edition, McGraw-Hill, 1963.

7. McAdams, W. H.: Heat Transmission. Third Edition, McGraw-Hill, 1954.

8. Kreith, F.: Principles of Heat Transfer. Third Edition, Intext Educational Publishers, 1973.

9. Kays, W. M. and A. L. London: Compact Heat Exchangers, Second Edition, McGraw-Hill, 1964.

10. Seifert, W. F., L. L. Jackson, and C. E. Sech: Design and Operational Consideration for High Temperature Organic Heat Transfer Systems. Paper presented at the Process Heat Transfer Symposium of the 71st National AIChE Meeting, February 22-24, 1972.

11. Anon.: Selecting High Temperature Heat Transfer Fluids. Dow Chemical Company Information Brochure.

12. Pullman, J.: Monsanto Industrial Chemicals Company, New York City, telephone conversation on November 21, 1980.

13. Rudinger, G.: "Relaxation in Gas-Particle Flow", Chapter in Non-Equilibrium Flows - Part I, P. P. Wegener, ed., pp. 119-161. Marcel Dekker, Inc., 1969.

14. Elliott, D. G., and L. G. Hays: Two-Phase Turbine Engines. Paper No. 769038, Proceedings of the Eleventh IECEC, pp. 222-228, 1976.

TABLE II.1
SENSITIVITY OF NOZZLE PERFORMANCE PREDICTIONS TO DROPLET BREAKUP

SIX-INCH NOZZLE LENGTH
STEAM/DTA MIXTURE
INLET 1060 R AND 1000 psia
EXIT 100 psia

		VALUES AT EXIT						
r	$We)_{crit}$	V_g	V_ℓ	V_ℓ/V_g	T_g	T_ℓ	D	η
		ft/sec			R		ft	
1	6	2570	2226	0 866	806.6	924.1	2.23×10^{-5}	0 930
1	3	2554	2272	0.890	811.8	914.7	1.71×10^{-5}	0.942
1	1	2532	2331	0 921	818.3	902.8	1.16×10^{-5}	0 957
5	6	1661	1381	0.831	942.6	1004.6	3.19×10^{-5}	0.883
5	3	1633	1406	0 861	948.3	1001.7	2.46×10^{-5}	0.903
5	1	1598	1438	0.890	954.9	998.0	1.68×10^{-5}	0 930
10	6	1310	1064	0 812	985.7	1028.2	4.03×10^{-5}	0 873
10	3	1281	1082	0 845	990.3	1026 7	3.11×10^{-5}	0 895
10	1	1244	1104	0 888	995.6	1024.7	2.12×10^{-5}	0 923
40	6	837 1	653 4	0.781	1031.3	1051 0	7.04×10^{-5}	0.890
40	3	809 5	661 0	0 817	1034 0	1050 7	5.42×10^{-5}	0 908
40	1	775 2	671 0	0 866	1037 1	1050 2	3.68×10^{-5}	0 933

TABLE II.2
SENSITIVITY OF NOZZLE PERFORMANCE PREDICTIONS TO DROPLET DRAG

SIX INCH NOZZLE LENGTH
STEAM/DTA MIXTURE
INLET 1060 R AND 1000 psia
EXIT 100 psia

		VALUES AT EXIT						
r	C_D	V_g	V_ℓ	V_ℓ/V_g	T_g	T_ℓ	D	η
	%	ft/sec			R		ft	
1	80	2579	2216	0.859	812.1	918.4	2.05×10^{-5}	0.930
1	100	2570	2226	0.866	806.7	924.1	2.24×10^{-5}	0.930
1	120	2562	2233	0.872	802.0	929.1	2.40×10^{-5}	0.930
5	80	1671	1376	0.823	949.1	1003.5	2.91×10^{-5}	0.880
5	100	1661	1381	0.831	942.6	1004.6	3.19×10^{-5}	0.883
5	120	1653	1384	0.837	936.8	1005.6	3.44×10^{-5}	0.885
10	80	1320	1060	0.804	990.0	1027.8	3.67×10^{-5}	0.869
10	100	1310	1064	0.812	985.7	1028.2	4.03×10^{-5}	0.873
10	120	1303	1066	0.819	980.8	1028.5	4.35×10^{-5}	0.876
40	80	844.7	651.7	0.772	1034.2	1051.0	6.41×10^{-5}	0.886
40	100	837.1	653.4	0.781	1031.3	1051.0	7.05×10^{-5}	0.890
40	120	831.2	654.7	0.788	1028.6	1051.0	7.62×10^{-5}	0.893

TABLE II.3
SENSITIVITY OF NOZZLE PERFORMANCE PREDICTIONS TO HEAT TRANSFER

SIX-INCH NOZZLE LENGTH
STEAM/DTA MIXTURE
INLET 1060 R AND 1000 psia
EXIT 100 psia

		VALUES AT EXIT					
r	HTC	V_g	V_ℓ	V_ℓ/V_g	T_g	T_ℓ	η
	%	ft/sec			R		
1	80	2564	2224	0.867	799.4	932.7	0.927
1	100	2570	2226	0.866	806.6	924.1	0.930
1	120	2575	2227	0.865	812.1	917.5	0.933
5	80	1657	1378	0.832	933.6	1006.7	0.880
5	100	1661	1381	0.831	942.6	1004.6	0.883
5	120	1664	1382	0.830	949.2	1003.0	0.886
10	80	1308	1063	0.813	978.1	1029.0	0.871
10	100	1310	1064	0.812	985.7	1023.2	0.873
10	120	1312	1065	0.811	991.0	1027.6	0.875
40	80	836.5	653.2	0.781	1027.0	1051.1	0.889
40	100	837.1	653.4	0.781	1031.3	1051.0	0.890
40	120	837.9	653.7	0.780	1034.3	1050.9	0.890

80-11-64-1

TABLE II.4

RELATIVE EFFECT OF GOVERNING PARAMETERS ON NOZZLE PERFORMANCE

O - NEGLIGIBLE
X - SMALL
✓ - SIGNIFICANT

PARAMETER	EFFECT ON EXIT VALUE					
	V_ℓ	V_g	V_ℓ / V_g	T_ℓ	T_g	η
LOADING RATIO	✓	✓	✓	✓	✓	✓
INLET PRESSURE	X	X	O	X	X	X
EXIT PRESSURE	X	✓	✓	X	✓	✓
PRESSURE RATIO	X	✓	✓	X	✓	✓
INLET TEMPERATURES	X	X	X	X	X	X
INLET TEMPERATURE DIFFERENTIAL	O	O	O	X	X	X
GAS SPECIFIC HEAT	O	O	O	O	X	O
GAS DENSITY	✓	✓	X	✓	✓	✓
LIQUID SPECIFIC HEAT	O	O	O	X	X	O
LIQUID DENSITY	X	X	O	O	O	X
LIQUID SURFACE TENSION	✓	X	✓	X	X	✓
INLET VELOCITY	X	X	O	O	O	X
DROPLET SIZE	✓	X	✓	X	X	✓
NOZZLE LENGTH	O	X	X	O	X	✓

TABLE II.5
EFFECT OF INLET TEMPERATURE ON NOZZLE PERFORMANCE PREDICTIONS

STEAM DTA
SIX-INCH NOZZLE
FLOW CONDITIONS P_{in} = 600 psi $P_{ex\,t}$ = 100 psi

	INLET VALUES		EXIT VALUES					
r	T_g	T_ℓ	V_g	V_ℓ	$T_\ell)_{in} - T_\ell$	$T_\ell - T_g$	D	η
	R		ft/sec		R		ft	
10	1160	1160	1164	961	26.3	32.0	4.43×10^{-5}	0.860
10	1060	1060	1129	912	24.5	32.3	5.16×10^{-5}	0.847
10	960	960	1088	866	23.2	31.9	5.84×10^{-5}	0.839
40	1160	1160	711	561	7.2	13.7	7.75×10^{-5}	0.862
40	1060	1060	701	540	6.8	14.3	9.17×10^{-5}	0.853
40	960	960	685	519	6.5	14.6	1.5×10^{-4}	0.850

TABLE II.6
EFFECT OF GAS SPECIFIC HEAT ON NOZZLE PERFORMANCE PREDICTIONS

GAS DTA
SIX-INCH NOZZLE
FLOW CONDITIONS $T_{g_{in}} = T_{\ell_{in}} = 1060$ R $P_{in} = 1000$ psia
$P_{exit} = 100$ psia

SPECIFIC HEAT $C_{pg}/C_{p_{steam}}$	LOADING RATIO r	THERMAL CAPACITY RATIO $(C/C_{pg})_{in}$ r	EXIT VALUES				
			V_g	V_ℓ	T_g	T_ℓ	η
			ft/sec		R		
2	40	17.8	857.6	653.7	1033.5	1051.6	0.8902
1	40	35.7	857.3	653.5	1031.3	1051.0	0.8898
0.5	40	71.4	[illegible]	653.4	1029.9	1050.7	0.8896
2	10	4.5	1313	1066	997.9	1033.0	0.875
1	10	8.9	1310	1064	985.7	1028.2	0.873
0.5	10	17.8	1308	1062	977.1	1025.0	0.871

TABLE II.7
EFFECT OF INLET VELOCITY ON NOZZLE PERFORMANCE PREDICTIONS

STEAM/DTA
SIX-INCH NOZZLE
FLOW CONDITIONS $T_\ell)_{in} = T_g)_{in} = 1060R$ $P_{in} = 1000$ psia.
$P_{exit} = 100$ psia

				EXIT VALUES					
	r	$V_g)_{in}$	$V_\ell)_{in}$	V_g	V_ℓ	V_ℓ/V_g	T_g	T_ℓ	η
		ft/sec		ft/sec			R		
a)	10	100	70	1310	1064	0.812	986	1028	0.873
	10	200	140	1320	1073	0.813	985	1028	0.876
	10	300	210	1334	1087	0.815	985	1028	0.880
	20	100	70	1035	822	0.794	1014	1043	0.874
	20	200	140	1046	833	0.796	1014	1043	0.878
	20	300	210	1064	850	0.799	1013	1043	0.883
	40	100	70	837	654	0.781	1031	1051	0.890
	40	200	140	850	666	0.784	1031	1051	0.894
	40	300	210	871	687	0.789	1030	1051	0.899
b)	20	100	70	1035	822	0.794	1014	1043	0.874
	20	100	80	1036	823	0.794	1014	1043	0.875
	20	100	90	1038	824	0.794	1014	1043	0.875
	20	300	210	1064	850	0.799	1013	1043	0.883
	20	300	240	1072	858	0.801	1013	1043	0.885
	20	300	270	1081	868	0.802	1012	1043	0.887

TABLE II.8
OPERATING TEMPERATURE LIMITATIONS AND DEGRADATION CHARACTERISTICS OF SELECTED FLUIDS

TRADE NAME	COMPOSITION	MAXIMUM OPERATING TEMPERATURE(R)	RELATIVE RATE OF DEGRADATION AT 1060R IN "PURE" SYSTEM
DOWTHERM A	DIPHENYL-DIPHENYL OXIDE EUTECTIC	1210	1
DOWTHERM G	DI- AND TRI-ARYL ETHERS	1110	3 4
THERMINOL 66	HYDROGENATED TERPHENYLS	1110	60
MOBILTHERM 603	ALKYL-AROMATIC PETROLEUM OIL	1060	780
HUMBLETHERM 500	ALIPHATIC PETROLEUM OIL	1060	780
DOW CORNING 710	PHENYLMETHYL POLYSILOXANE FLUID	960	NOT AVAILABLE
DOW CORNING SYLTHERM 444	SILICONE FLUID	860	NOT AVAILABLE

TABLE II.9
SIMPLIFIED NOZZLE SIZING PROCEDURE

1. NOZZLE LENGTH — AS LONG AS POSSIBLE WITHIN GEOMETRIC CONSTRAINTS

2. INLET DIAMETER

$$d_{in} = \sqrt{\frac{4}{\pi}\left(\frac{\dot{m}_g}{\rho_g V_g}\right)_{in}\left[1 + rK\frac{\rho_{g,in}}{\rho_l}\right]} \qquad \text{(Eg II .12)}$$

where $K \equiv V_g / V_l = \text{constant}$

3. THROAT LOCATION — AT 50% OF NOZZLE LENGTH
THROAT PRESSURE IS HALF WAY BETWEEN INLET AND EXIT PRESSURES

4. THROAT DIAMETER

$$\epsilon_m = \frac{1}{1 + \frac{K\rho_l}{r\rho_{g,in}}} \quad ; \quad \epsilon_{thr} = \frac{1}{1 + \frac{K\rho_l}{r\rho_{g,thr}}}$$

$$V_{g,thr} = \sqrt{V_{g,in}^2 + \frac{2RT_{g,in}}{1+rK}\left[\ell n\frac{P_{in}}{P_{thr}} + \left(\frac{\epsilon_{in}}{1-\epsilon_{in}}\right)\left(1 - \frac{P_{thr}}{P_{in}}\right)\right]} \qquad \text{(Eg II .13)}$$

$$d_{thr} = d_{in}\sqrt{\frac{V_{g,in}}{V_{g,thr}} \times \frac{P_{in}}{P_{thr}} \times \left(\frac{1-\epsilon_{in}}{1-\epsilon_{thr}}\right)} \qquad \text{(Eg II .15)}$$

5 EXIT DIAMETER

$$\epsilon_{exit} = \frac{1}{1 + \frac{K\rho}{r\rho_{g,exit}}}$$

$$V_{g,exit} = \sqrt{V_{g,in}^2 + \frac{2RT_{g,in}}{1+rK}\left[\ell n\frac{P_{in}}{P_{exit}} + \left(\frac{\epsilon_{in}}{1-\epsilon_{in}}\right)\left(1 - \frac{P_{exit}}{P_{in}}\right)\right]} \qquad \text{(Eg II .17)}$$

$$d_{exit} = d_{in}\sqrt{\frac{V_{g,in}}{V_{g,exit}} \times \frac{P_{in}}{P_{exit}} \times \left(\frac{1-\epsilon_{in}}{1-\epsilon_{exit}}\right)} \qquad \text{(Eg II .18)}$$

FIG II 1

COMPARISON OF TWO-PHASE NOZZLE WITH ONE-PHASE NOZZLE AT EQUAL EXIT KINETIC ENERGY

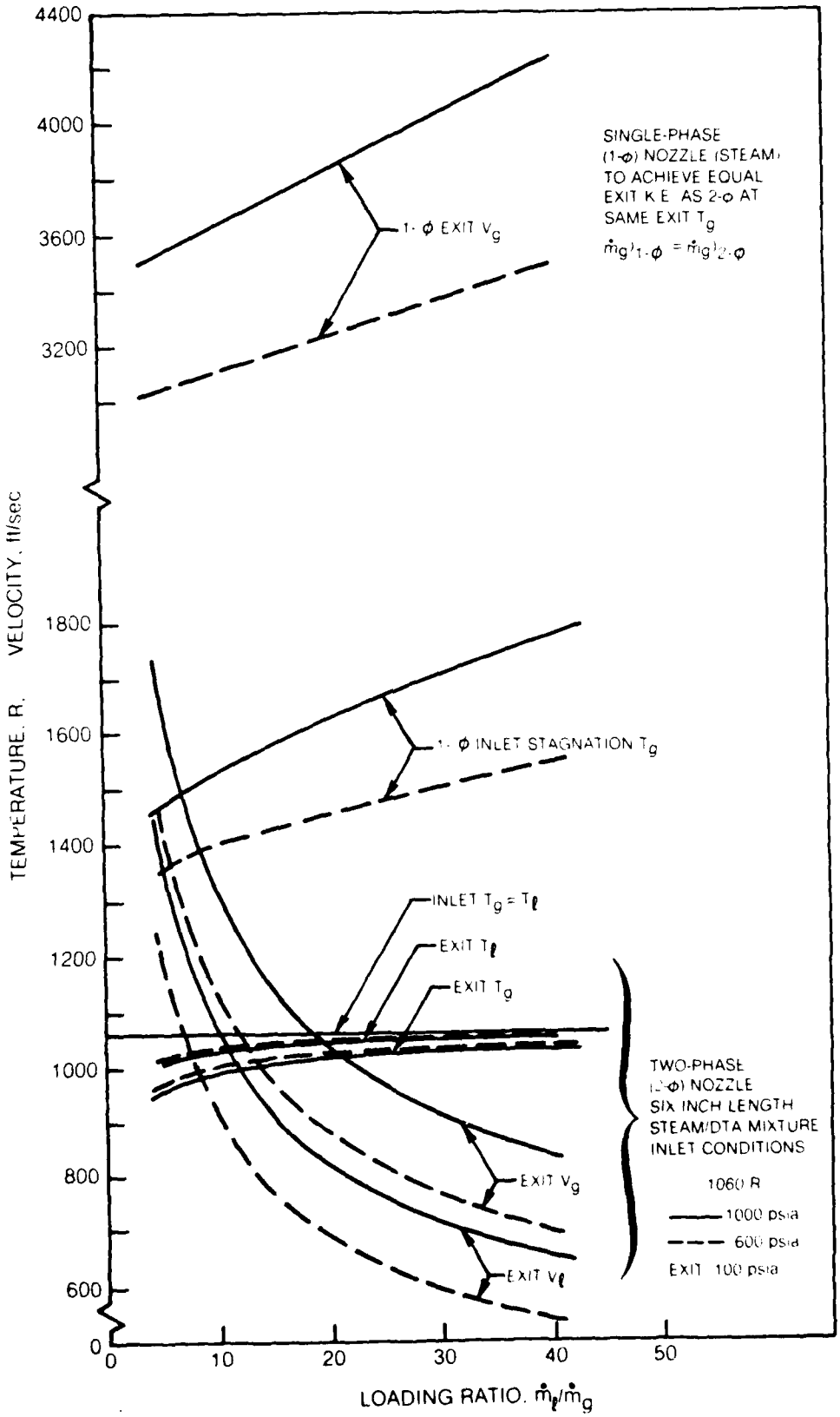

80-11-64-6

EFFECT OF LOADING RATIO ON TWO-PHASE NOZZLE PERFORMANCE PREDICTIONS

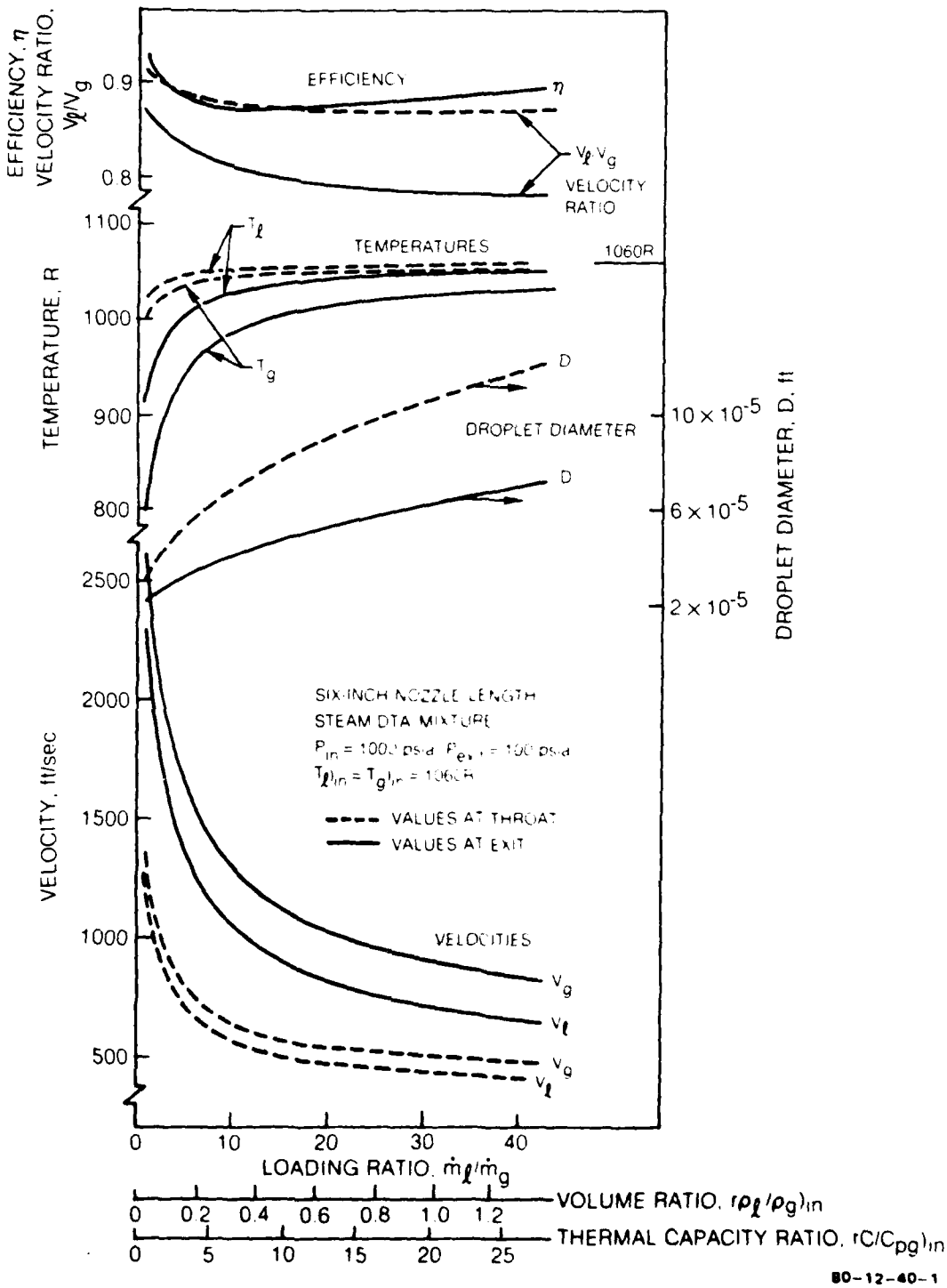

EXIT SPECIFIC POWER OF TWO-PHASE NOZZLE

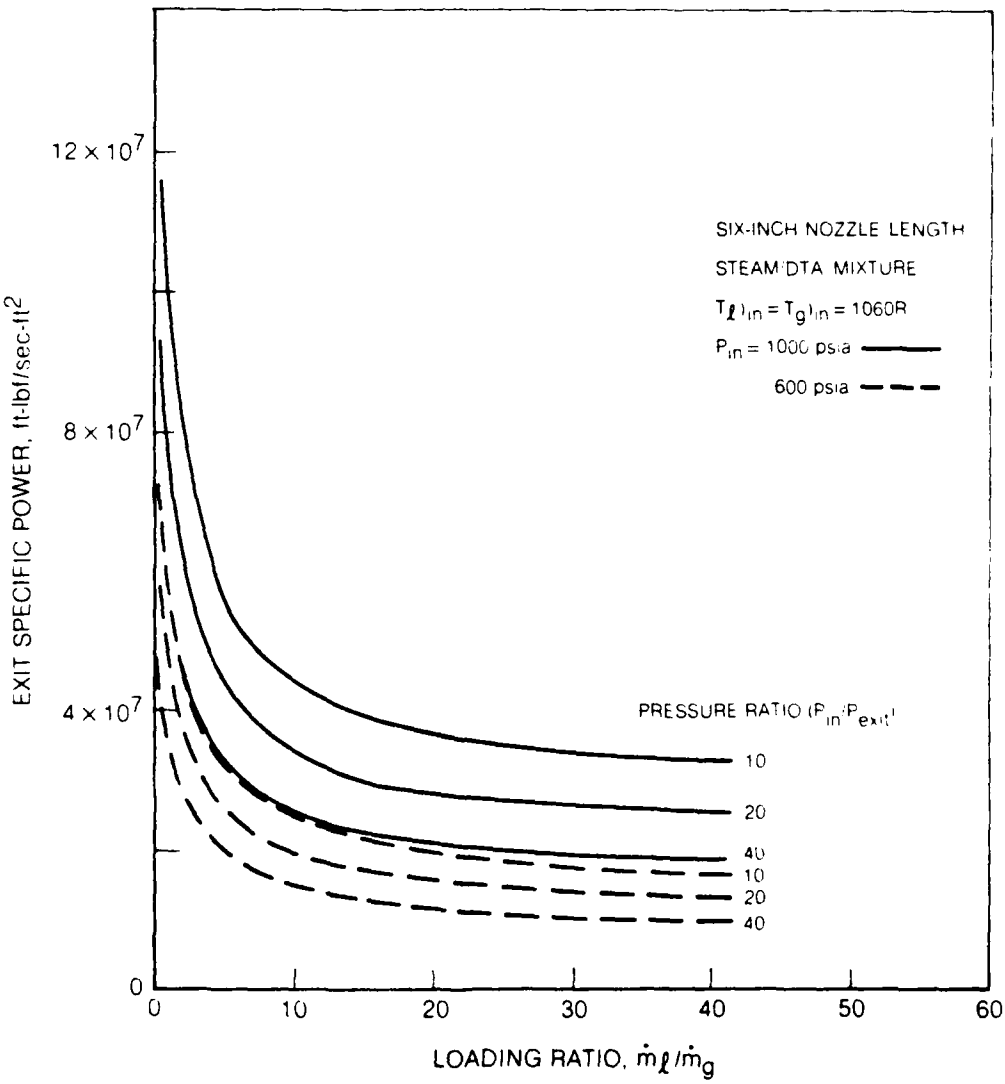

81-6-3-5

FIG II 4

EFFECT OF INLET PRESSURE ON NOZZLE PERFORMANCE PREDICTIONS

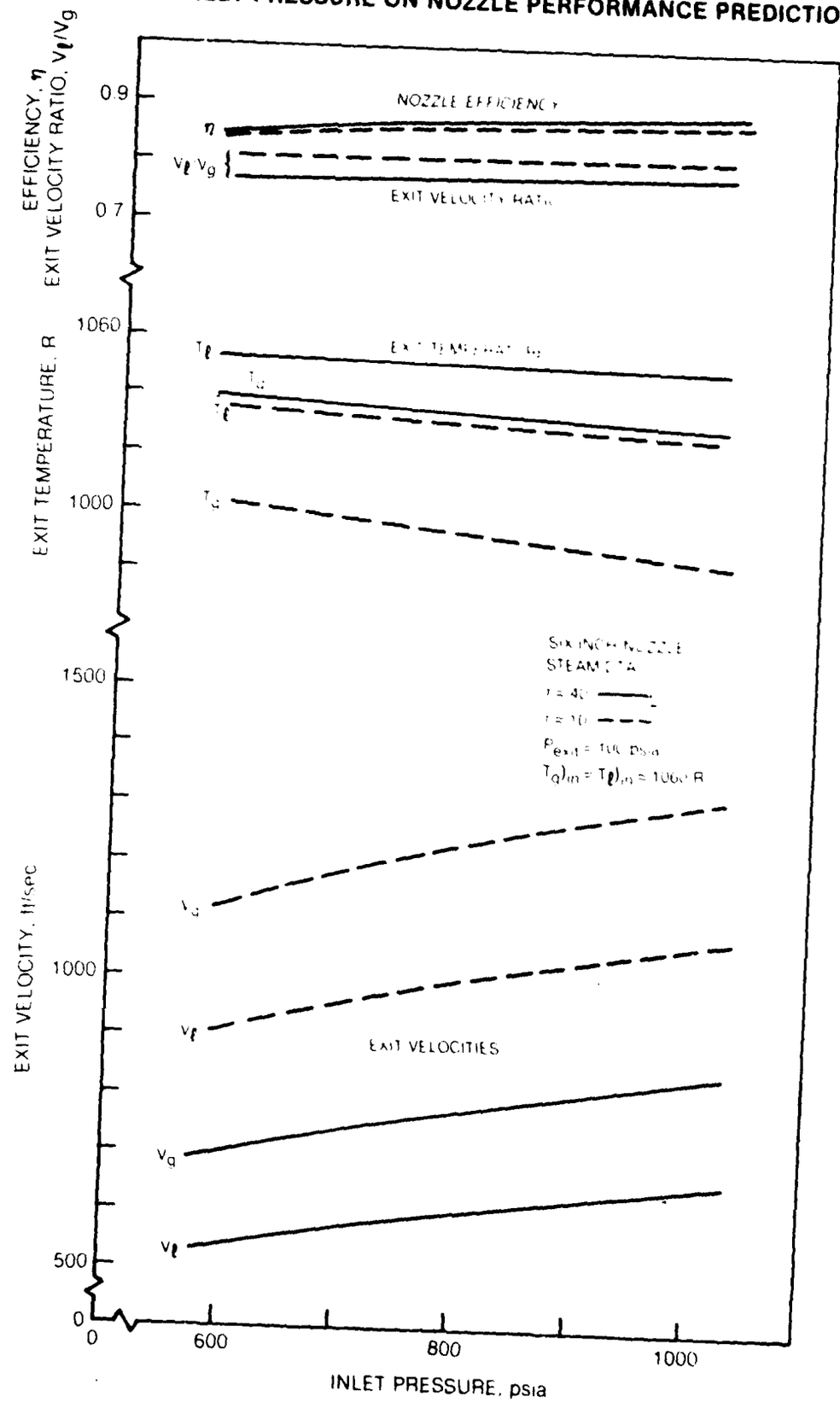

80-11-64-10

FIG II 5

EFFECT OF EXIT PRESSURE ON NOZZLE PERFORMANCE PREDICTIONS

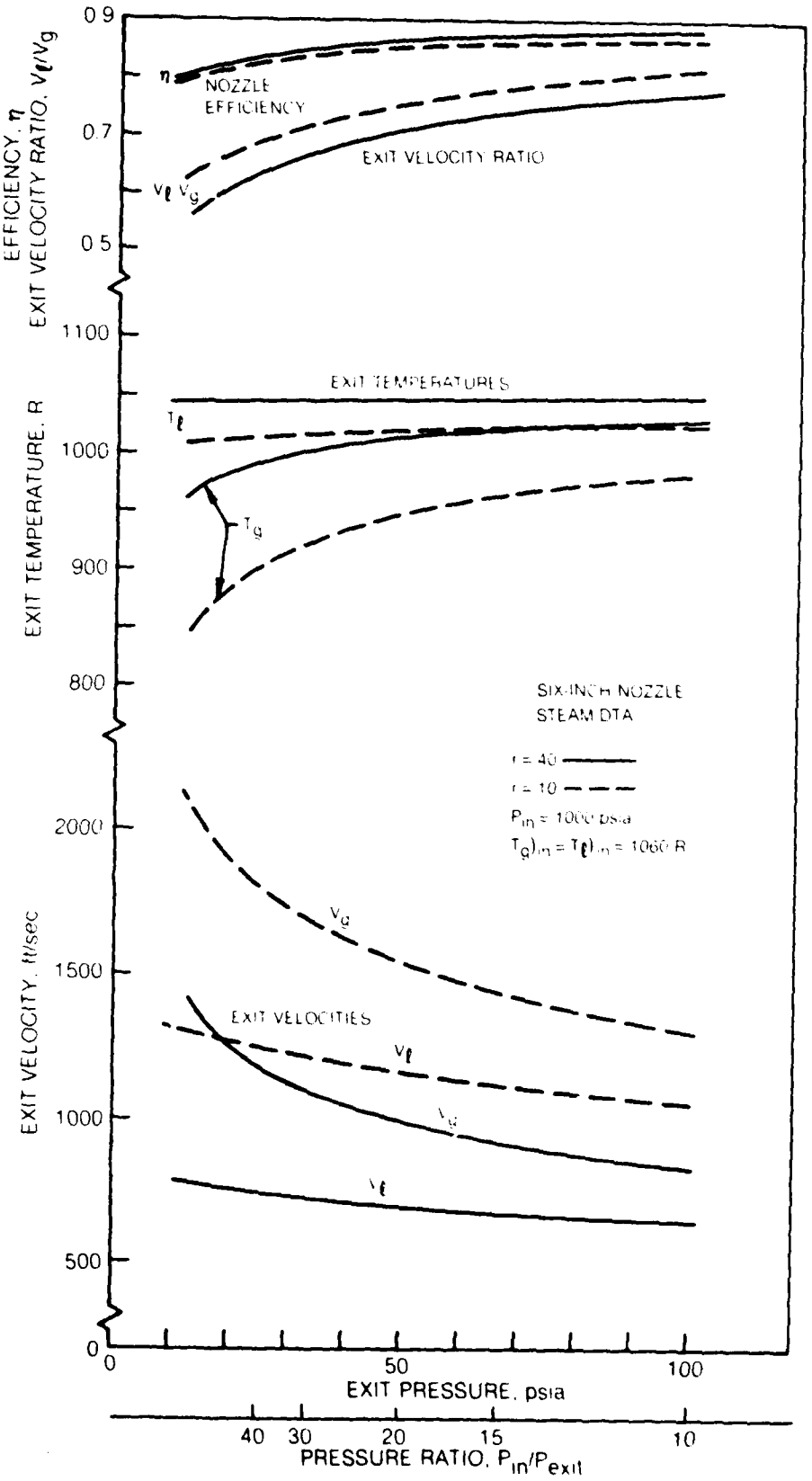

80-11-64-9

FIG II.6

EFFECT OF PRESSURE RATIO ON NOZZLE PERFORMANCE CHARACTERISTICS

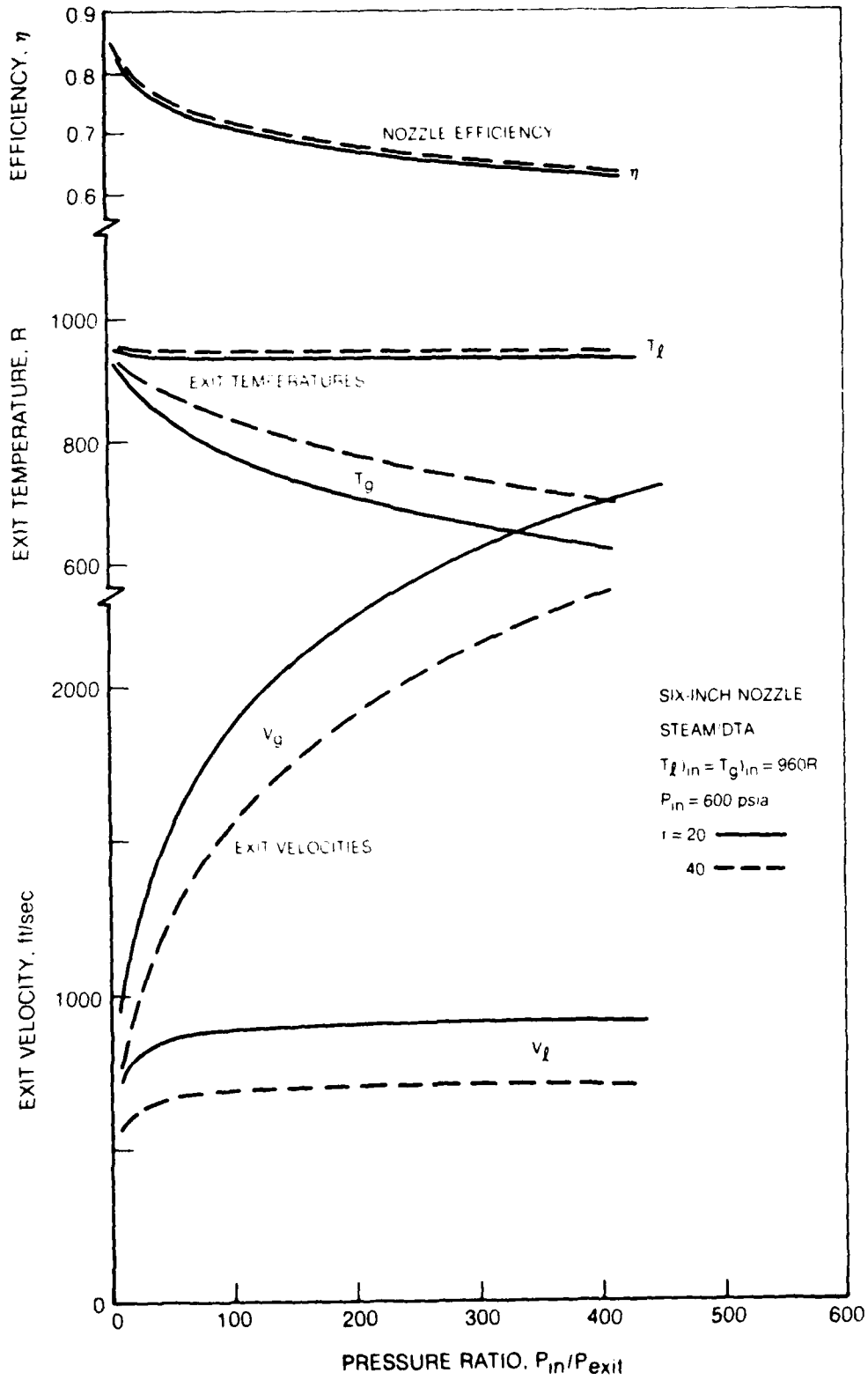

81-6-3-6

FIG II 7

TWO-PHASE NOZZLE DESIGN AT LOW EXIT PRESSURE

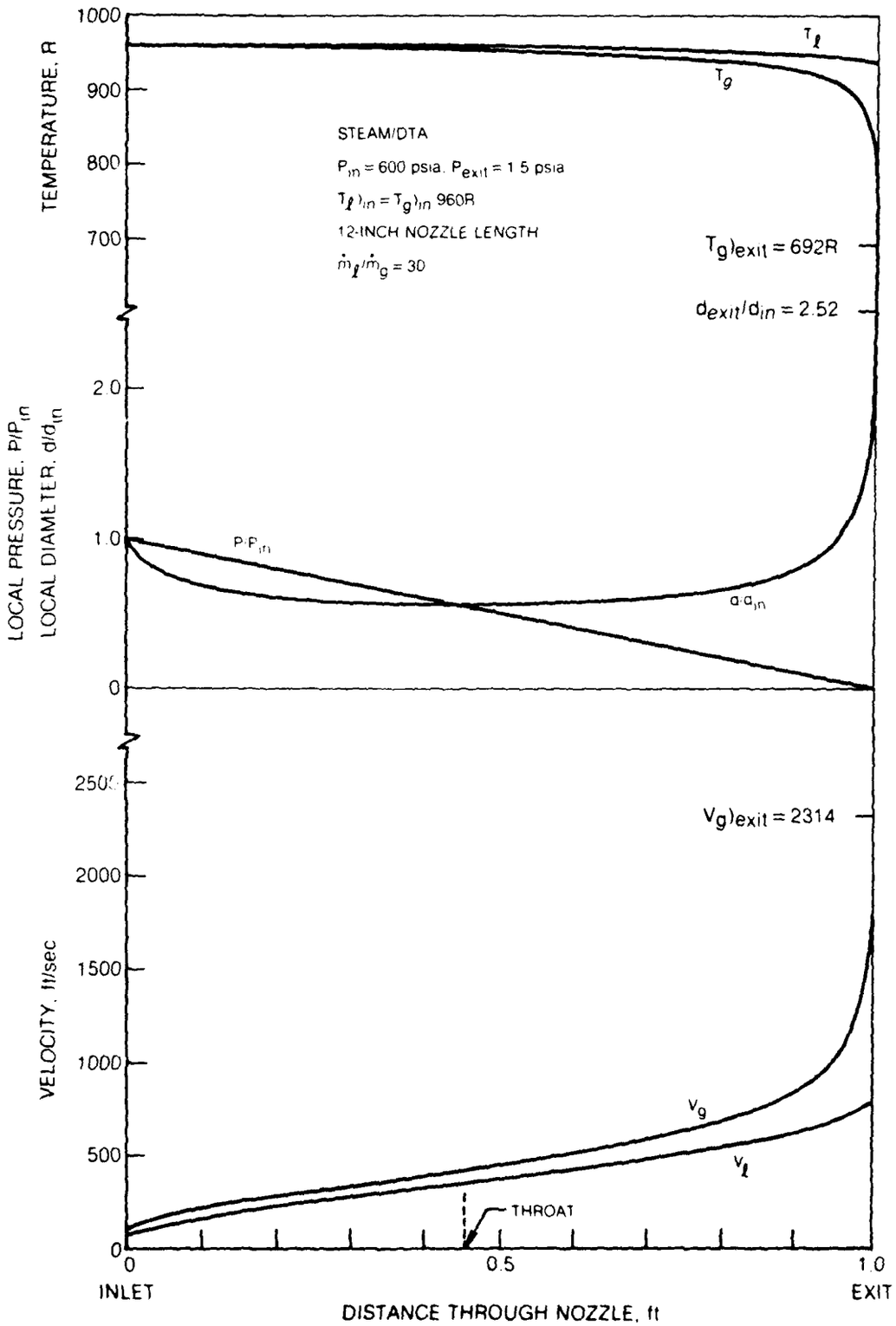

81-6-3-21

EFFECT OF EXIT PRESSURE ON NOZZLE SHAPE

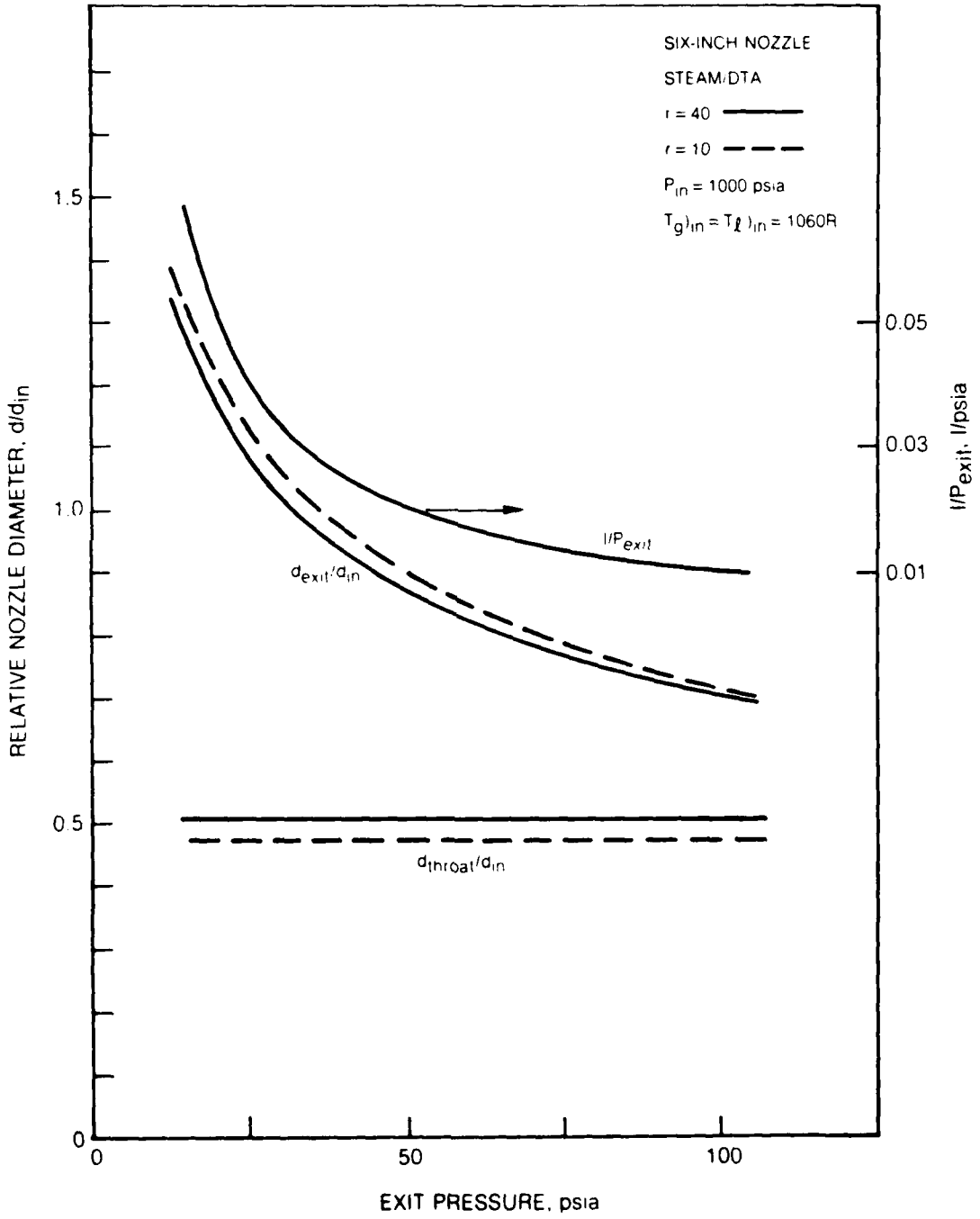

81-6-3-7

FIG II 9

EFFECT OF INLET TEMPERATURE DIFFERENCE ON NOZZLE PERFORMANCE PREDICTIONS

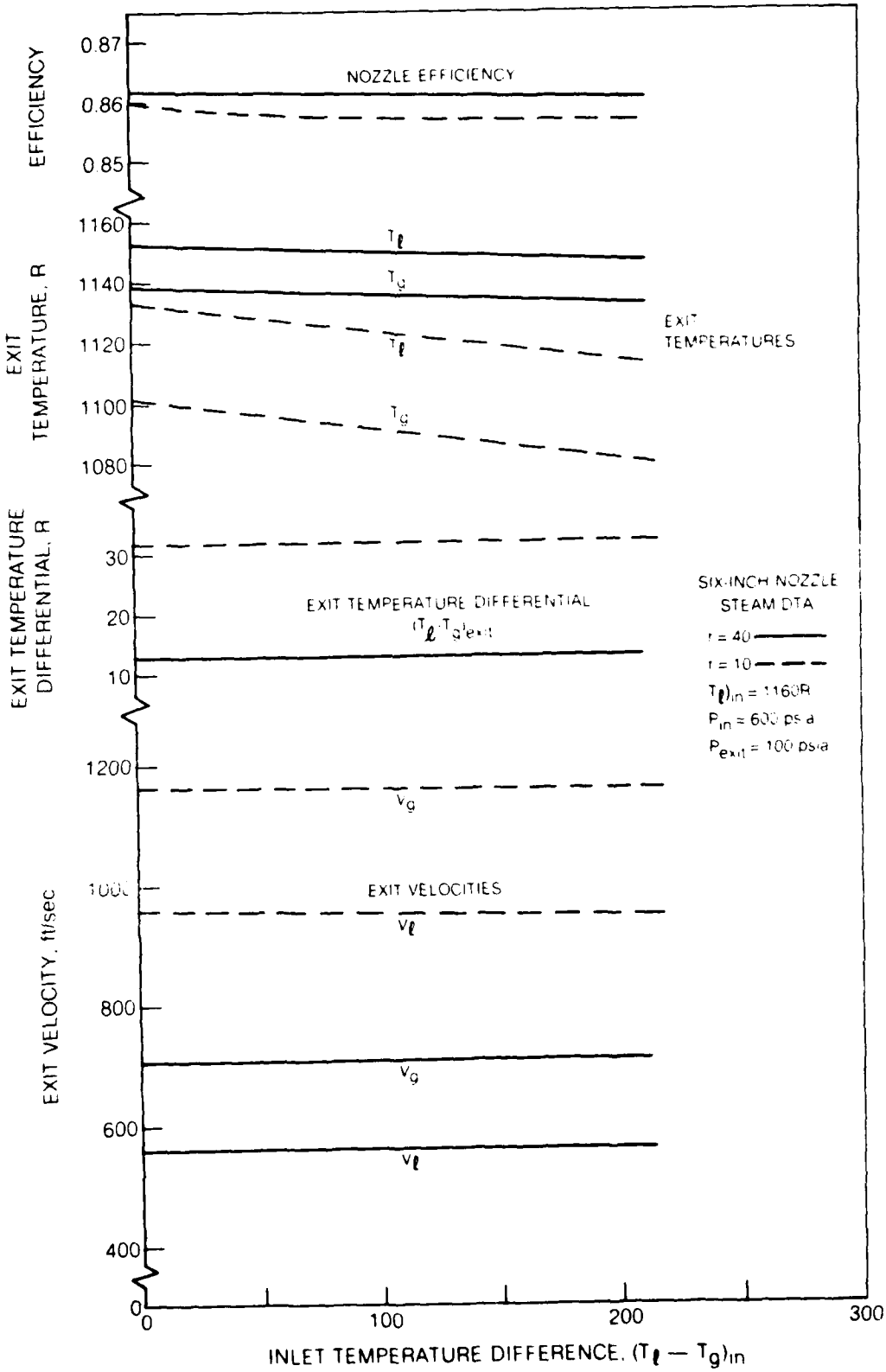

80-11-64-11

FIG. II.10

EFFECT OF INLET TEMPERATURE DIFFERENCE ON NOZZLE PERFORMANCE PREDICTIONS (AS FUNCTION OF LOADING RATIO)

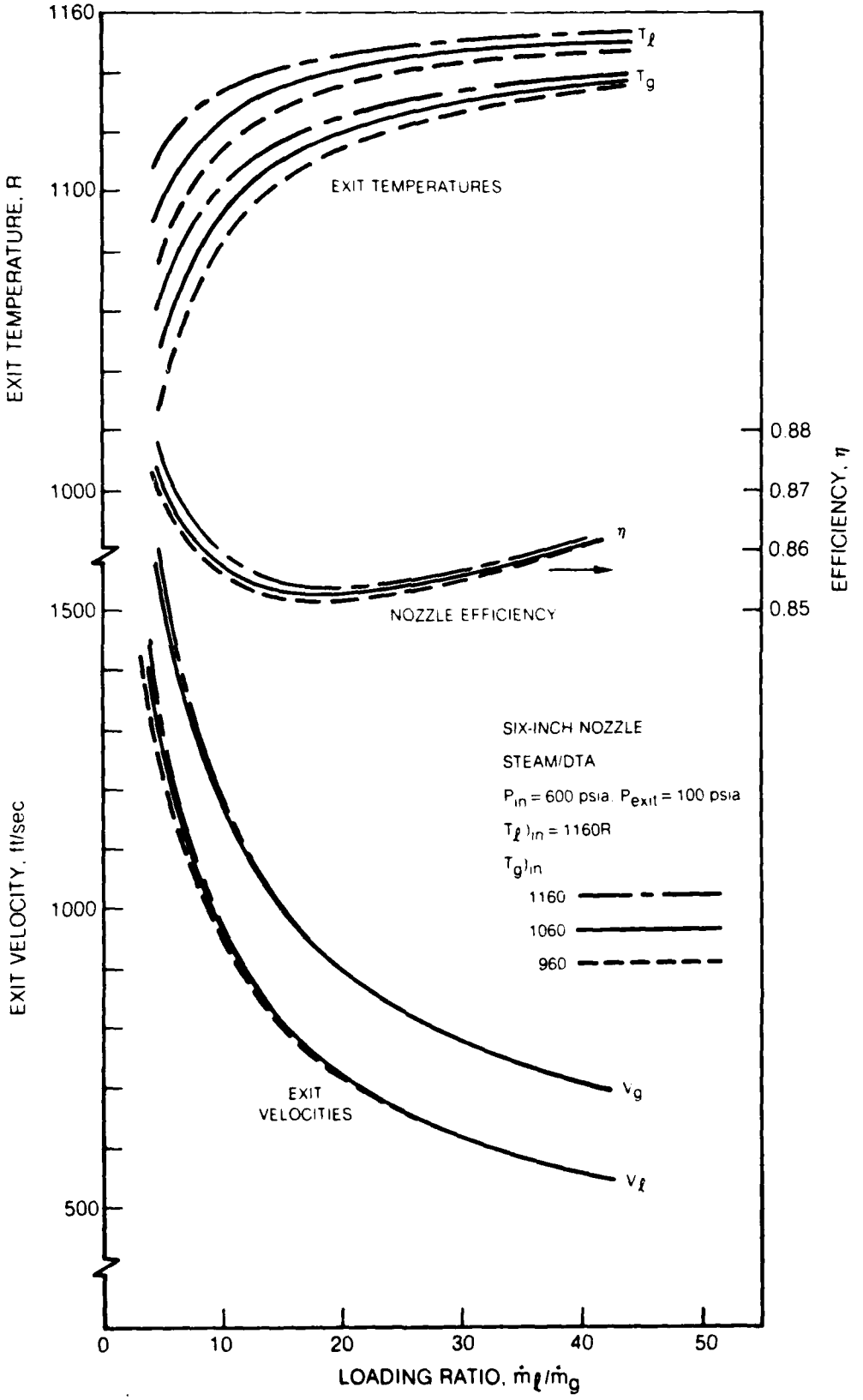

81-6-3-8

FIG II 11

EFFECT OF GAS DENSITY ON NOZZLE PERFORMANCE PREDICTIONS

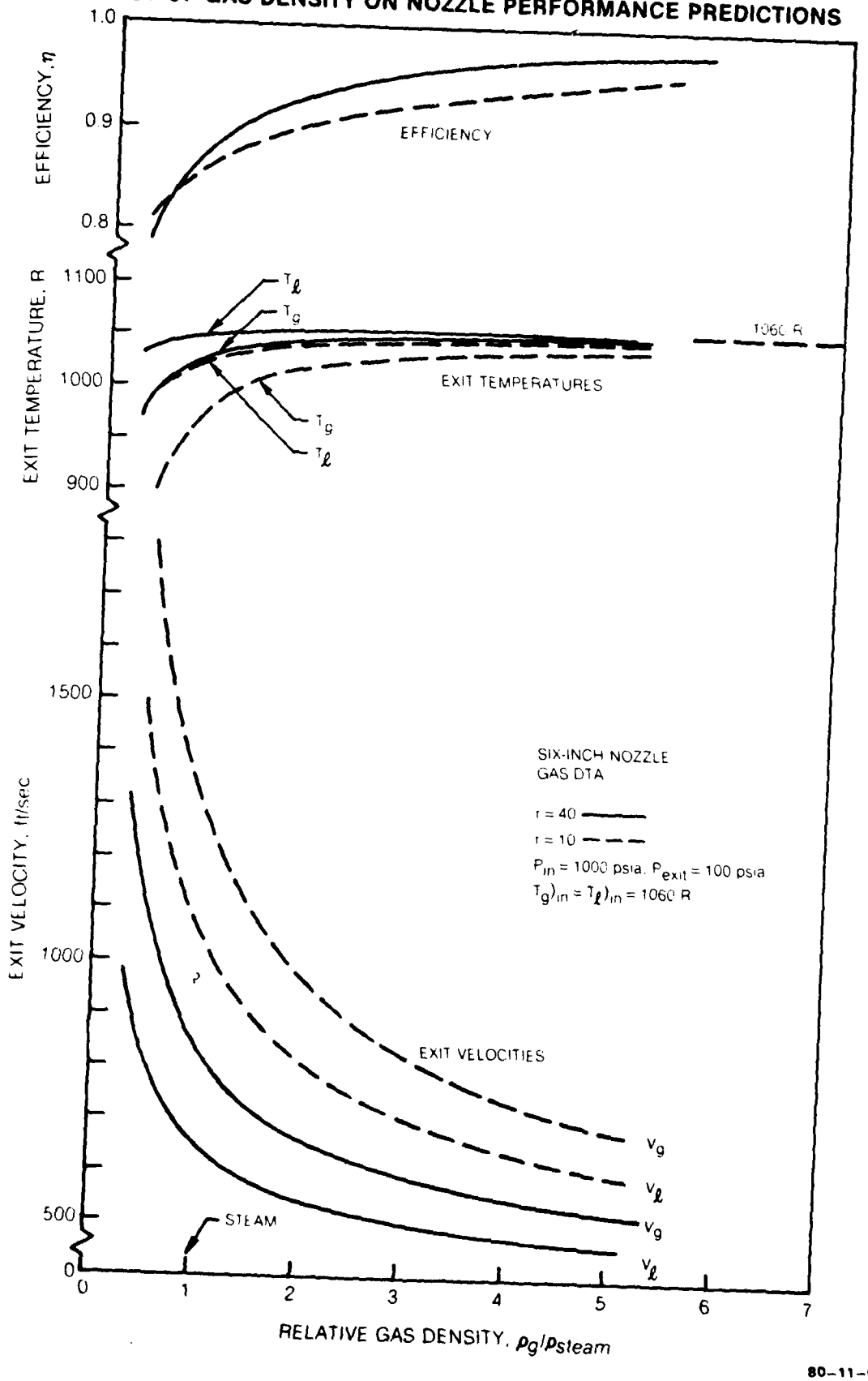

80-11-64-8

FIG II.12

EFFECT OF LIQUID SPECIFIC HEAT ON NOZZLE PERFORMANCE PREDICTIONS

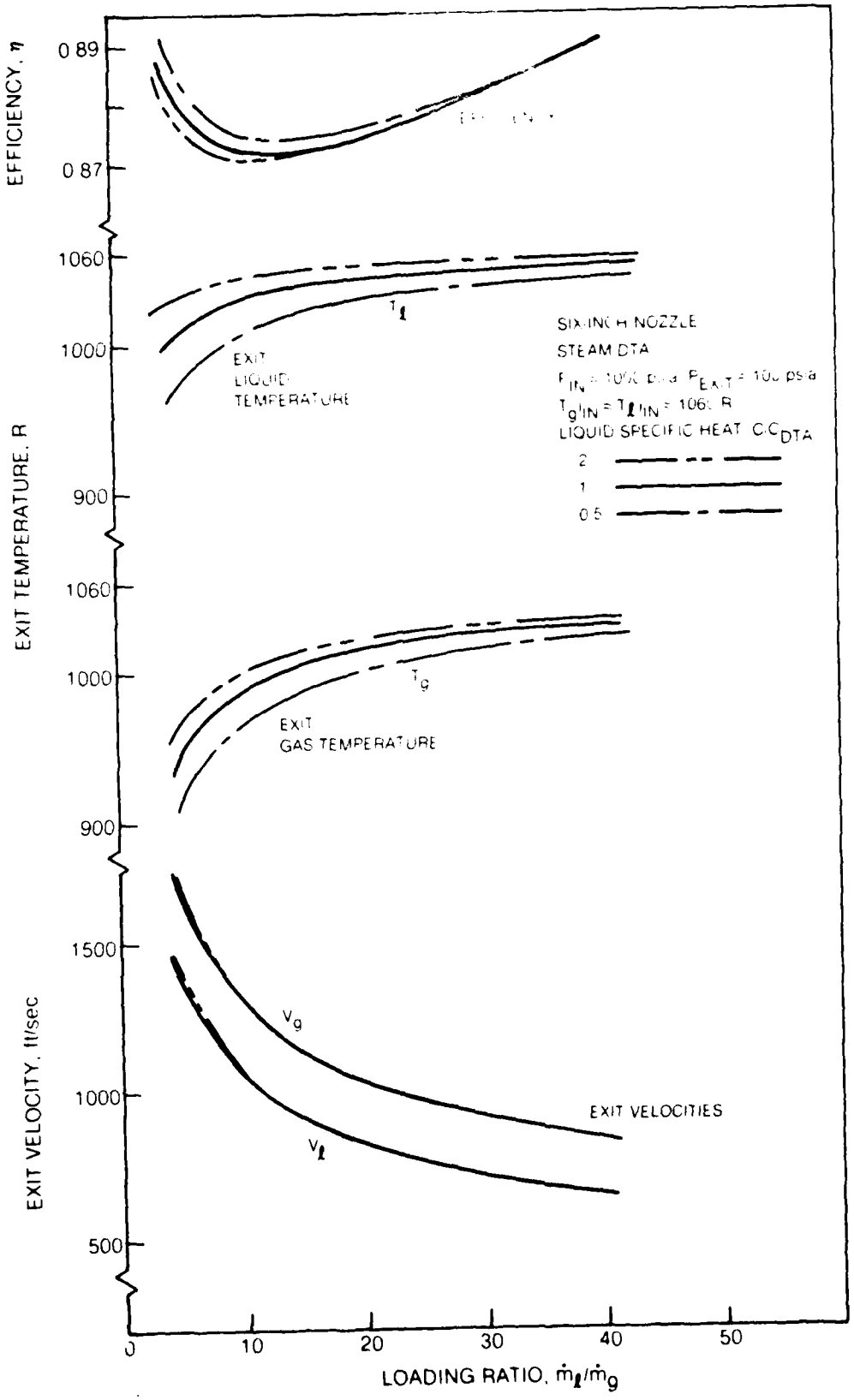

81-2-132-4

EFFECT OF SURFACE TENSION ON NOZZLE PERFORMANCE PREDICTIONS

FIG. II.13

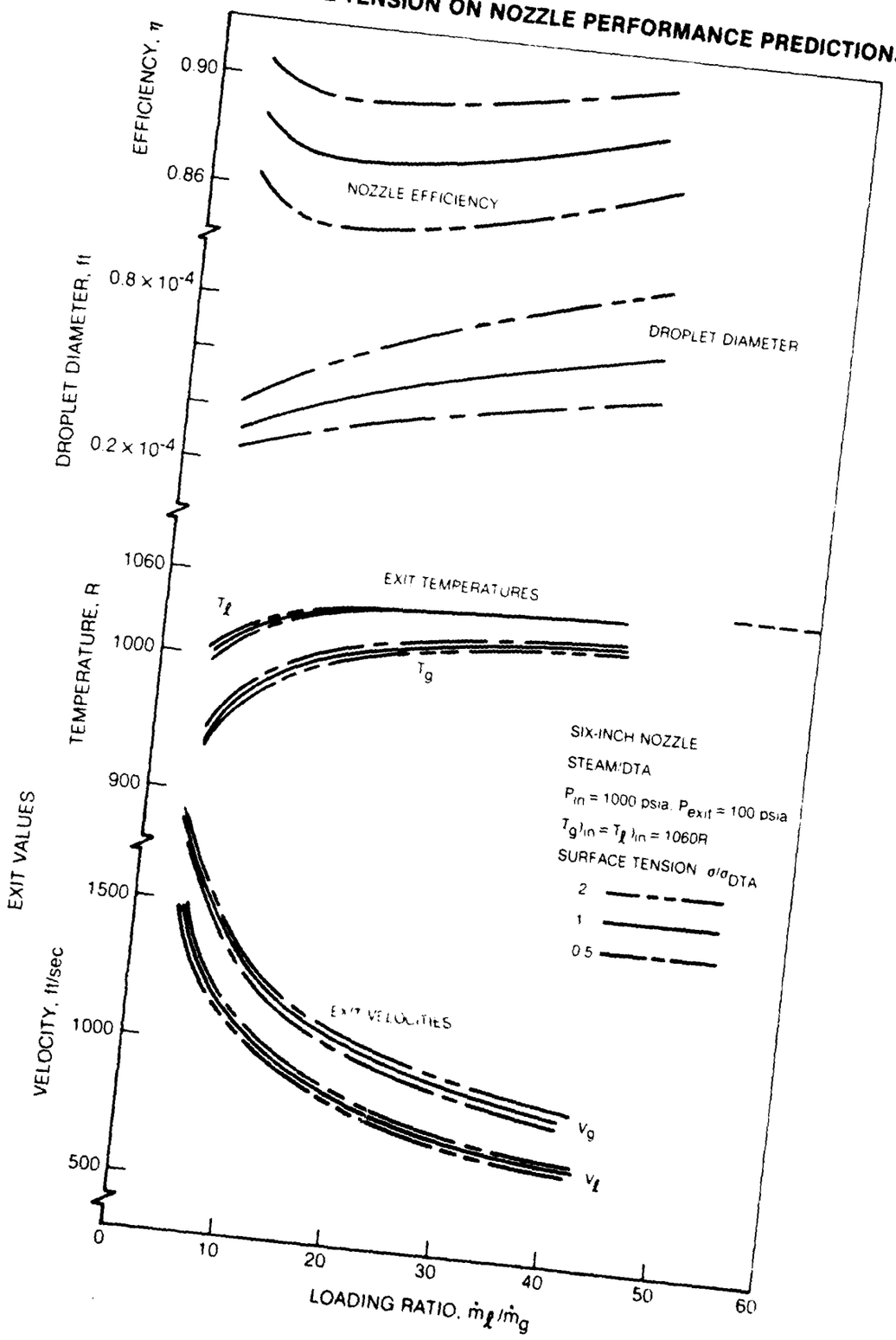

81-6-3-9

EFFECT OF LIQUID DENSITY ON NOZZLE PERFORMANCE PREDICTIONS

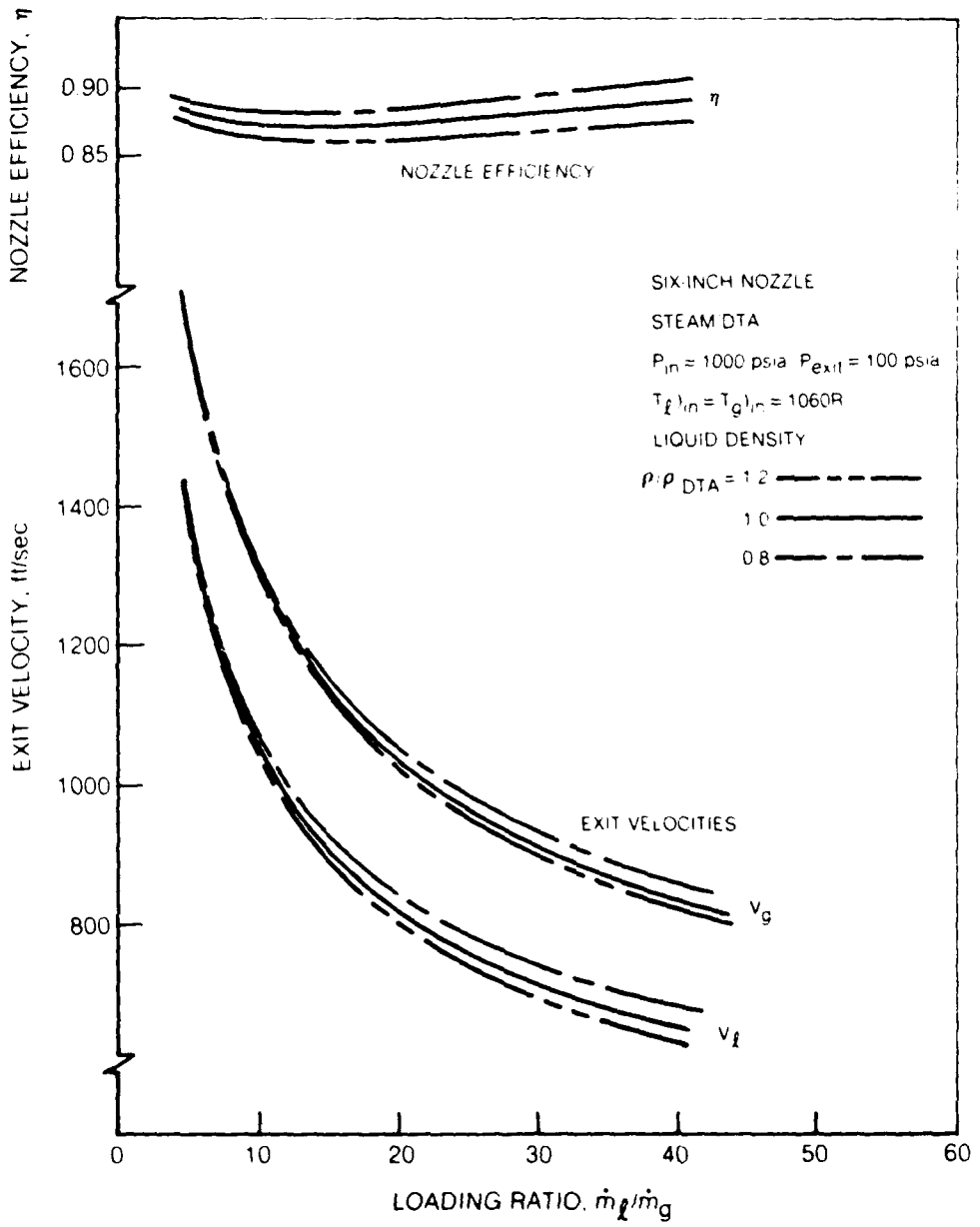

81-6-3-10

FIG. II 15

EFFECT OF DROPLET SIZE ON NOZZLE PERFORMANCE PREDICTIONS

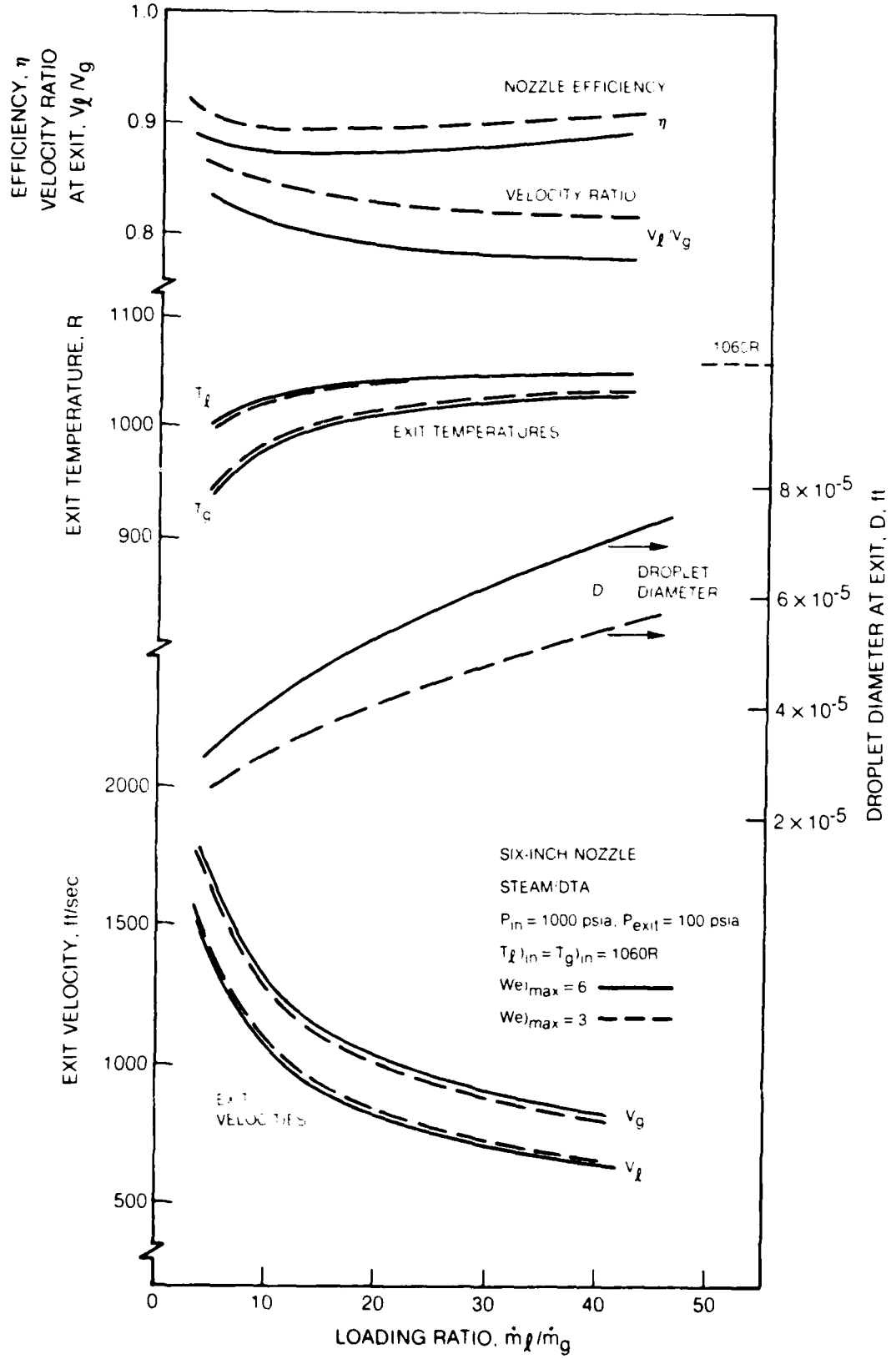

81-6-3-11

FIG II 16

EFFECT OF NOZZLE LENGTH ON NOZZLE PERFORMANCE PREDICTIONS

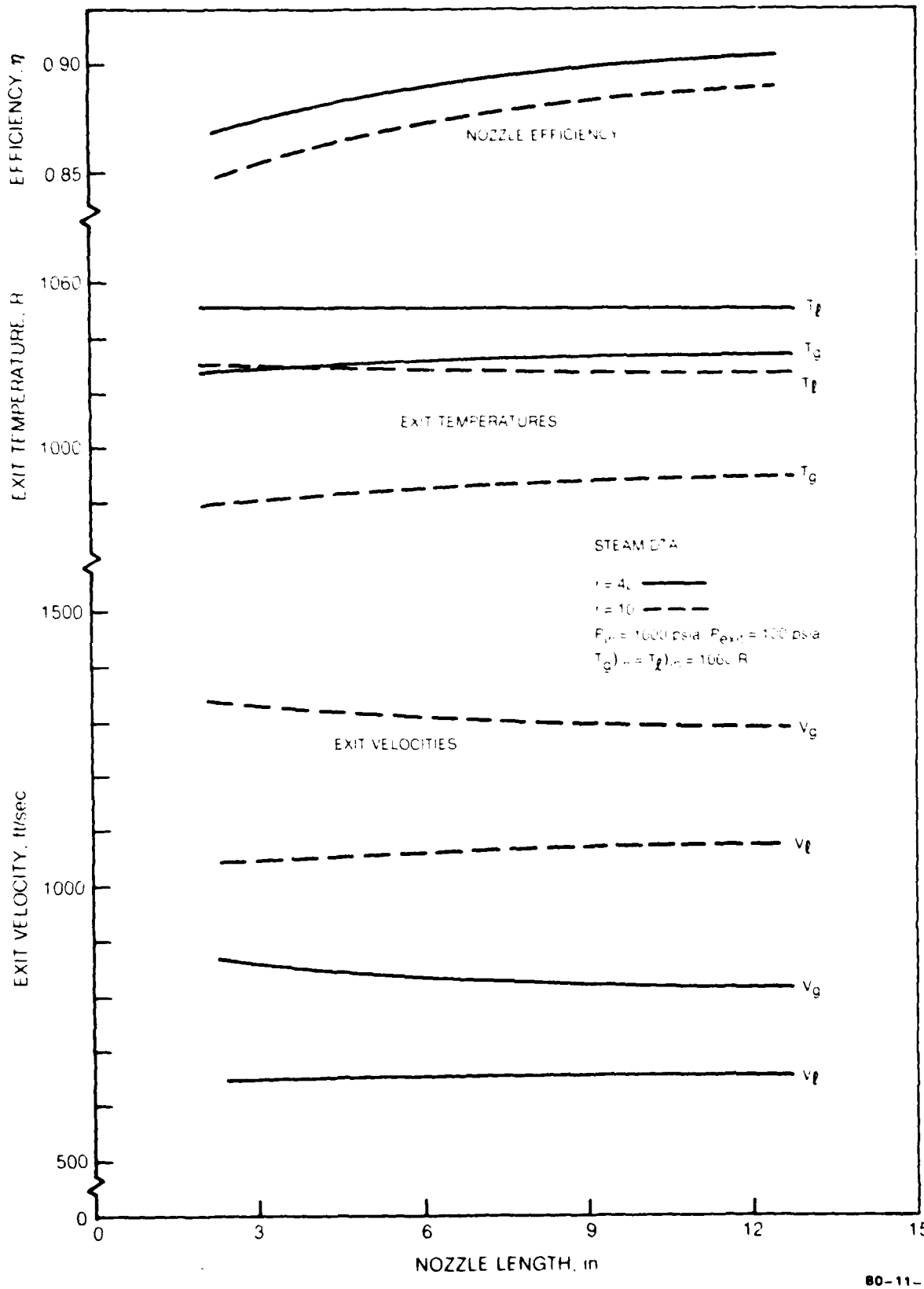

80-11-64-7

POWER SPLIT AND LIQUID ENERGY FRACTION OF TWO-PHASE NOZZLE

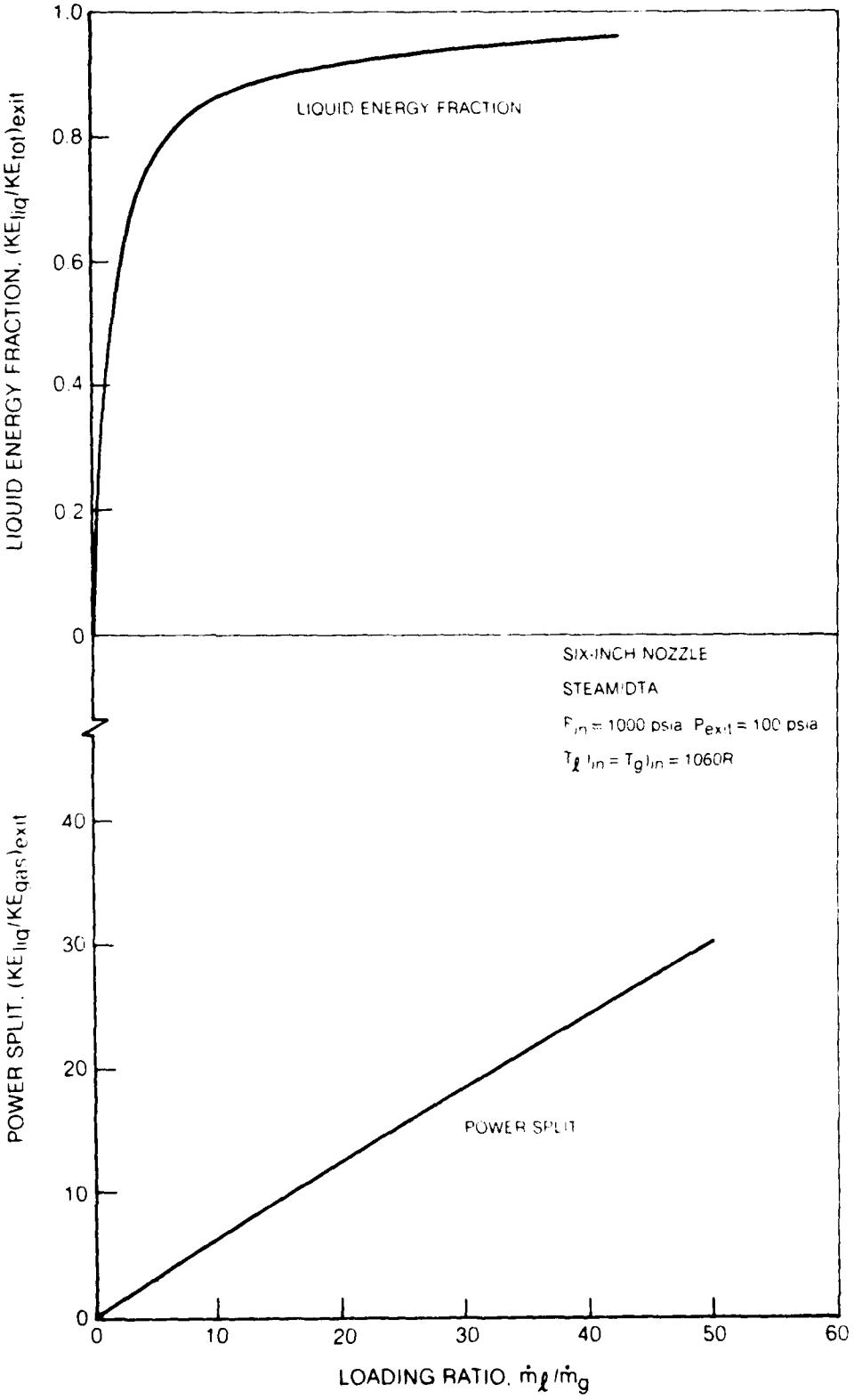

81-6-3-12

TWO-PHASE NOZZLE EFFICIENCY MAP — PRESURE EFFECTS

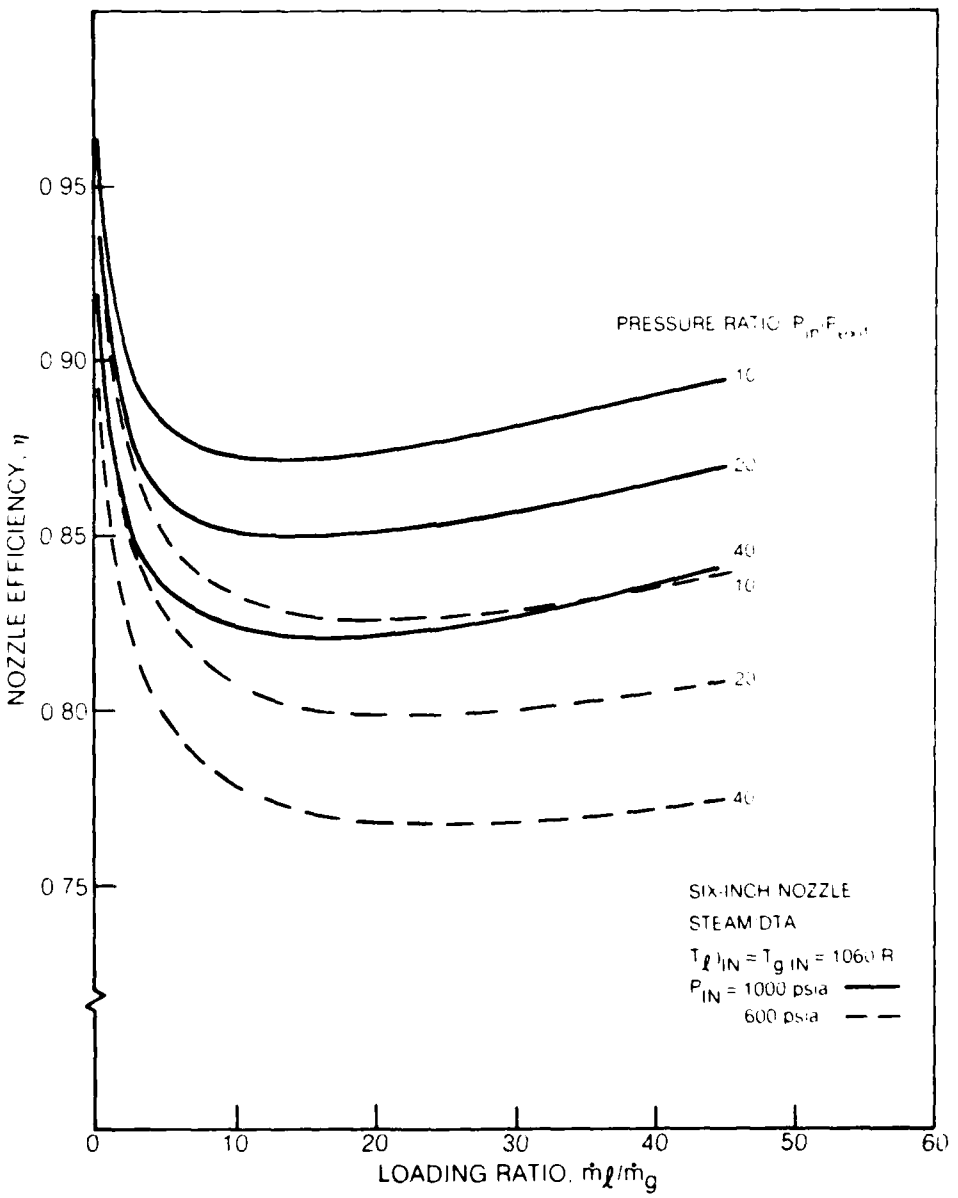

81-2-132-1

TWO-PHASE NOZZLE EFFICIENCY MAP — TEMPERATURE EFFECTS

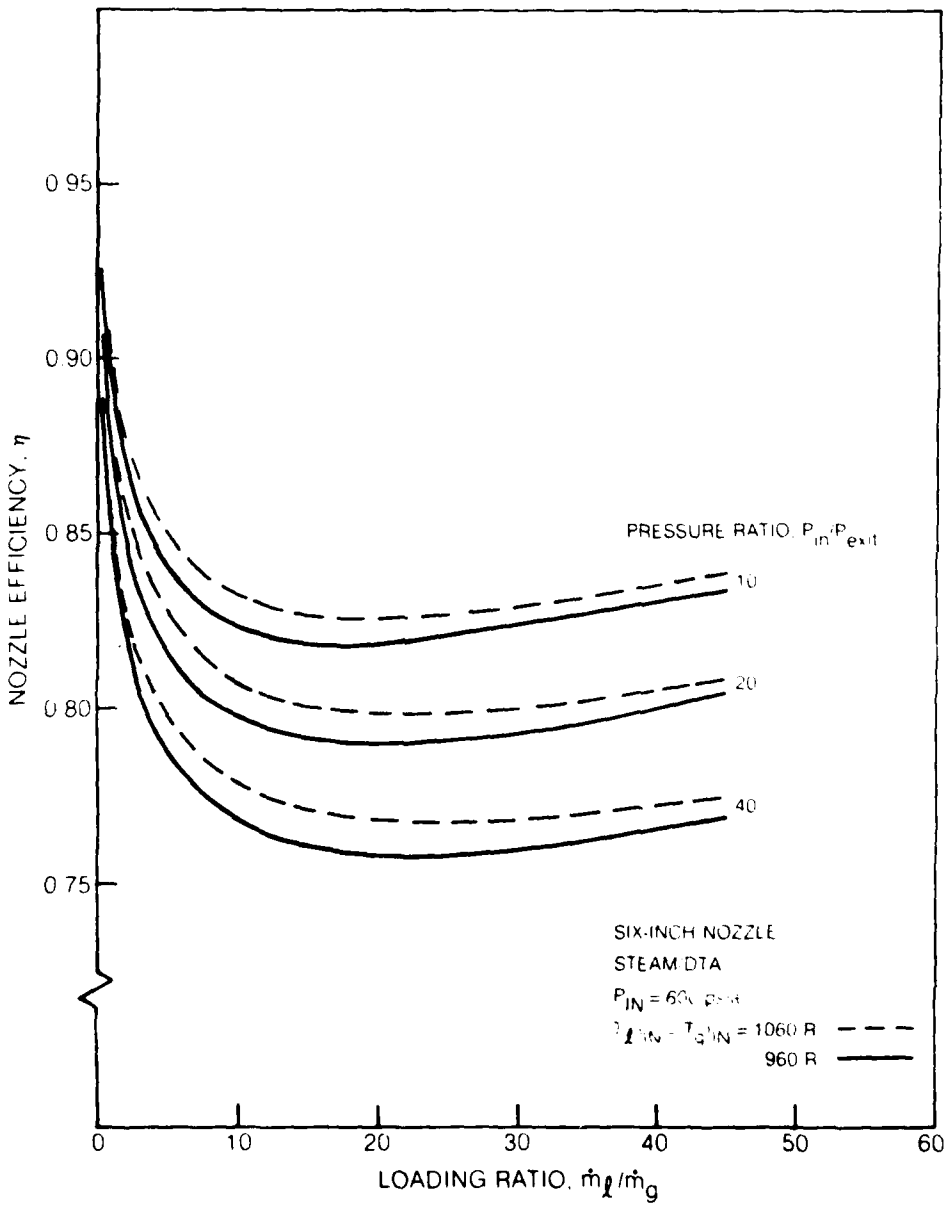

81-2-132-2

TWO-PHASE NOZZLE EFFICIENCY MAP — TEMPERATURE DIFFERENCE EFFECTS

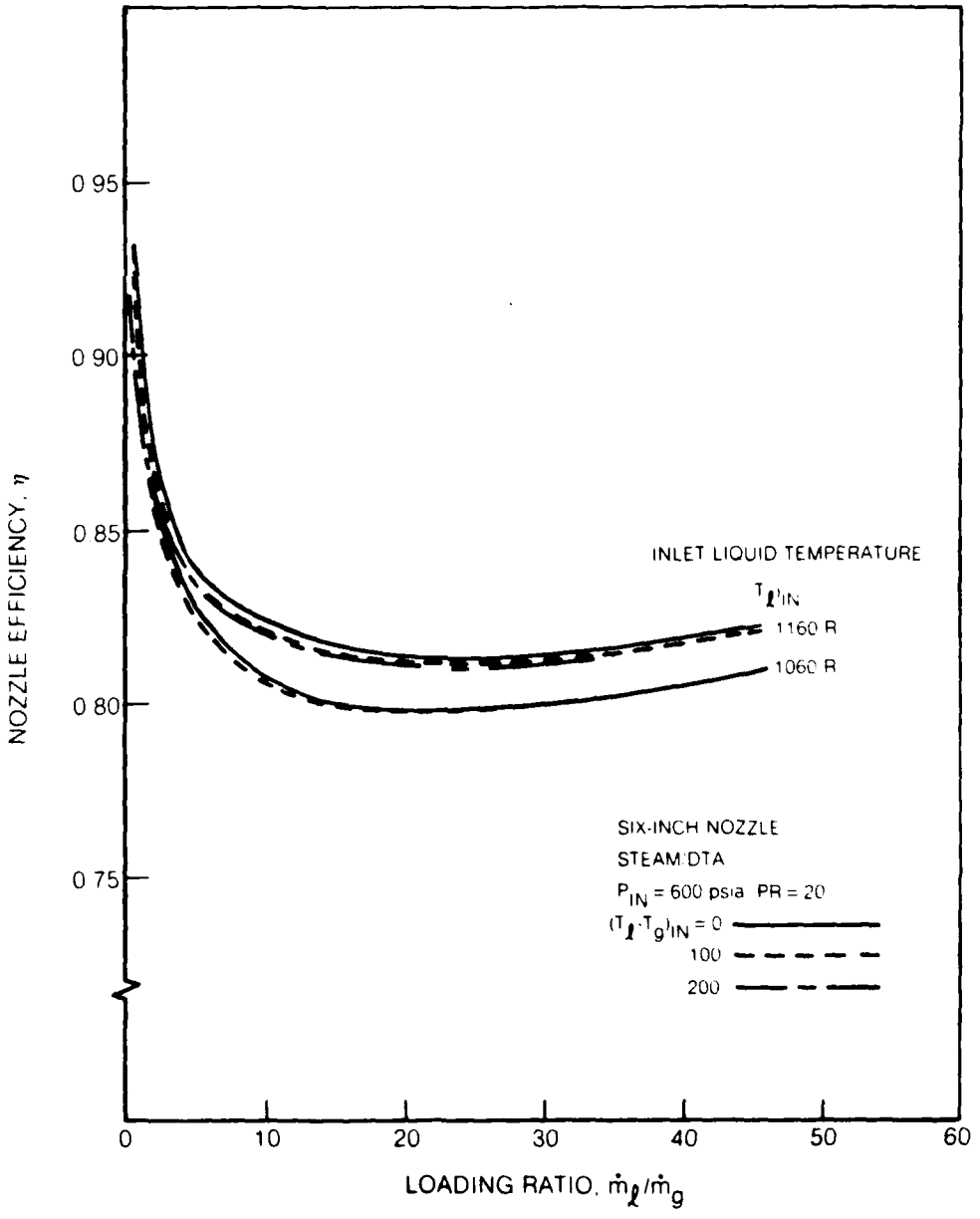

81-2-132-3

COMPARISON OF MODEL WITH DROPLET HEAT TRANSFER TO EXPERIMENTAL WATER-NITROGEN RESULTS AT NOZZLE INLET PRESSURE OF 150 psia

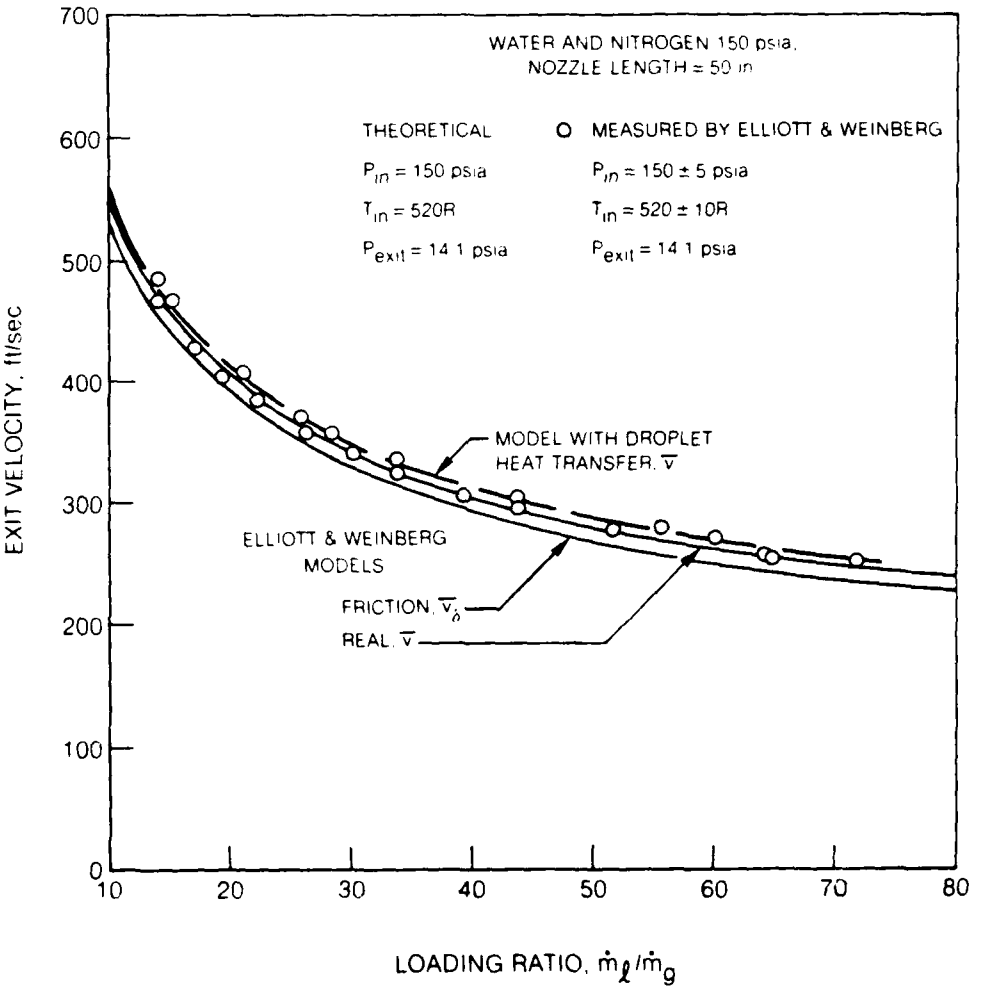

81-6-3-23

COMPARISON OF MODEL WITH DROPLET HEAT TRANSFER TO EXPERIMENTAL WATER-NITROGEN RESULTS AT NOZZLE INLET PRESSURE OF 190 psia

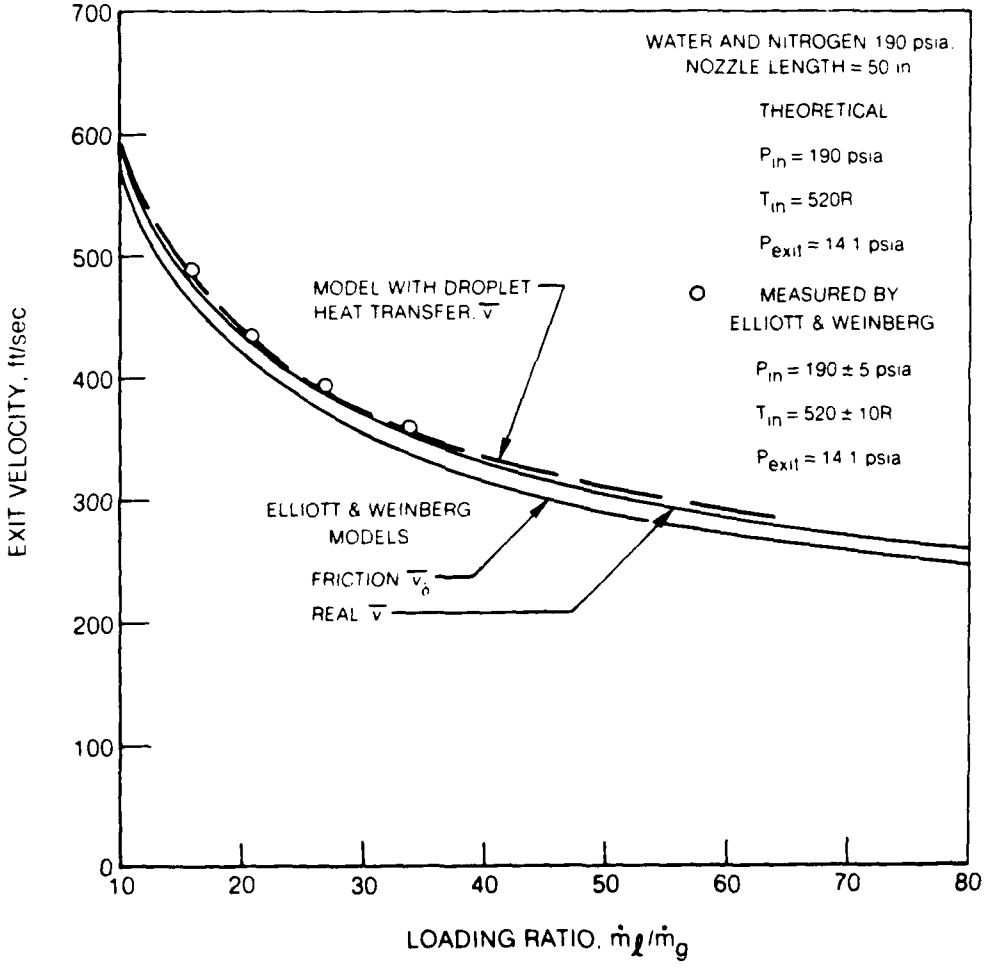

81-6-3-24

COMPARISON OF MODEL WITH DROPLET HEAT TRANSFER TO EXPERIMENTAL WATER-NITROGEN RESULTS AT NOZZLE INLET PRESSURE OF 230 psia

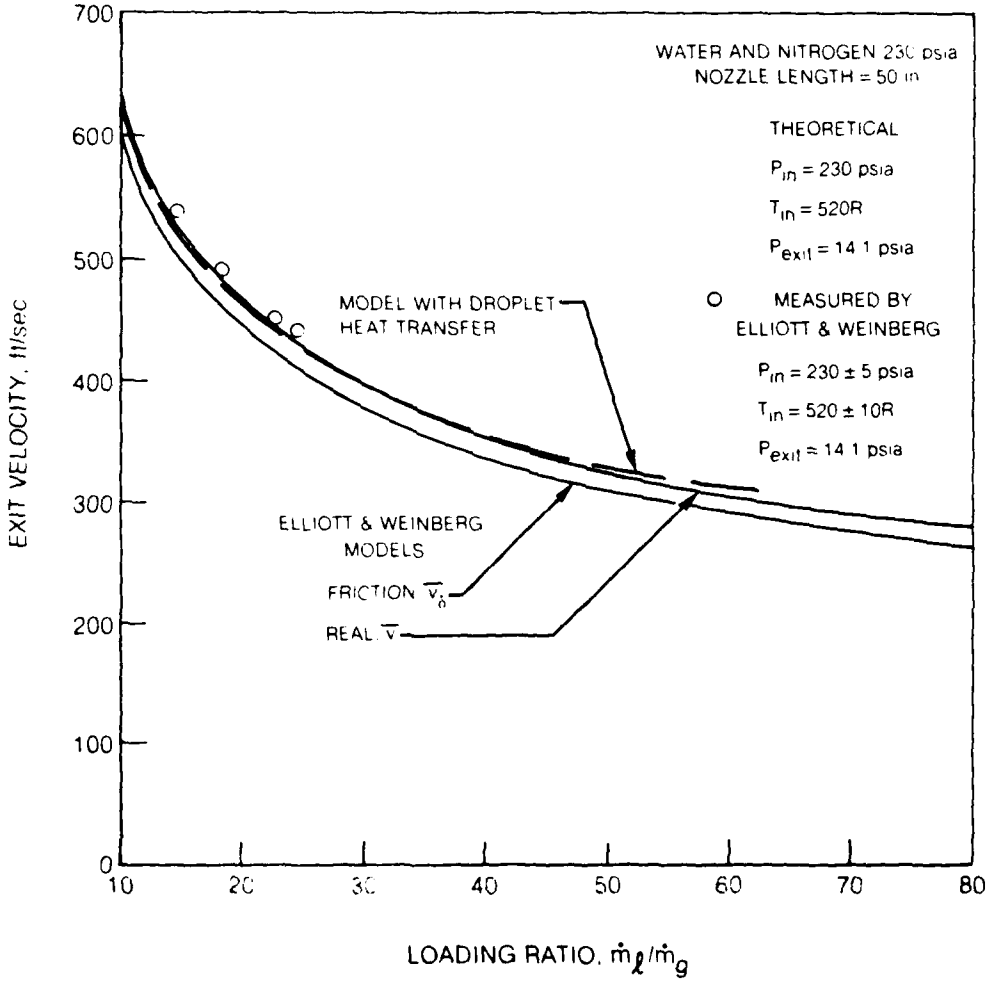

81-6-3-22

EFFECTS OF DTA vs DTG ON NOZZLE PERFORMANCE PREDICTIONS

FIG. 11.24

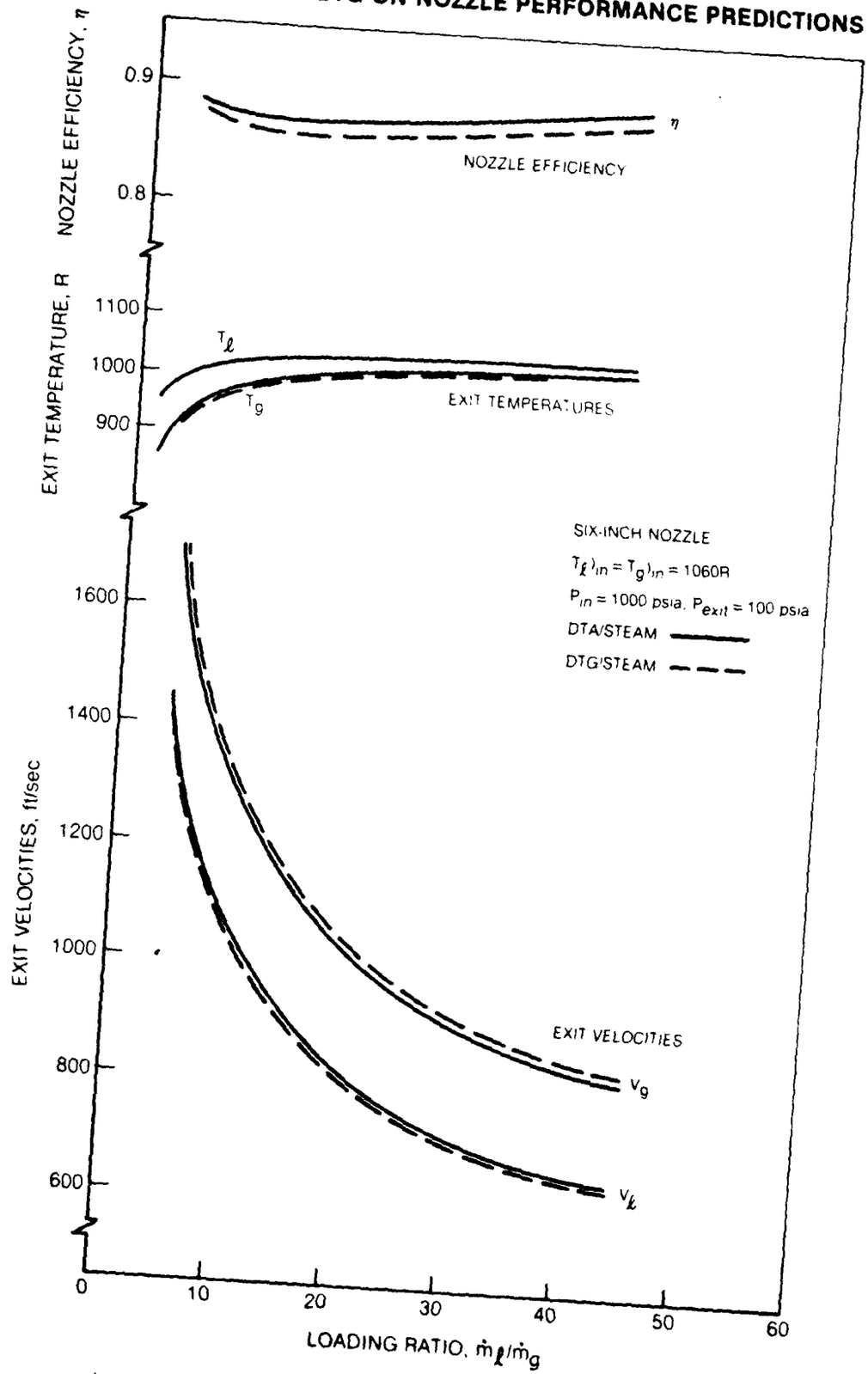

81-6-3-13

FIG. II.25

COMPARISON OF SIMPLIFIED SIZING PROCEDURE TO DROPLET HEAT TRANSFER MODEL

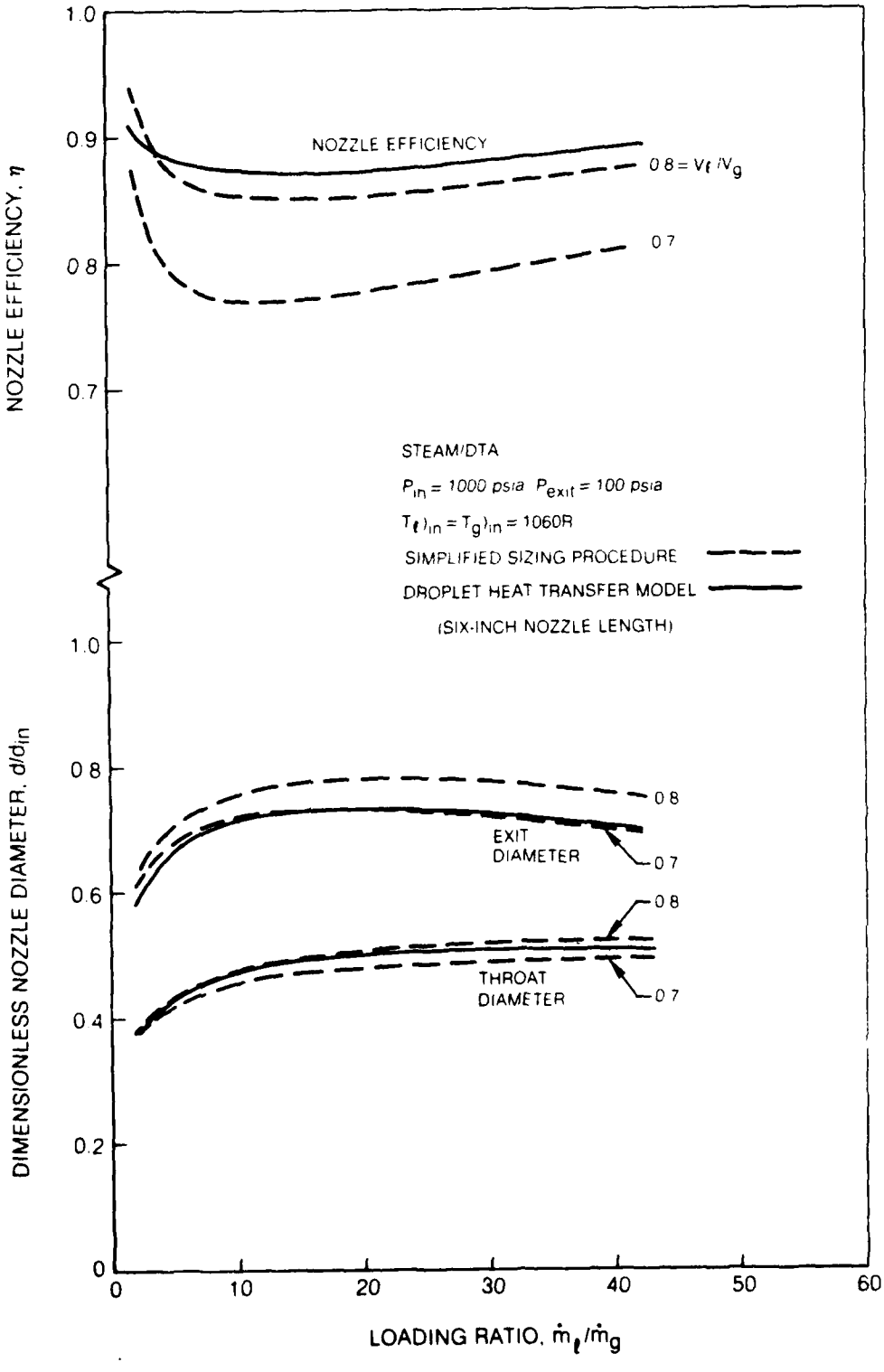

81-6-3-14

COMPARISON OF CALCULATED EXIT VELOCITIES

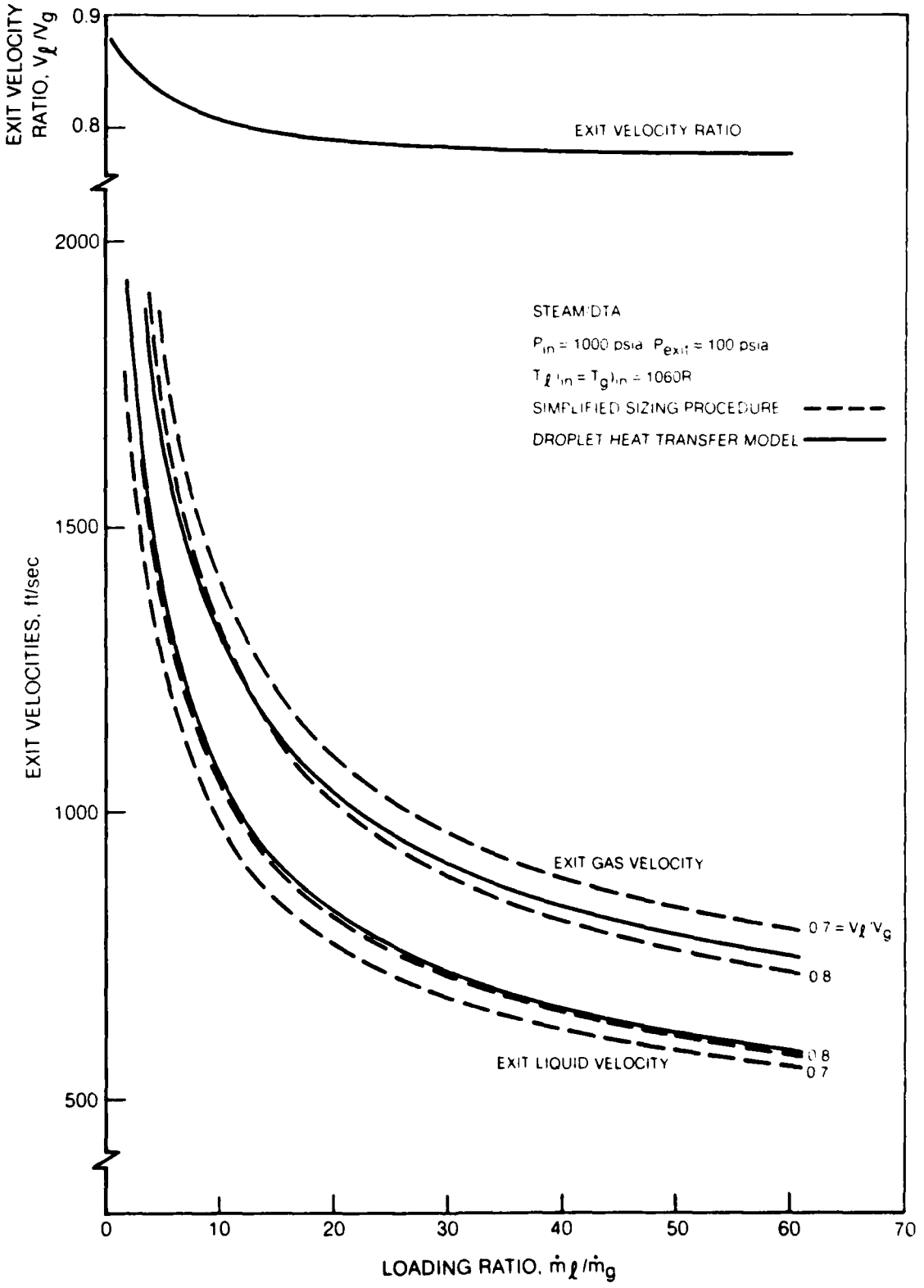

81-6-3-15

SIMPLIFIED SIZING PROCEDURE vs DROPLET HEAT TRANSFER MODEL

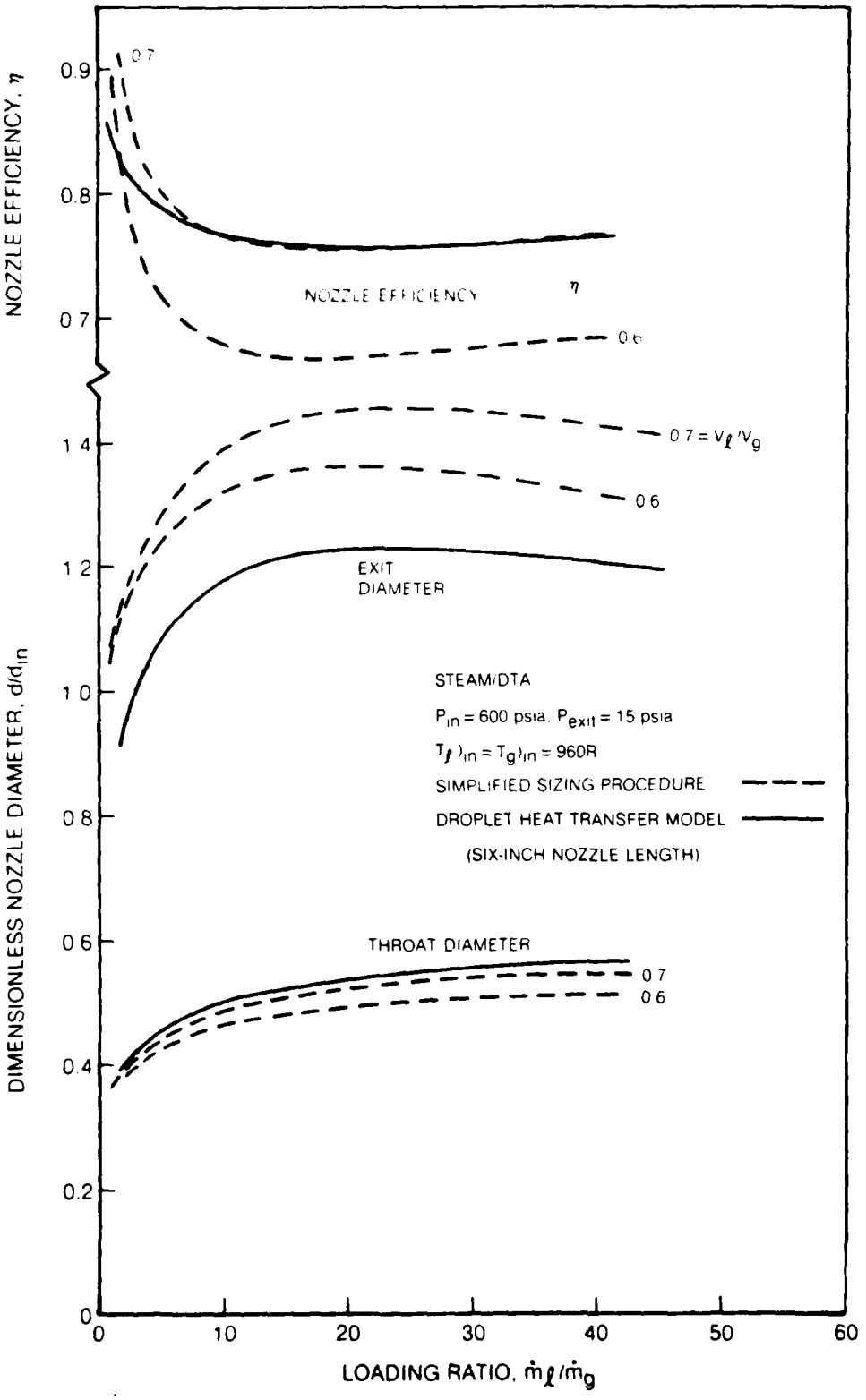

81-6-3-16

FIG. II.28

SCHEMATIC OF WORK EXTRACTION SYSTEM WITH TWO-PHASE NOZZLE

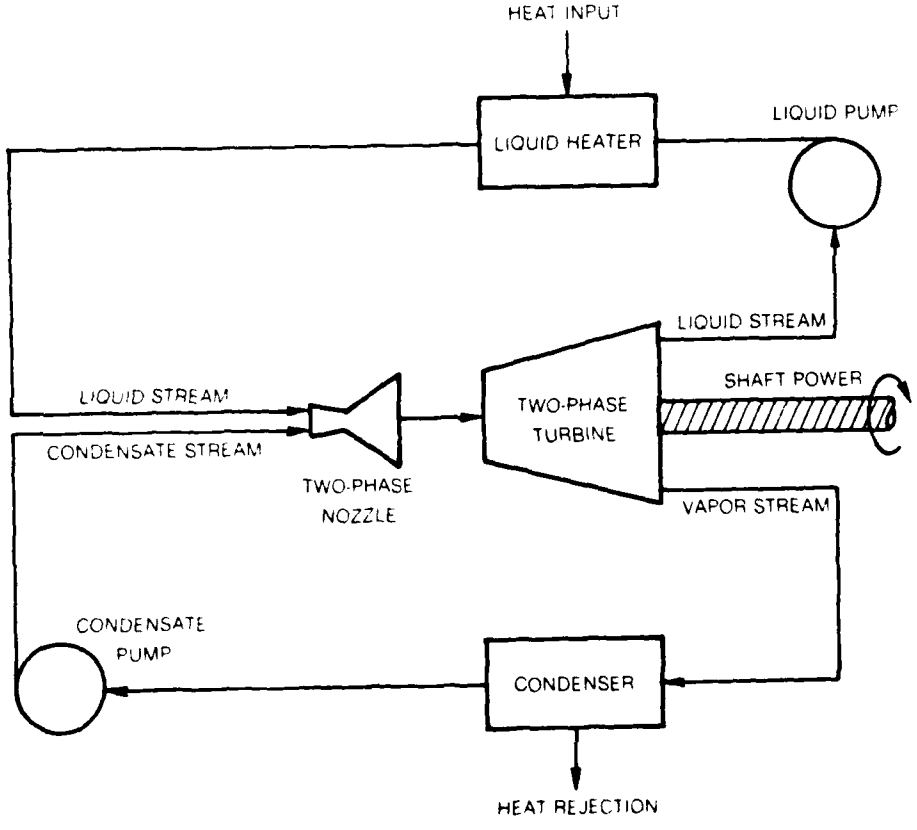

81-6-3-17

FIG. II.29

SIMPLIFIED OFF-DESIGN PERFORMANCE PREDICTIONS

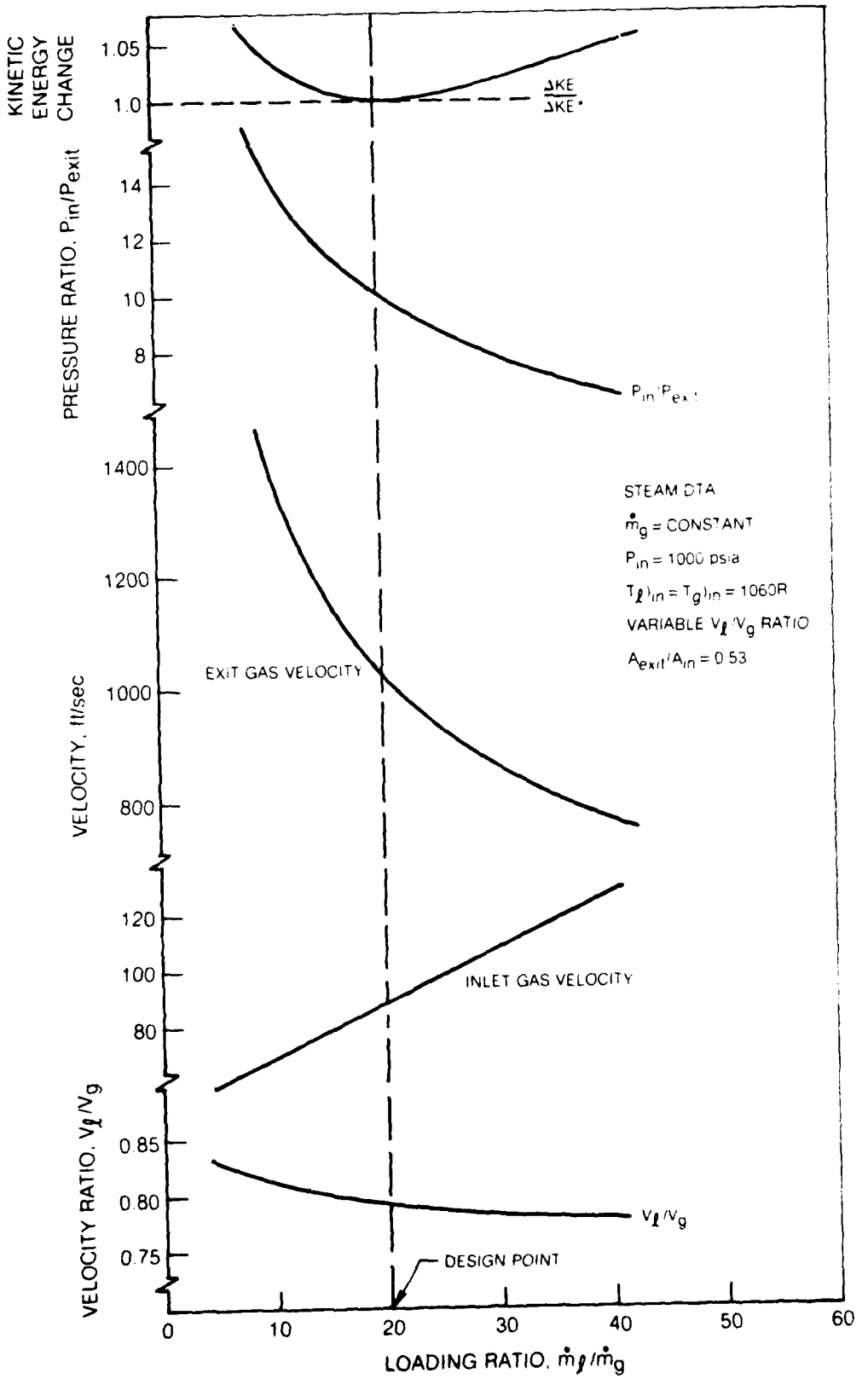

81-6-3-18

FIG. II.30

SIMPLIFIED OFF-DESIGN PERFORMANCE PREDICTIONS

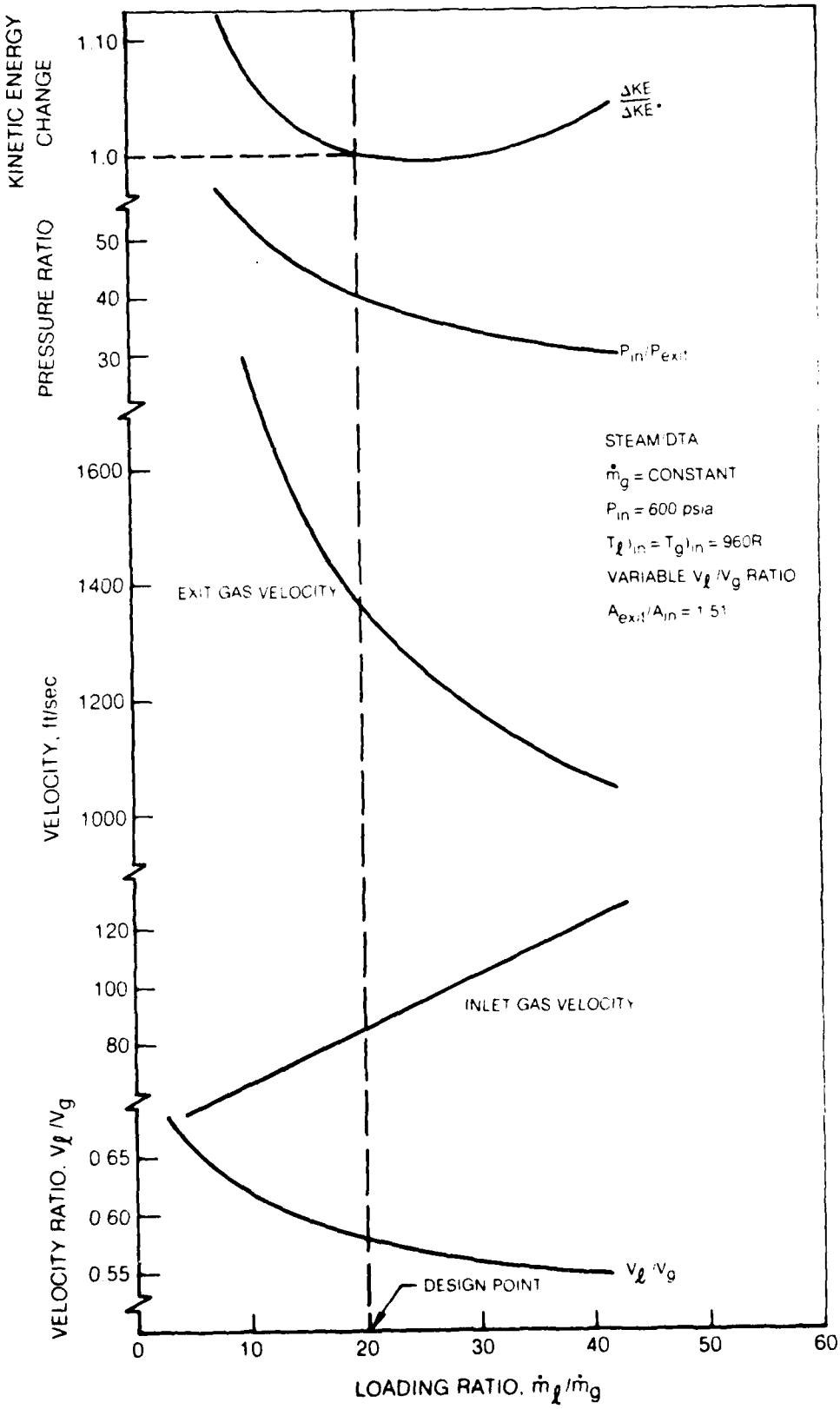

B1-6-3-19

FIG. II-31

SIMPLIFIED OFF-DESIGN PERFORMANCE PREDICTIONS — AT CONSTANT LOADING RATIO

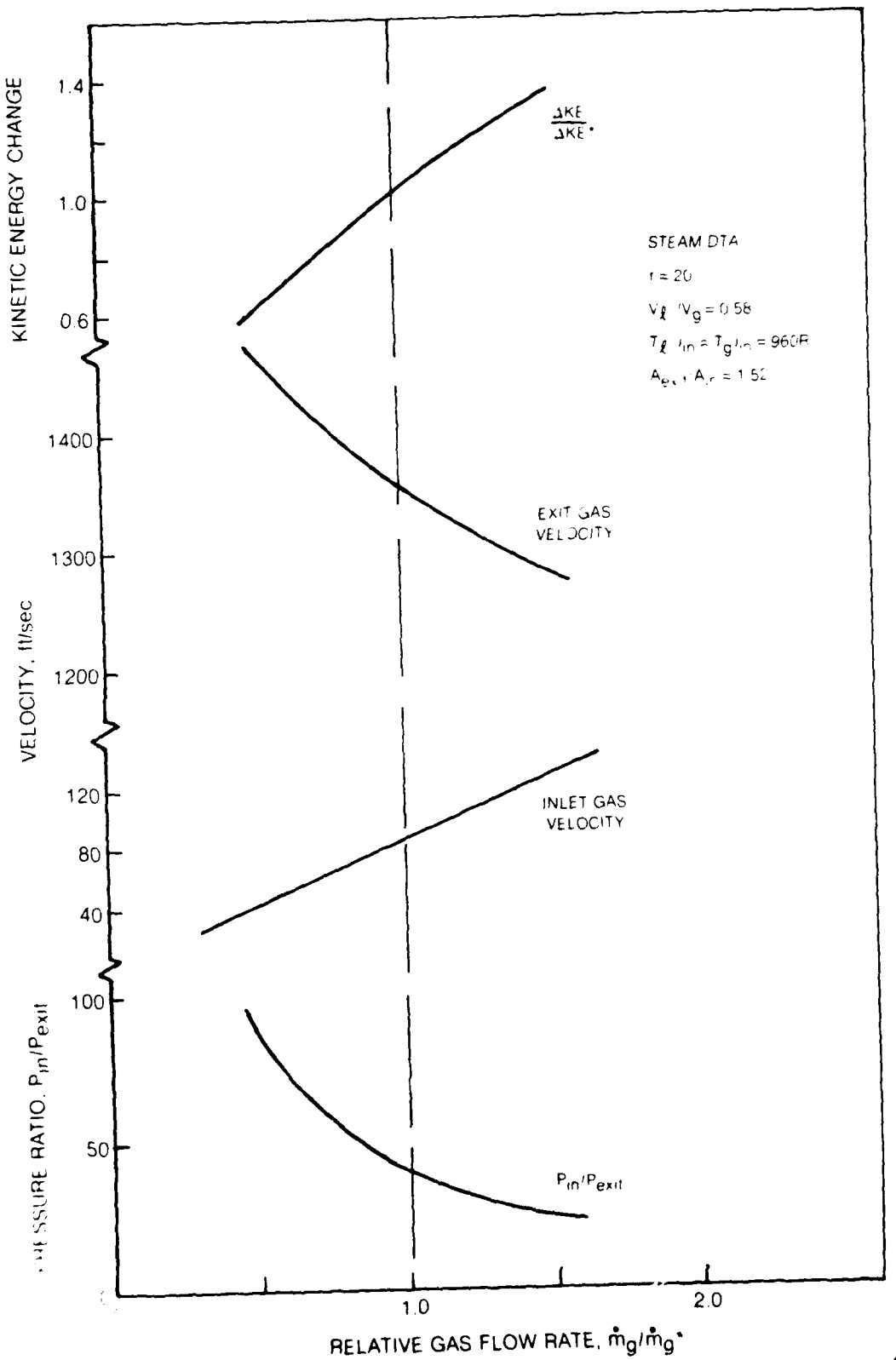

81-6-3-20

R81-955229-4

DISTRIBUTION LIST

TWO PHASE FLOW

	One copy except as noted
Mr. M. Keith Ellingsworth Power Program, Code 473 Office of Naval Research 800 N. Quincy Street Arlington, VA 22217	5
Defense Documentation Center Building 5, Cameron Station Alexandria, VA 22314	12
Technical Information Division Naval Research Laboratory 4555 Overlook Avenue SW Washington, DC 20375	6
Professor Paul Marto Department of Mechanical Engineering US Naval Post Graduate School Monterey, CA 93940	
Professor Bruce Rankin Naval Systems Engineering US Naval Academy Annapolis, MD 21402	
Dr. Al Wood Office of Naval Research Eastern/ Central Regional Office Bldg. 114, Section D 666 Summer Street Boston, Massachusetts 02210	
Mr. Mike Chaszeyka Office of Naval Research Branch Office 536 South Clark Street Chicago, Ill. 60605	

Mr. Charles Miller, Code 05R13
Crystal Plaza #6
Naval Sea Systems Command
Washington, DC 20362

Steam Turbines Branch, Code 5221
National Center #4
Naval Sea Systems Command
Washington, DC 20362

Mr. Ed Ruggiero, NAVSEA 08
National Center #2
Washington, DC 20362

Dr. Earl Quandt Jr., Code 272
David Taylor Ship R&D Center
Annapolis, MD 21402

Mr. Wayne Adamson, Code 2722
David Taylor Ship R&D Center
Annapolis, MD 21402

Dr. George Lea, Director
Fluid Mechanics Program
National Science Foundation
Washington, DC 20550

Mr. Michael Perlsweig
Department of Energy
Mail Station E-178
Washington, DC 20545

Professor J. A. C. Humphrey
Department of Mechanical Engineering
University of California, Berkeley
Berkeley, CA 94720

Professor Brian Launder
Thermodynamics and Fluid Mechanics Division
University of Manchester
Institute of Science & Technology
P088 Sackville Street
Manchester M601QD England

R81-955229-4

Professor Shi-Chune Yao
Department of Mechanical Engineering
Carnegie-Mellon University
Pittsburgh, PA 15213

Dr. Branko Leskovar
Electronics R&D Group
Lawrence Berkeley Laboratory
University of California
Berkeley, CA 94720

Dr. Ryszard Gajewski, Director
Division of Advanced Energy Projects
Office of Basic Energy Sciences
Department of Energy
Washington, DC 20545

Dr. David Elliot
NASA Jet Propulsion Laboratory
4800 Oak Grove Drive
Stop 67-201
Pasadena, CA 91103

Mr. Lance Hays, President
BiPhase Energy Systems
2800 Airport Blvd.
Santa Monica, CA 90405

Professor Paul A. Libby
Department of Applied Mechanics and Engineering Sciences
University of California San Diego
P.O. Box 109
La Jolla, CA 92037

Professor C. Forbes Dewey Jr.
Fluid Mechanics Laboratory
Massachusetts Institute of Technology
Cambridge, Massachusetts 02139

Professor Warren Rohsenow
Mechanical Engineering Department
Massachusetts Institute of Technology
77 Massachusetts Avenue
Cambridge, Massachusetts 02139

R81-955229-4

Professor A. Louis London
Mechanical Engineering Department
Bldg. 500, Room 501B
Stanford University
Stanford, CA 94305

Professor T. N. Veziroglu
Clean Energy Research Institute
University of Miami
Coral Gables, Florida 33124

Professor Daryl Metzger
Chairman, Mechanical and Energy
Systems Engineering
Arizona State University
Tempe, Arizona 85281

Professor T. H. Gawain
Department of Aeronautics
Naval Postgraduate School
Monterey, California 93940

Dr. J. E. Minardi
University of Dayton
Research Institute
Dayton, Ohio 45469

Professor Frank E. Marble
Mail Code 205-45
California Institute of Technology
Pasadena, California 91125

Dr. Oscar Manley
Div. of Engineering, Math., & Geo-Sciences
US Department of Energy
Washington, DC 20545


DAT
FILM